2005

OPTIMIZATION OF MACHINING PERFORMANCE IN CONTOUR FINISH TURNING OPERATIONS

Masaya Hagiwara
University of Kentucky

ABSTRACT OF THESIS

OPTIMIZATION OF MACHINING PERFORMANCE IN CONTOUR FINISH TURNING OPERATIONS

Unlike straight turning, the effective cutting conditions and tool geometry in contour turning operations are changing with changing workpiece profile. This causes a wide variation in machining performance such as chip flow and chip breakability during the operation. This thesis presents a new methodology for optimizing the machining performance, namely, chip breakability and surface roughness in contour finish turning operations. First, a computer program to calculate the effective cutting conditions and tool geometry along the contour workpiece profile is developed. Second, a methodology to predict the chip side-flow for complex grooved tool inserts is formulated and integrated in the current predictive model for contour turning operations. Third, experimental databases are established and numerical data interpolation is applied to predict the cutting forces, chip shape and size, and surface roughness for 1045 steel work material. Finally, based on the machining performance predictions, a new optimization program is developed to determine the optimum cutting conditions in contour finish turning operations.

KEWORDS: Optimization, Chip side-flow, Chip control, Contour turning,
Finish turning operations

Masaya Hagiwara

05 / 03 / 2005

OPTIMIZAITON OF MACHINING PERFORMANCE IN CONTOUR FINISH TURNING OPERATIONS

By

Masaya Hagiwara

I.S. Jawahir
Director of Thesis

G. Huang
Director of Graduate Studies

05 / 03 / 05
Date

RULES FOR THE USE OF THESES

Unpublished theses submitted for the Master's degree and deposited in the University of Kentucky Library are as a rule open for inspection, but are to be used only with due regard to the rights of the author. Bibliographical references may be noted, but quotations or summaries of parts may be published only with permission of the author, and with the usual scholarly acknowledgments.

Extensive copying or publication of the dissertation in whole or in part also requires the consent of the Dean of the Graduate School of the University of Kentucky.

A library that borrows this thesis for use by its patrons is expected to secure the signature of each user.

Name Date

THESIS

Masaya Hagiwara

The Graduate School

University of Kentucky

2005

OPTIMIZATION OF MACHINING PERFORMANCE IN CONTOUR FINISH TURNING OPERATIONS

THESIS

A thesis submitted in partial fulfillment of the requirements
for the degree of Master of Science in Mechanical Engineering
in the College of Engineering
at the University of Kentucky

By
Masaya Hagiwara

Director: Dr. I.S. Jawahir, Professor of Mechanical Engineering

Lexington, Kentucky
2005

ACKNOWLEDGEMENTS

I would like to express my sincere gratitude to Professor I.S. Jawahir for the help and guidance he provided to me during my studies here at the University of Kentucky. His constructive criticism, constant encouragement instilled in me the motivation to develop skills as a researcher. Thanks are also due to my committee members, Dr. J.M. Parker, and Dr. R. Molzon, for their support of my work.

I would like to specially thank Mr. Shi Chen (PhD Candidate) for his outstanding guidance and continuous support not only in my research work, but also in my daily life.

Grateful acknowledgement is extended to the UK Center for Manufacturing, University of Kentucky, for providing administrative support and for the use of the facilities to carry out research.

Finally, I would like to thank to my parents as well as my friends for their constant encouragement.

TABLE OF CONTENTS

LIST OF TABLES

LIST OF FIGURES

CHAPTER 1

INTRODUCTION AND THESIS OVERVIEW

1.1 Introduction

In machining operations, chip control is one of the most important factors for achieving good surface finish and part quality, operator safety, machine productivity, cost efficiency, and tool sustainability. However, chip control tends to be overlooked because of the complexity of the process. The need for research on improved methods of chip control was emphasized in a major review on chip control by Jawahir and Luttervelt [1]. However, chip control itself is not an independent factor in machinability assessments, as it relates to several other factors such as tool-life and surface finish [2]. Figure 1.1 shows the most common machinability assessment criteria involving several interrelated machining performance measures [3].

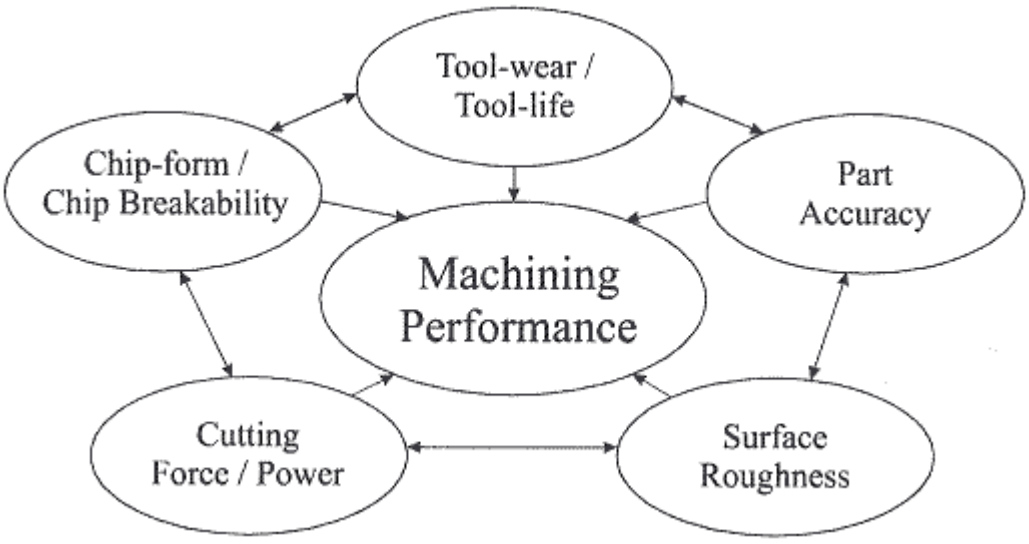

Figure 1.1: The machinability assessment criteria [3]

Several researchers have worked on developing chip flow predictive models since Colwell proposed the earliest model in 1954 [4]. However, most researchers focus on the straight turning process and these models cannot be simply applied to contour profiles of the workpiece. This is because the effective cutting conditions and tool geometry are changing with changing workpiece profile. Since almost all machining products are not from a simply straight turning bar, but have curved profiles including corner fillets or complex profiles such as the automotive wheels, developing the chip flow predictive model in contour turning operations is significant. In machining processes, it often happens that chip strikes the machined surface and affects the finish surface. This problem has to be taken care of especially in finishing operations. In finishing operations, the surface quality is the major issue and even a small scratch may make products scrap. When it comes to complex workpiece geometry, the effects of chip become more severe because of the difference of elevation in each segment and the wide variations in chip flow direction along the workpiece profile. Thus, the use of a chip flow predictive model in more practical operations, such as contour turning, becomes necessary.

Once the predictive model is established, the next step is the optimization. Since computer simulation programs of the predictive model can be developed as long as the model has a mathematical form, it is always possible to associate this program with an optimization program. The benefits of this connection between the simulation and optimization processes are not only to obtain the optimal machining performance, but also to make the process planning much easier. With regards to the chip flow predictive model, it can lead to control chip flow in a more favorable direction by changing cutting parameters, such as cutting conditions and tool geometry.

Cutting conditions, especially feed and depth of cut, are among the major factors influencing the machining performance. In contour turning, the machining surface can be divided into small segments according to the shapes such as concave and convex. The optimal cutting condition would be different in each segment due to the various effective parameters. The depth of cut cannot be changed through the contour profile, but feed can vary between segments when a CNC machine is used. Therefore, the optimal feed in each segment can be achieved at a given optimal depth of cut through the profile.

The main objective of this thesis work is to optimize the machining performance in contour finish turning operations. In finishing operations, surface roughness is a major concern. Hence, to quantify the machining performance in finish turning operations, two criteria are used in this thesis; chip breakability and surface roughness. Chip breakability takes care of chip shape and size, and chip side-flow. By finding optimal depth of cut and feed in each segment through the profile, the machining performance in contour turning can be improved.

To achieve this aim, the chip flow prediction program developed by Redetzky et al. [5] and Ghosh [6] at the University of Kentucky was extended in this thesis work. The chip shape, size and surface roughness are predicted from the experimental database. Then, these factors are used as input to the optimization program to find the optimal cutting conditions.

1.2 Overview of the Thesis

Chapter 2 contains the literature review on chip side-flow predictive models, and optimization methods developed for machining. A summary of major work on chip flow and chip control published in the past few decades is presented in this chapter.

Chapter 3 introduces the chip flow predictive model for machining with flat-faced tools based on Redetzky et al [5] and with grooved tool based on Ghosh [6]. Details of their analytical modeling are also described in this chapter.

Chapter 4 presents the optimization process developed for contour turning. Two criteria (chip breakability and surface roughness) are used to evaluate the machining performance in finish contour turning operations. The chip breakability criterion considers two factors which are chip shape and size, and chip side-flow angle. A numerical analysis based on the experimental database to predict the cutting force in complex grooved tool, surface roughness, and chip shape and size, is then presented. This chapter also includes an explanation and general procedure for using the Simulated Annealing (SA) method in this optimization problem.

Chapter 5 is a case study. A sample contour workpiece that contains a range of likely workpiece geometry combinations is selected. The results of the optimization program are shown in plotted figures as well as numerical tables.

Chapter 6 summarizes the current research findings and presents a list of future work.

Figure 1.2 shows an overview of the thesis work proposed.

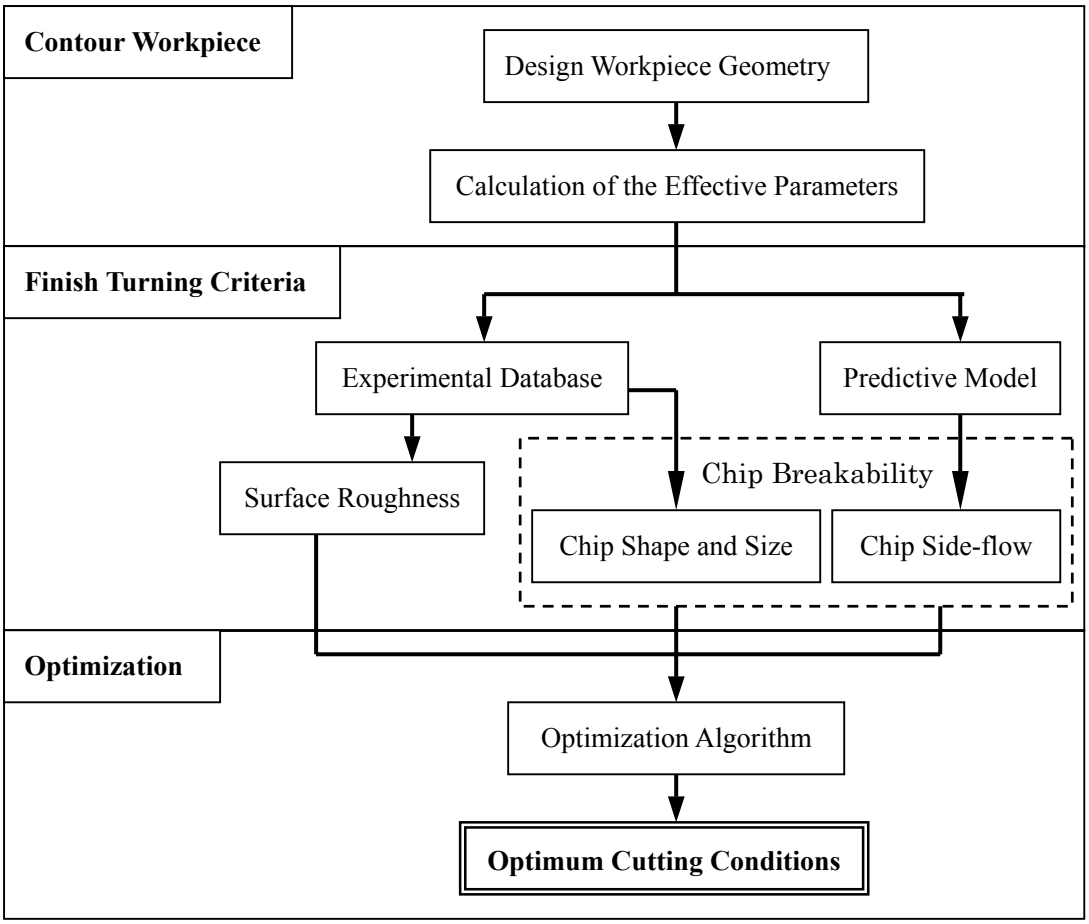

Figure 1.2: Overview of the thesis work

CHAPTER 2

A SUMMARY OF PREVIOUS WORK

2.1 Introduction

In past half century, many researchers have attempted to model the chip flow and the process of chip formation. Now that most of industrial products depends on Computer Integrated Manufacturing (CIM) environments, automatic selection of cutting tools and conditions by Computer Aided Process Planning (CAPP) system are needed. The assumption that the machining performance can be predicted within a reasonable degree of accuracy is the basis for the development of machining information systems (models, databases, etc.) which form the core of CAPP-systems [1]. Therefore, chip flow predictive model is not only likely to give us a better understanding of the chip formation process, but also it enables the selection of effective cutting conditions and tool geometry and leads to optimized machining performance. Once the predictive model is established, we can then consider how the machining performance can be improved, or the cost can be reduced, and optimization is the next concern. By integrating the predictive model and optimization for a computer program, it is possible to obtain the best machining performance and production cost, and process planning can be successful.

This chapter presents a review of considerable amount of work in the past several decades on chip flow modeling, and optimization methods developed for machining processes.

2.2 Previous Work

2.2.1 Chip Side-flow Model

One of the earliest chip flow models was established by Colwell [4]. Chip flow is substantially perpendicular to the side-cutting edge for the sharp-nosed tools but the direction swung progressively toward the tool axis as the nose radius is increased. He assumed that the chip-flow over the cutting face of the tool was perpendicular to the major axis of the projected area of cut (Figure 2.1). Cutting pattern was classified in terms of tool nose radius and depth of cut and derived the equations of chip-flow prediction based on the condition that the cutting was approximately orthogonal, i.e., both the rake and inclination angles were zero degrees.

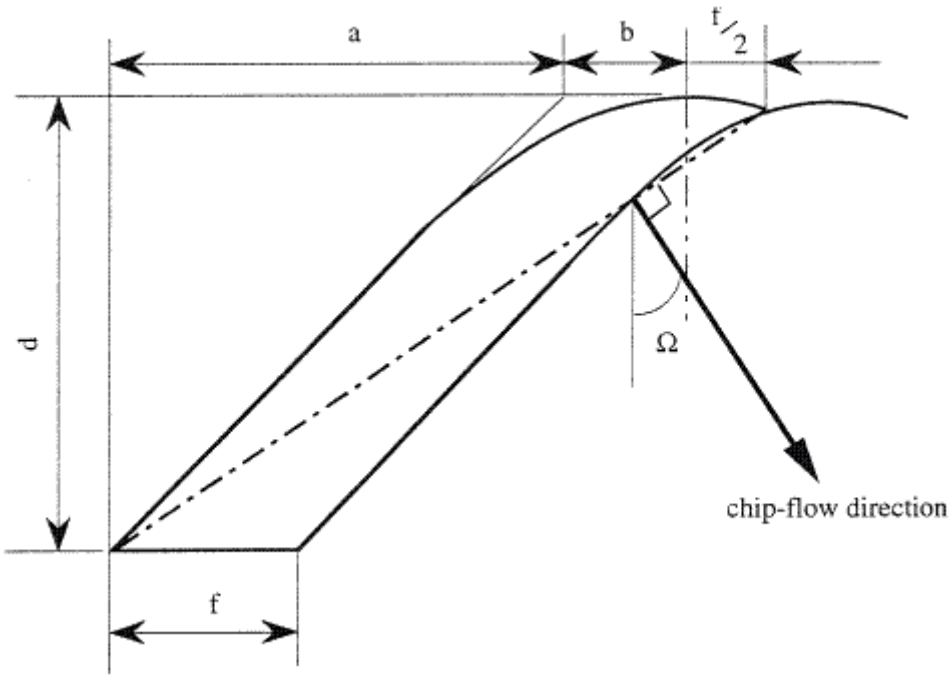

Figure 2.1: Colwell's chip flow model [4]

Okushima and Minato [7] mathematically developed the chip flow model for nose radius tools. They experimentally showed that the cutting speed does not affect the chip flow angle. The cutting edge was divided into small elements, and it was assumed that chip flow angles were perpendicular to the cutting edge in each segment. Then, the elemental chip flow angles were summed up along the cutting edge to obtain the overall chip flow angle (Figure 2.2). Based on this assumption, they developed six different mathematical expressions by classifying the cutting patterns.

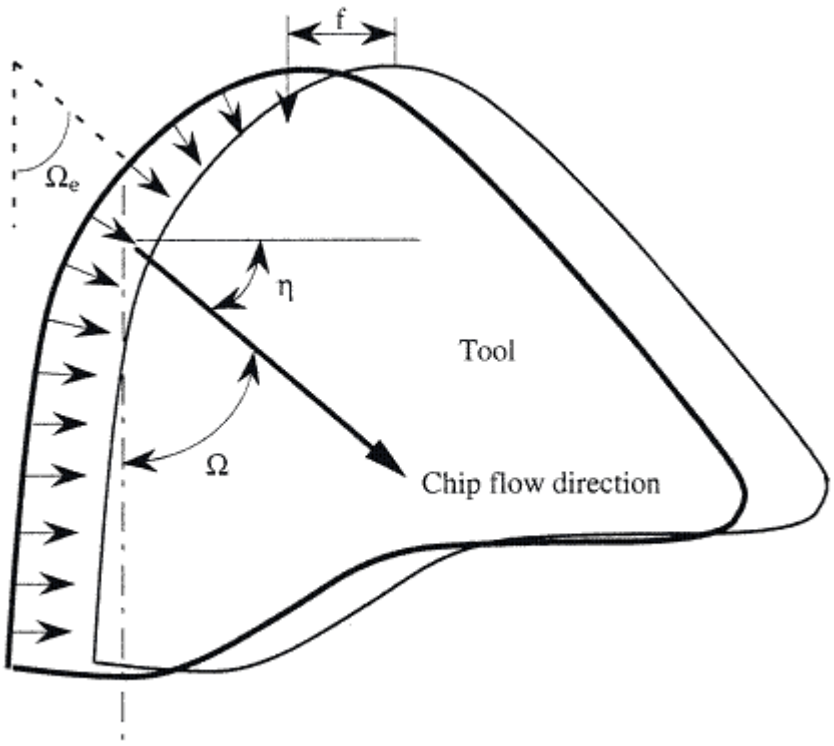

Figure 2.2: Chip flow model by Okushima and Minato [7]

Stabler [8] considered the chip flow on the primary and secondary cutting edges separately. He made the geometrical analysis of a cutting tool edge and proposed that the chip flow angle is equal to the inclination angle of the cutting edge. Later, he modified his model and introduced a constant of proportionality K_m which varied

between 0.9 to1.0 depending on materials and cutting conditions [9].

Nakayama [10] and Nakayama et al. [11] developed a mathematical expression to determine the chip geometry. They assumed that if all conditions were kept unchanged during some period of cutting time, the chip-form had to be constant and the chip geometry was spiral plane tangential to tool rake face. They expressed the chip side-curl and up-curl with curvature radii separately, and determined the actual chip geometry by superposing them (Figure 2.3).

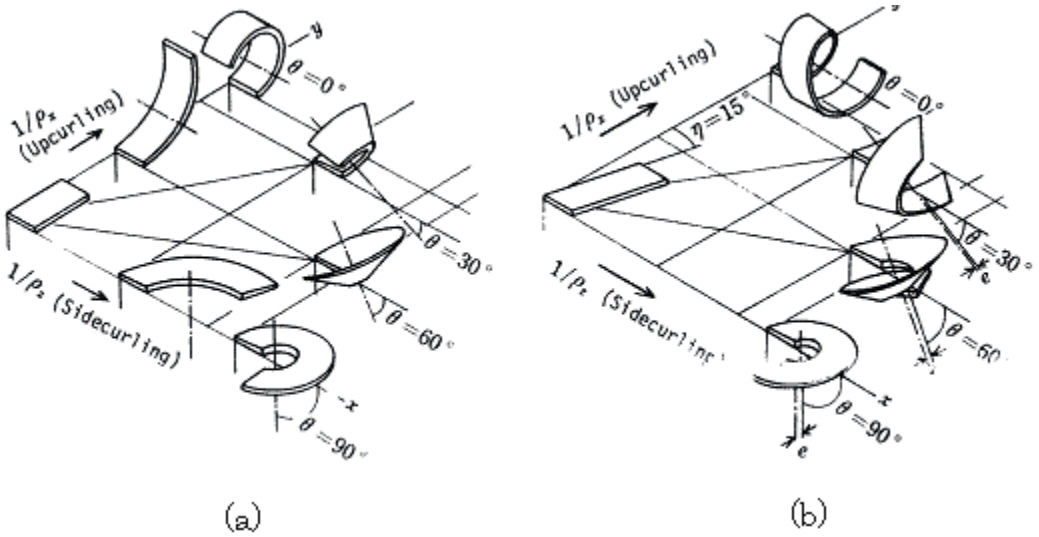

Figure 2.3: Variations of chip-forms by up-curling and side-curling when (a) $\eta = 0$ deg. and (b) $\eta = 15$ deg. [11]

Young et al. [12] treated the chip as a series of independent elements of infinitesimal width. They assumed that the thickness and orientation of the undeformed chip section corresponding to each chip element varied, and thus, the friction force component for each element changed in magnitude as well as direction. Then, these friction force components were summed up to find their resultant force and it was assumed that the direction of the resultant force coincided with the chip flow direction. However, this work is restricted to nose radius tools with zero rake and inclination angles.

Wang and Mathew [13] and Wang [14] extended the model by Young et al. [12] and predicted the chip flow angle from tool geometry and cutting conditions. They took into account the inclination angle effects by defining the equivalent cutting edge in the tool rake face which is taken to be at right angles to the chip flow direction. However, their model ignored the workpiece and tool material effects, thus, it gave the same value even though different material was used.

Arsecularatne et al. [15] proposed a model for chip flow direction with rake and inclination angles. Their model took care of the effects of nose radius and inclination angle separately, and predicted chip flow angle by superposition of these effects. The main weakness of this model is the consideration of work material properties through Stabler's empirical material constant. Also, variations of effective inclination and rake angles along the rounded cutting edge is not considered in the analysis. In their later work [16], they applied the modified tool angles based on Wang and Mathew's [13] model to include the variations of effective inclination and rake angles.

Ghosh and Jawahir [17] developed an online estimation method for chip flow predictions based on measured cutting forces and tool geometry (Figure 2.4). They considered the equivalent cutting edge, which was an imaginary line on the toolface, by joining the extremities of the feed and depth of cut and assumed that cutting force acted on this line. In a same manner as by Young et al. [12], they assumed colinearity between the friction forces on the rake face and the chip flow direction. Later, they developed a chip flow predictive model for machining with grooved tools as well [18]. They showed that the chip flow angle with grooved tools is larger than with flat-faced tools and formulated a semi-empirical relationship using the measured cutting force. Since this model incorporated the force ratio between the flat-face and grooved tools,

it can be applied to highly complex groove geometry. More details of this model will be introduced in Chapter 3.

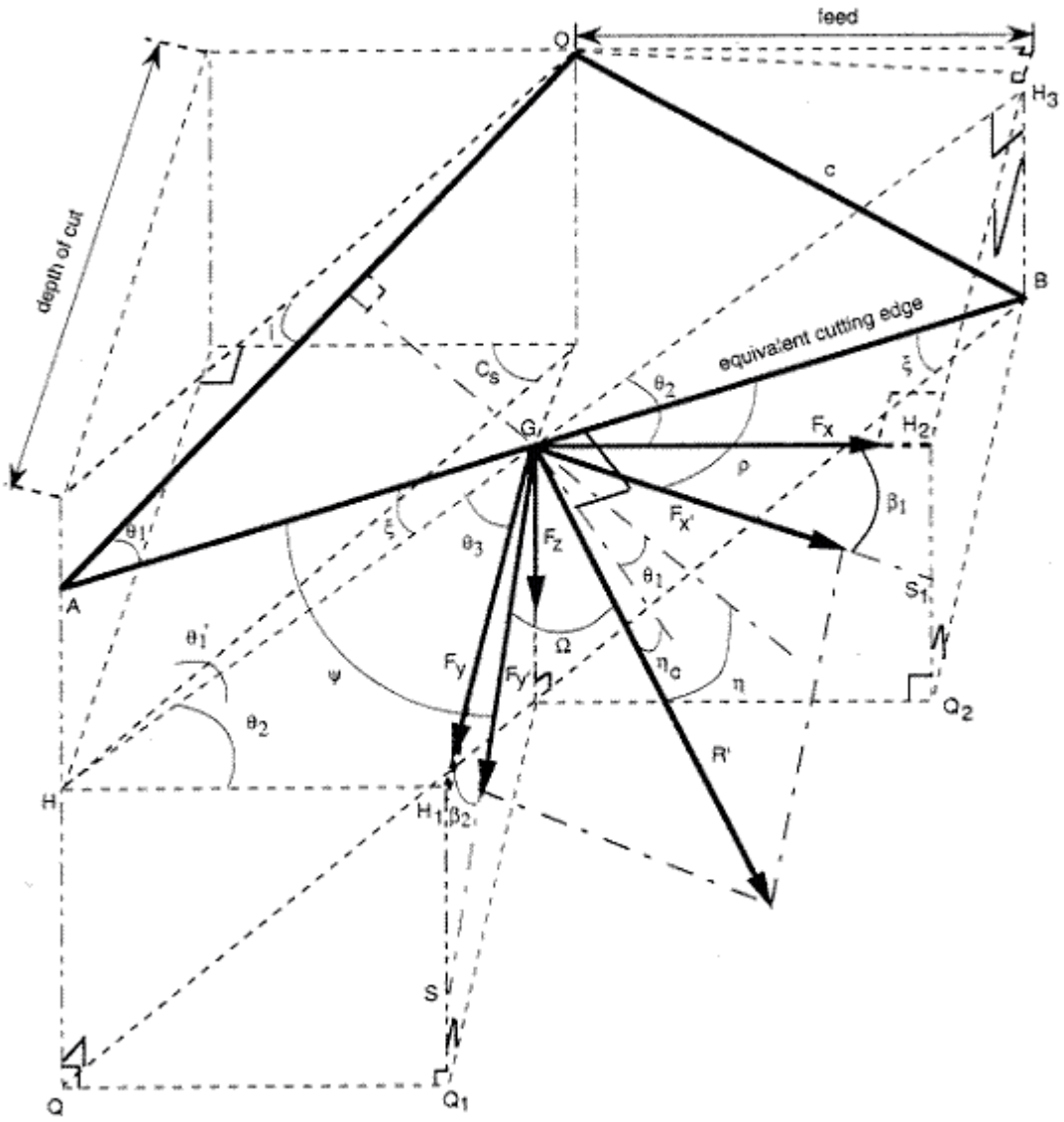

Figure 2.4: Model by Ghosh and Jawahir [17]

Redetzky [19-21] has done considerable amount of work on modeling of the cutting forces and chip flow with flat-faced tools. In a series of later work, Redetzky et al. [5, 22] developed a more accurate model by dividing the undeformed area of cut into infinitesimally small elements. The effective rake, inclination, side and end cutting

edge angles along the rounded cutting edge were considered. Also, the work material variations were taken into account in this model. More details of this work will be presented in Chapter 3.

Although the models shown above have contributed to the development of accurate chip side-flow prediction, all these methods can be applied only to straight turning. This is not practical since almost all products have some curvature or a profile. In contour turning operations, the cutting conditions and the geometry relationship between the tool and the workpiece will continuously change with changing workpiece profile. Thus, those effects have to be taken into account when the model is applied to contour turning operations.

2.2.2 Optimization of Machining Processes

Taylor first realized the importance of machining optimization [23]. He found that it was necessary to take into account not only the tooling cost, but also machining cost to achieve the optimum economical machining performance. It is because more often tools can be replaced, the higher cutting speed can be reached and therefore the larger amount of material can be removed. On the other hand, there are four opposing considerations which may cause a greater expense. These considerations are:

1. The time to replace the worn-out tool.
2. The time to grind the tool
3. The cost of dressing a tool
4. The cost of the tool steel which is lost every time a tool is redressed.

He took care of these problems and developed a definite mathematical form by using some assumptions on the different costs and derived an analytical expression. Finally, it was concluded that in order to achieve optimum economical machining

performance, a tool should be allowed to cut continuously without grinding at least seven times the time lost in changing the tool, plus the proper portion of the time for redressing, time for grinding and the time equivalent of the cost of the tool steel.

Since then, much work has been done on machining optimization. Gilbert [24, 25] took care of two criteria, maximum production rate and minimum cost, in order to determine the appropriate cutting speed for machining operations. Okushima and Hitomi [26] considered the maximizing profit rate in machining processes. In a similar manner, but more practical condition, Tee et al. [27] produced an analysis by employing a computer to search for the condition yielding maximum rate of profit.

Boothroyd and Rusek [28] tried to optimize cutting conditions by compromising between the conditions for minimum cost and minimum production time within a given time period. Their analysis also included the effect of worker incentive schemes and batch production on the machining conditions for maximum efficiency.

In most of the works above, the problems are simplified by considering only one variable, the cutting speed, in order to maximize the economical machining performance. However, not only the cutting speed, but also many other factors, for example, feed and depth of cut, are contributing to machining performance, such as tool-life, surface roughness, chip breakability, material removal rate and machining accuracy. Once these factors are taken into account in the optimization problem, the objective function will be highly complex with some equality or inequality equations and constraints. In this case, the problem cannot be solved properly or it takes too much time to find an optimal solution if a classical optimization method is used. It is useless if the method cannot reach optimal solution in practical time although it has

the capability to solve the problem. Then, the main focus of the optimization problem is not only solving the problem itself, but also how efficiently it can solve the problem. Many methods for optimization have been investigated and used in machining.

Ermer [29] analyzed a nonlinear objective function with inequality constraints to determine the optimal machining conditions by geometric programming. This optimization method is effective when the objective function is of more than second degree and the constraints are nonlinear comparing to conventional indirect method such as Lagrange's.

Agapiou [30] focused on a combination of the minimum production cost and minimum production time requirements as an objective function to determine optimal machining conditions. The two criteria of production cost and production time were used through their weighted factors while a constant multiplier was used to normalize the objective function. The power limitation, surface roughness limitations, temperature constraint, and limitation of the maximum cutting force were considered as constraints by expressing them as power functions of the process parameters. The Nelder-Mead simplex method was used in this optimization problem.

Da et al. [31, 32] developed a hybrid process model for finish turning operations by including machining performance parameters such as surface roughness, chip breakability, cutting force, tool-life and material removal rate. They treated three independent variables, cutting speed, feed, and depth of cut, to maximize the machining performance based on the weighed factors which was determined by the operator. To solve this problem, a sequential quadratic programming algorithm was used.

Chen and Su [33] presented an optimization method for cutting conditions in multi-pass operations in continuous profile machining in order to minimize the unit production cost. Actual machining time, machine idling cost due to loading and unloading operations and idling tool motion, the tool replacement cost and the tool cost were considered. This objective function was a quite complex nonlinear equation with 7 variables and multiple constraints were included such as the limitation of cutting speed, feed, surface roughness, cutting force, power consumption, and tool-life. Simulated Annealing (SA) method was used to solve this optimization problem.

Wang et al. [3] extended their previous work [31, 32] to multi-pass turning operations. Since the total depth of cut through the passes was fixed, feasible region of this problem became very tight comparing to single pass problems. Therefore, they used Genetic Algorithm (GA) to solve this problem. Wang [34] also developed the web-based user interface for this optimization problem so that researchers or process planners could determine optimum cutting condition with ease.

Saravanan et al. [35] showed an optimization method for cutting conditions in continuous profile machining in order to minimize the production cost. For the optimization method, they used GA and SA and compared the results. According to their results of test example, GA reached a relatively good fitness from the initial stage of the iteration but did not improve much at the end of iterations while SA produced the minimum fitness and continuously improved with increasing iteration. As a result, SA gave better results than GA at the end of iteration point, which was small production cost.

Unlike linear programming problems, nonlinear programming problems are quite difficult to reach global optimal points due to the complicated objective functions, constraints and the existence of local optimal points. Many methods to achieve global optimum in practical time are still under investigation, and even prevailing methods such as Genetic Algorithm (GA) and Simulated Annealing (SA) have disadvantages as well as advantages.

As shown above, most optimization problems in machining are nonlinear problems and these are quite complicated. GA and SA are frequently used in these problems because of their capability to solve the problem, wide range of application potential and reliability. The main advantage of GA is that it is quite fast to find a relatively good solution no matter how complicated the problem is. On the other hand, SA needs more time to find direction to reach global optimal, but is capable of reaching there faster than GA. In this thesis work, SA is used and the details of optimization by SA will be presented in Chapter 4.

CHAPTER 3

DEVELOPMENT OF A CHIP SIDE-FLOW MODEL FOR CONTOUR TURNING OPERATIONS WITH GROOVED TOOLS

3.1 Introduction

With the growing dependence of machining processes on computer aided manufacturing (CIM) environments, the process planning activity has become an important process for manufacturers. The process plan is not randomly selected, but has to be based on the profound experience or simulation results. However, the experience cannot be obtained or found easily. On the other hand, anyone can have simulation results once a computer based predictive model is developed. Predictive models in machining processes help to determine the parameters and factors which affect the machining performance, such as cutting conditions, cutting tool, and the work material. It is possible to develop a predictive model on the computer program base, and this program can, not only predict the process, but also add more advantages. Since all information needed for input and output is stored as data in a computer, the application can become wide, for example, integration into the optimization program to obtain the best machining performance, integration into CNC machining center to automatically input the optimized data, and visualization and the simulation of results as movie animation.

This chapter presents a new method to apply the extended chip flow predictive model in contour turning operations. The model by Redetzky et al. [5] dealing with

flat-faced tool and the model by Ghosh et al. [18] dealing with grooved tool will be explained first. Then, how to treat the changing parameters of cutting conditions and tool geometry under contour turning operations will be explained. Details of the computer program, mathematical form of workpiece profile generator and effective parameters, as well as the overall flowchart, showing the prediction of the chip side-flow angle in flat-faced and grooved tools will also be presented in this chapter.

3.2 Chip Flow Predictive Model for Flat-faced Tools Based on Redetzky et al. [5]

Redetzky et al. [5] performed a considerable amount of work on modeling the cutting forces and chip flow in machining with flat-faced tool. Their predictive model is based on the integration of two distinct sub-models:

1. The geometric model which defines the complete geometry of the machining operations based on cutting conditions (cutting speed, feed and depth of cut) and tool geometry (cutting edge angle, rake angle, inclination angle and the nose radius)
2. The force model, which establishes the force coefficients for a work material - cutting tool combinations as a function of cutting conditions and tool geometry, based on limited single edge cutting experiments.

These two sub-models are finally integrated to predict the cutting forces for machining operations with a nose radius tool. The calculated cutting forces are also used in predicting the chip side-flow angle based on the effective direction of the resultant friction force on the rake face of the cutting tool. The effective rake, inclination, side- and end-cutting edge angles along the rounded cutting edge are

considered. Also, the work material variations are taken into account in this model.

3.2.1 The Geometric Model and the Force Model

The geometric model is developed based on the assumption that the active cutting edge is treated as a series of small single cutting edges. Therefore, the geometric model is based on the division of the cut area *A* as a whole into regions, which are further subdivided into small elemental cut areas *dA* (Figure.3.1). Later, when integrated with the force model, the elemental cut areas develop force elements at each elemental width *db* and at each elemental area of cut *dA* of the active cutting edge. The cut areas as well as other geometric parameters are located within the reference plane P_r (Figure.3.2). Since the shape of the cutting area is different according to the cutting conditions and tool geometry, it is classified on the basis of two parameters, depth of cut and feed-nose radius ratio.

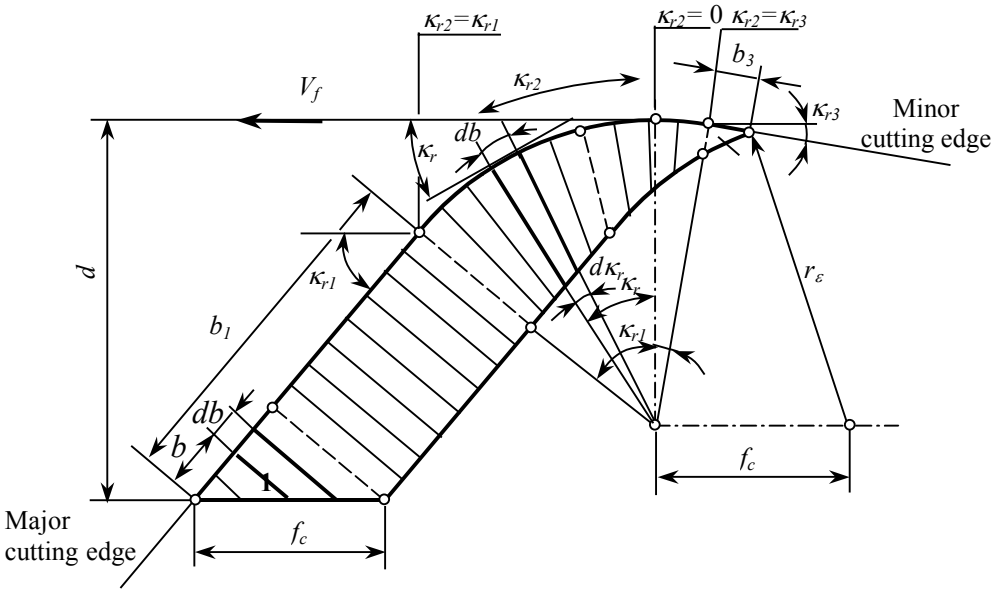

Figure 3.1: The undeformed cut area and the associated geometric parameters [5]

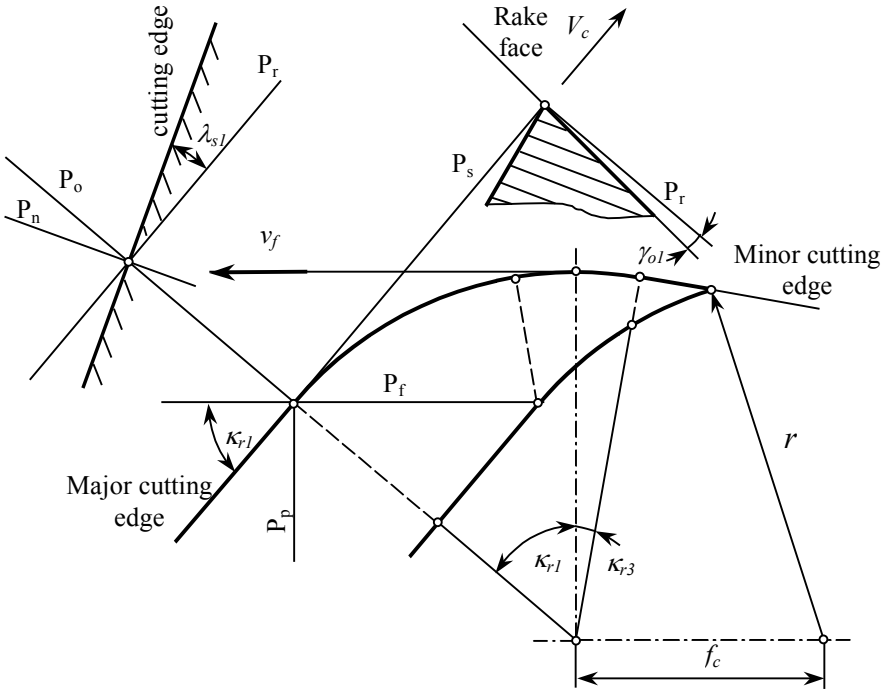

Figure 3.2: Planes for measurement of tool angles [5]

The fundamental assumption of the force model is that the force behavior in single edge machining (with a width of cut *b*) can be applied to each elemental width of cut (*db*) in machining with nose radius tools. The basic purpose of the force model is the establishment of force coefficients and correction factors for cutting speed and rake angle effects for each work material- cutting tool combination.

The primary (cutting tool-oriented) components of the resultant cutting force are calculated with work material-cutting tool combination coefficients in each element first. Then, the conversion of the local primary force elements into the local secondary force (in x-y-z directions) elements is conducted by means of the local cutting edge angle along the active cutting edge.

3.2.2 The Model for Predicting Chip Flow

Figure 3.3 shows the basic orientation of the force components and the method for converting them into force components on the rake face. The basic principle of colinearity of the rake face forces and the chip flow is used in the prediction of the chip side-flow angle. It is important to note the difference between the chip flow angles η and η_c. The angle η is measured in the reference plane P_r, whereas η_c is measured on the rake face. The parameters η_c and F are defined within the rake face from their components in planes P_s and P_n. They result from the partial "area of cut " forces F_{Aj} (j = *x, y, z*).

At first, the projection of F_{Ax} and F_{Ay} into the directions of planes P_n and P_s results in the force components F_{sr} and F_{nr} as follows:

$$F_{sr} = -F_{Ax}\cos\kappa_{r1} + F_{Ay}\sin\kappa_{r1} \tag{3.1}$$

$$F_{nr} = F_{Ax}\sin\kappa_{r1} + F_{Ay}\cos\kappa_{r1} \tag{3.2}$$

where κ_{r1} is the cutting edge angle.

Then, projecting these components and the additional component F_{Az} into the directions of planes P_s and P_n within the rake face, we get (Figure.3.3)

$$F_s = F_{sr}\cos\lambda_{s1} + F_{Az}\sin\lambda_{s1} \tag{3.3}$$

$$F_n = F_{nr}\cos\gamma_{s1} + (F_{Az}\cos\lambda_{s1} - F_{sr}\sin\lambda_{s1})\sin\gamma_{n1} \tag{3.4}$$

Thus, we get the chip flow force:

$$F = (F_s^2 + F_n^2)^{1/2} \tag{3.5}$$

and the resultant chip flow angle on the rake face

$$\eta_c = \tan^{-1}(F_s / F_n) \tag{3.6}$$

We now transform η_c into η (in the reference plane P_r) by using:

$$\eta = \tan^{-1}\left[\left(\tan\eta_c \cos\lambda_{s1} - \sin\gamma_{s1} \sin\lambda_{s1}\right)/\cos\lambda_{s1}\right] \qquad (3.7)$$

Thus, the chip flow angle η is predicted by using the predicted cutting force and the tool geometry.

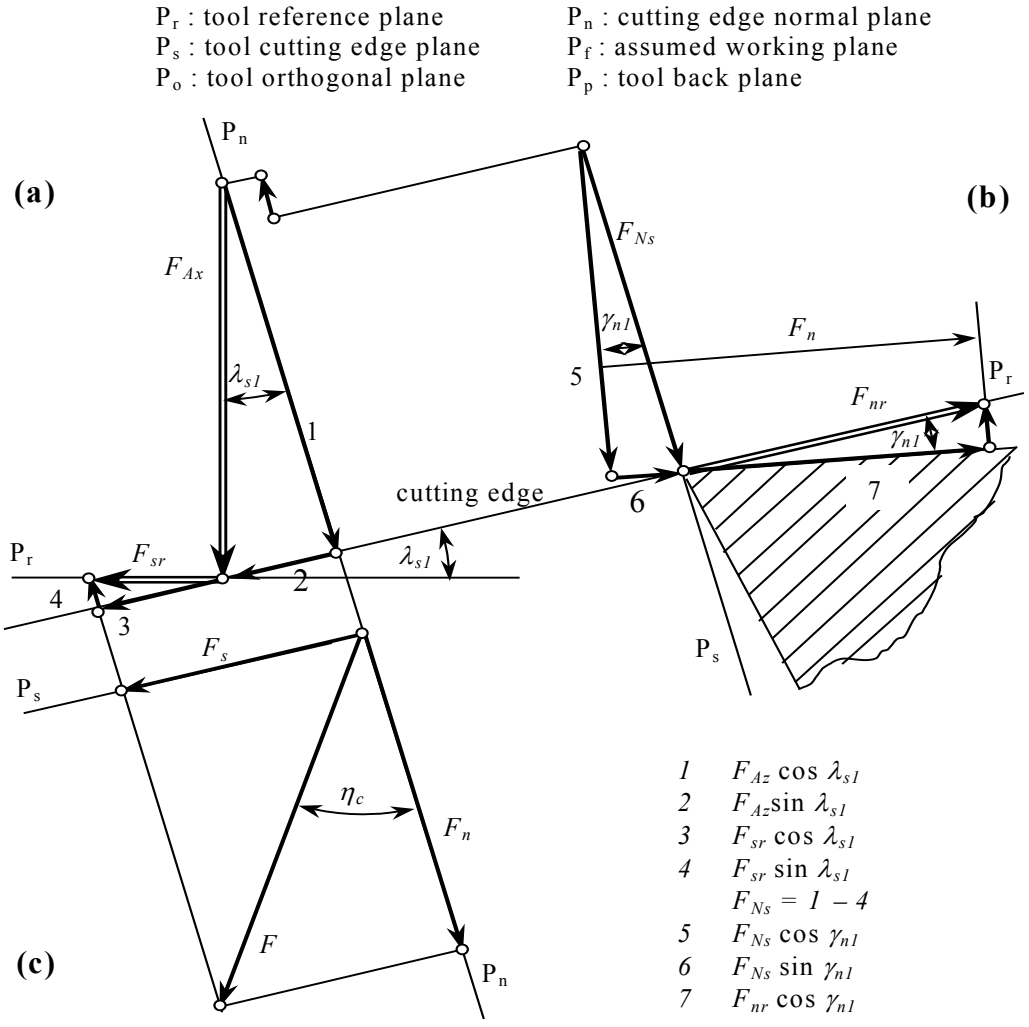

Figure 3.3: Derivation of the chip flow angle and chip flow force resulting from the partial secondary forces F_{Ax}, F_{Ay} and F_{Az}. [5]
(a) within plane P_s; (b) within Plane P_n; (c) on the rake face

3.3 Chip Flow Predictive Model for Grooved Tools Based on Ghosh et al. [18]

Ghosh et al. [18] proposed a new methodology for estimating the chip side-flow direction in grooved tools based on measured cutting forces in machining with flat-faced and grooved tools. A semi-empirical equation for chip side-flow has been formulated based on the estimated chip-flow direction in flat-faced tools and the cutting force ratio between flat-faced and grooved tools along with the effective tool geometry and cutting parameters.

The chip side-flow angles in grooved tools are higher than those in flat-faced tools for the same tool geometry and the cutting conditions. This is explained through a schematic diagram. Figures 3.4 (a) and (b) show diagrams of chip flow with an obstruction-type chip breaker for small and large depths of cut. For small depths of cut, the chip, after hitting the bump, would be deflected sideways, towards the main cutting edge, and this would result in a higher value of the chip side-flow angle as compared to a flat-faced tool. At higher depths of cut, the chip side-flow is only partially obstructed by the bump and the chip develops a mixed mode of side-curl and up-curl, with up-curl as the dominating factor.

This increase can be accounted for by two factors: (i) the chip-groove effect, and (ii) the effective inclination and the rake angle effect. For the chip-groove effects, they take into account the force ratio of the radial force F_x and the feed force F_y as an indicator $\left(FR = {F_y}/{F_x} \right)$. And, for changing depth of cut, the ratio of the FR for flat-faced tool and for the grooved tool $\left(K_1 = {FR_{flat}}/{FR_{groove}} \right)$ is considered significant, as this would indicate the change in the force ratio due to varying

utilization of the groove for different cutting conditions.

The second factor affecting chip flow in grooved tool is the effective rake and inclination angles. Since there are numerous commercial grooved tools and all of them have very complex shape, the effective tool geometry factor is considered as constant for each grooved tool. The constant K_2 is found to vary between 4.5 and 5.5.

Thus, they expressed the equation for chip side-flow angle (η_s) in grooved tools

$$\eta_s = \eta + \left[\frac{\left(F_y / F_x \right)_{flat}}{\left(F_y / F_x \right)_{groove}} \right] \left[K_2 / d \right] \tag{3.8}$$

where η_s and η denote the chip flow angles in grooved and flat-faced tools, respectively.

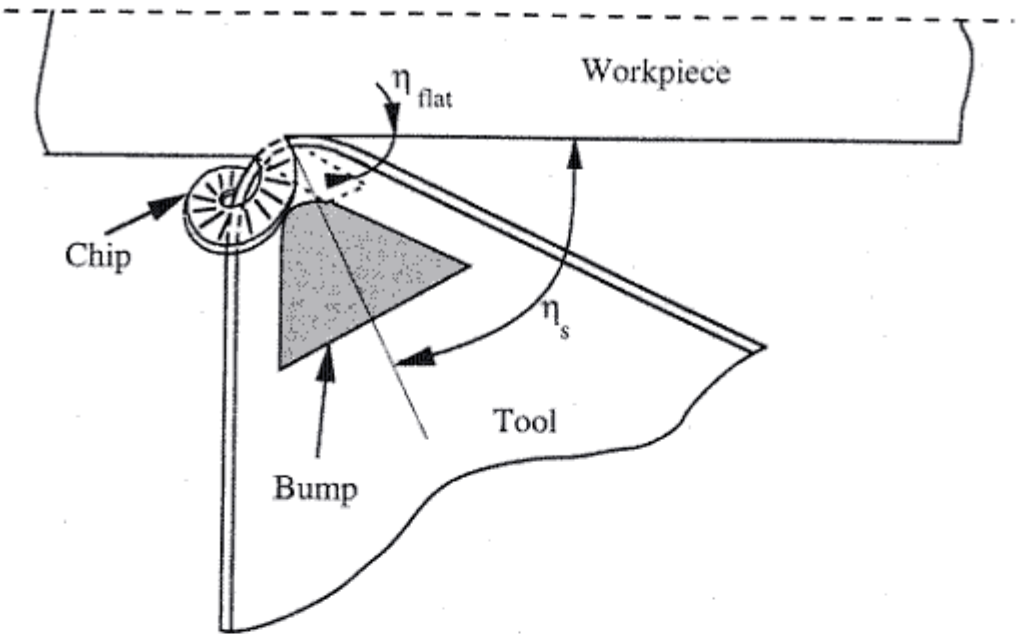

(a)

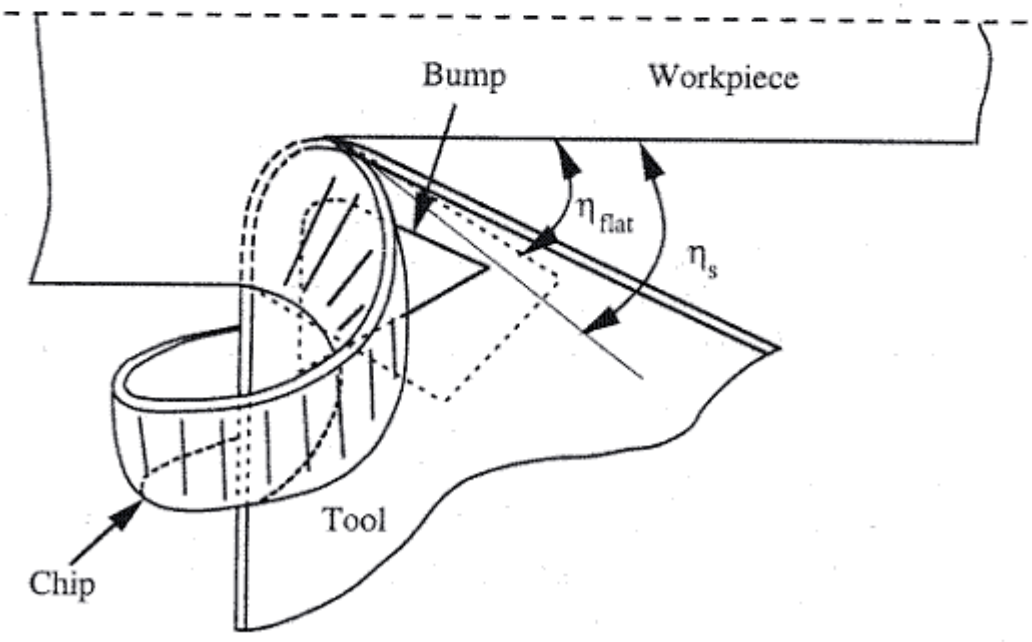

(b)

Figure 3.4: Schematic diagram of chip flow for changes in the depth of cut [18]
(a) small depth of cut (b) large depth of cut

3.4 Application to Contour Turning Operations

3.4.1 Background of the Predictive Model for Contour Turning

Due to the complex workpiece geometry in contour turning, most of the current theories are for straight bar turning. Changing workpiece profile causes varying effective cutting conditions, such as effective depth of cut and axial feed, and effective tool geometry, such as effective side-cutting edge angle and end-cutting edge angle (Figure. 3.5) [36].

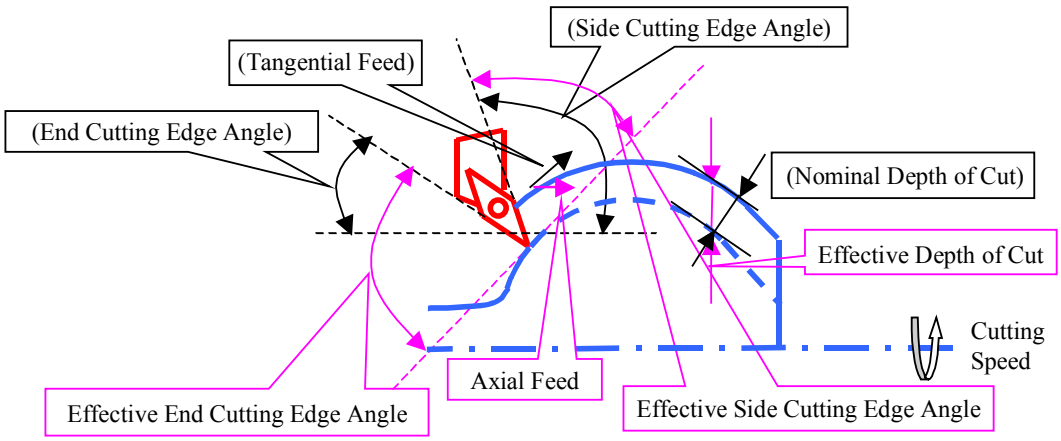

Figure 3.5: Variations of effective depth of cut, effective side-cutting edge angle and effective end-cutting edge angle along the length of contour profile [36]

Balaji and Jawahir [37] conducted an experimental study of contour turning of aluminum alloys using PCD flat-faced and diamond coated grooved tools. This work focuses on attaining the best machining performance under dry conditions. In order to study the effects of contour geometry on machining performance in aluminum machining, a contour shape with sudden changes from convex to concave and concave to convex geometries was specially designed by the authors to include various combinations of features (Figure.3.6).

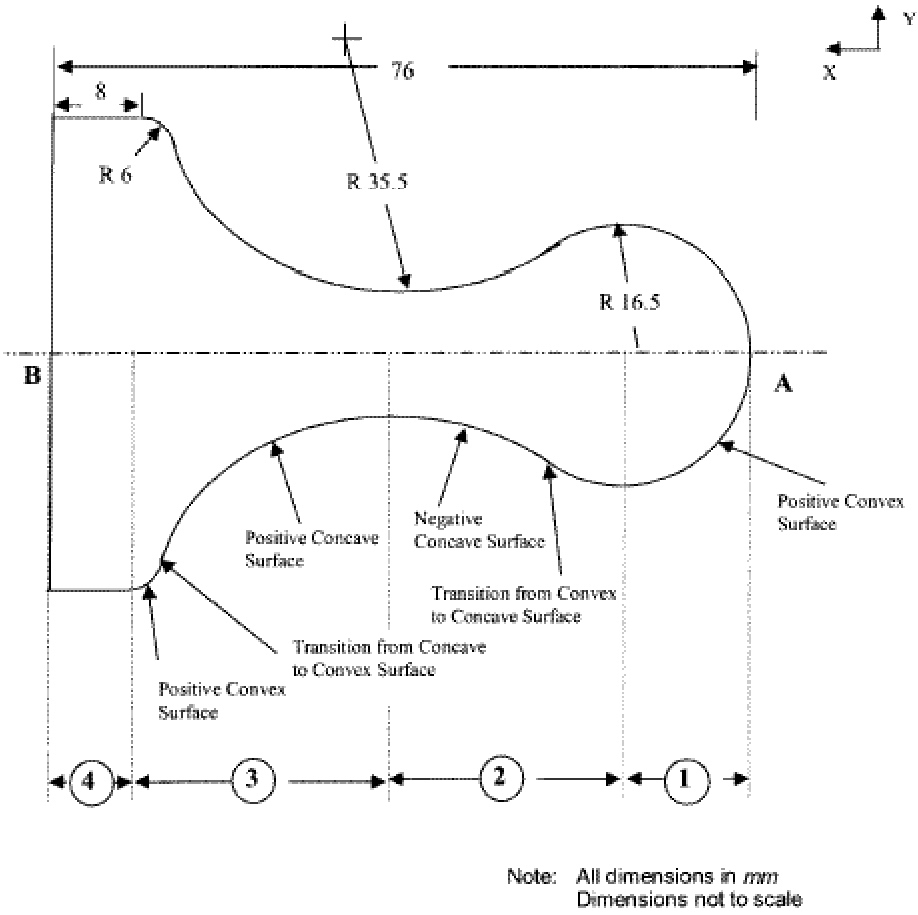

Figure 3.6: The specification of the workpiece used by Balaji and Jawahir [37]

The predictive model for chip side-flow angle used here was the model by Redetzky et al. [5], and the prediction results were successfully obtained (Figure 3.7). However, the cutting force used as an input for the chip flow model was experimentally measured in this study. Therefore, once workpiece geometry is changed, it requires experiments all over again to obtain cutting force data. To overcome this problem, Chen [36] extended the force and chip flow predictive model by Redetzky et al. [5] to specific contour turning profile for the cast aluminum wheel, by using the calculated effective depth of cut, effective side-cutting edge angle, and effective end-cutting edge angle as input.

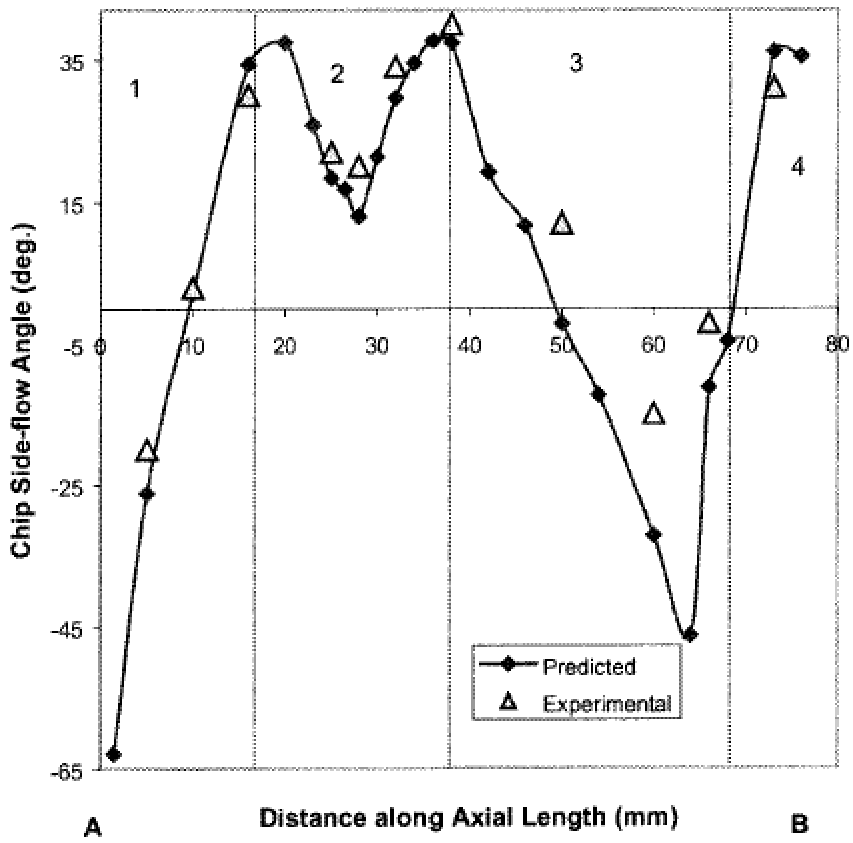

Figure 3.7: Variation of predicted and experimentally measured chip side-flow angle during roughing of 2011-T3 aluminum alloy with PCD flat-faced tools (V =394 m/min, f = 0.3 mm/rev, nominal depth of cut =2.5 mm) [37]

3.4.2 Contour Workpiece Determination

If the size, application and design of the products are different, the profile of the workpiece will be totally different and the number of contour profile used in practical world is countless. Therefore, to extend the chip flow predictive program for a generalized contour profile, the first step of calculation for the cutting force and chip side-flow angle in contour turning is to determine the workpiece geometry profile.

The geometry can be classified by three typical shapes, namely, convex, concave and the straight shape. Any given contour profile can be divided into small segments, and expressed by combinations of their shapes. Only two or three parameters are needed to determine each segment shape, namely, start angle, end angle and radius in

concave/convex shape, or slope angle and length in straight shape. Thus, once mathematical form is developed for these three shapes, any workpiece geometry can be drawn automatically, and can be stored as a data. Then, effective cutting conditions and tool geometry can be calculated easily. It has to be noted that the boundary area between each segment has to be taken care of in particular because the geometry has a sudden change in this region. Therefore, the same number of data points is calculated in each segment and additionally in the boundary area (Figure 3.8).

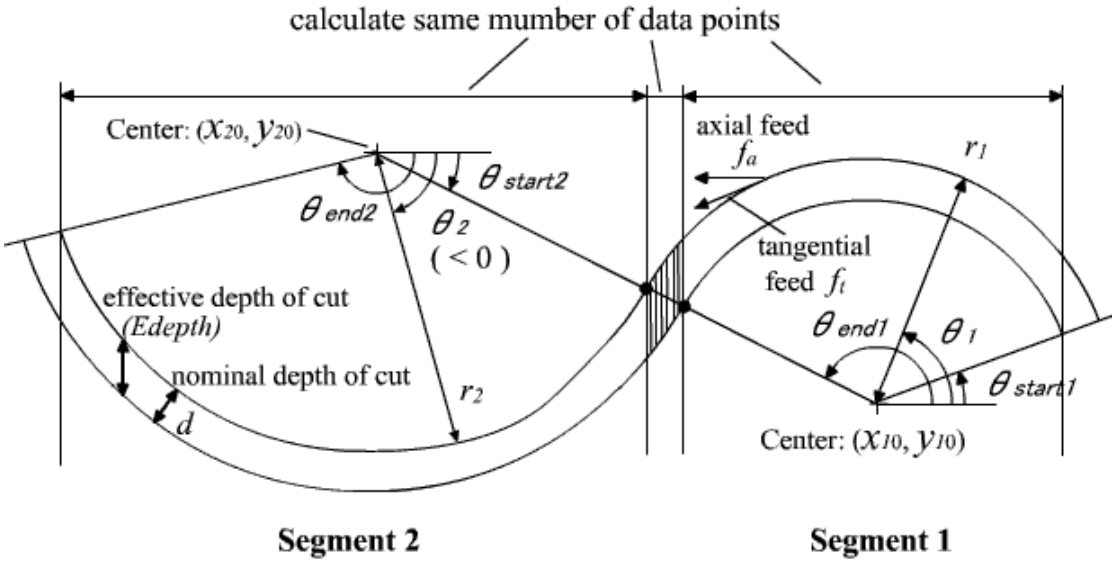

Figure 3.8: Workpiece geometry effects

3.4.3 Mathematical Form of Effective Cutting Conditions and Tool Geometry

Once the workpiece geometrical data is obtained as shown in the previous section, it is easy to calculate effective depth of cut, effective side- and end-cutting edge angles and axial feed. However, the equations to calculate these parameters are different depending on the segment shapes, which are concave, convex and straight line. The equations to calculate the effective cutting conditions and tool geometry in each shape are shown below.

(i) Convex shape ($\theta_1 > 0$)

Effective depth of cut (Edepth):

$$Edepth = \sqrt{r_1^2 - (x_1 - x_{10})^2} - \sqrt{(r_1 - d)^2 - (x_1 - x_{10})^2} \quad (3.9)$$

Axial feed: $f_a = f_t \times \sin\theta_1$ (3.10)

Effective side-cutting edge angle: $ECs = \theta_1 + Cs - \pi/2$ (3.11)

Effective end-cutting edge angle: $ECe = Ce - \theta_1 + \pi/2$ (3.12)

(ii) Convex shape ($\theta_2 < 0$)

Effective depth of cut (Edepth):

$$Edepth = \sqrt{(r_2 + d)^2 - (x_2 - x_{20})^2} - \sqrt{r_2^2 - (x_2 - x_{20})^2} \quad (3.13)$$

Axial feed: $f_a = f_t \times \sin(-\theta_2)$ (3.14)

Effective side-cutting edge angle: $ECs = \theta_2 + Cs + \pi/2$ (3.15)

Effective end-cutting edge angle: $ECe = Ce - \theta_2 - \pi/2$ (3.16)

(iii) Straight shape (θ_3 = slope angle)

Effective depth of cut: $Edepth = d/\cos\theta_3$ (3.17)

Axial feed: $f_a = f_t \times \cos\theta_3$ (3.18)

Effective side-cutting edge angle: $ECs = Cs - \theta_3$ (3.19)

Effective end-cutting edge angle: $ECe = Ce + \theta_3$ (3.20)

Figure 3.9 shows the relation between the workpiece shape and effective side- and end-cutting edge angles.

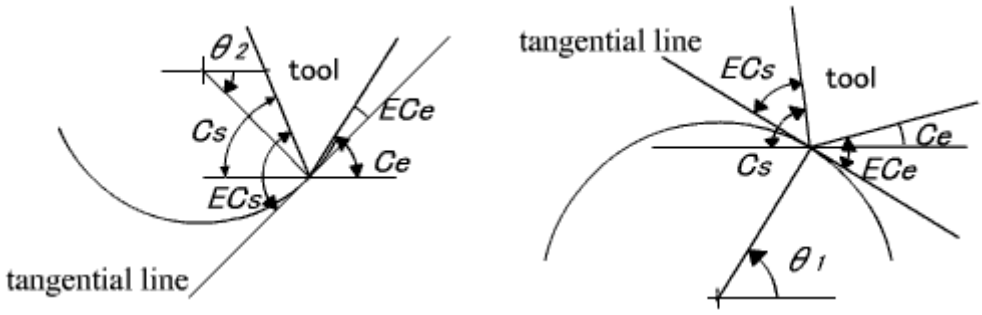

Figure 3.9: Effective side- and end-cutting edge angles in convex and concave shape

3.4.4 Extended Predictive Model for Chip Side-flow in Contour Turning Operations with Grooved Tools

In order to extend the chip side-flow predictive model for flat-faced tools by Redetzky et al. [5], and for grooved tools by Ghosh et al. [18] to contour turning, the first step is to input the workpiece geometry data. By allowing the geometry shapes in each segment, geometry data can be stored in the program. From this data, the effective cutting conditions, such as effective depth of cut, axial feed, and effective tool geometry, such as side-cutting edge angle, end-cutting edge angle, can be calculated. Then, these parameters are used as input for the program to apply the model by Redetzky et al. [5], and the chip side-flow angle with flat-faced tool can be obtained. For a grooved tool, the model by Ghosh et al. [18] can be applied. The obtained cutting forces and chip side-flow angle data for flat-faced tool and cutting forces data for grooved tool from database are used as input to calculate the chip side-flow angle for grooved tools. Since it is quite difficult to predict cutting forces in grooved tools due to the complex and various groove geometry in the commercial tool inserts, a numerical method, such as cubic spline interpolation from database, can be used to obtain the radial and feed forces functions. Figure 3.10 shows the overall flowchart of the procedure.

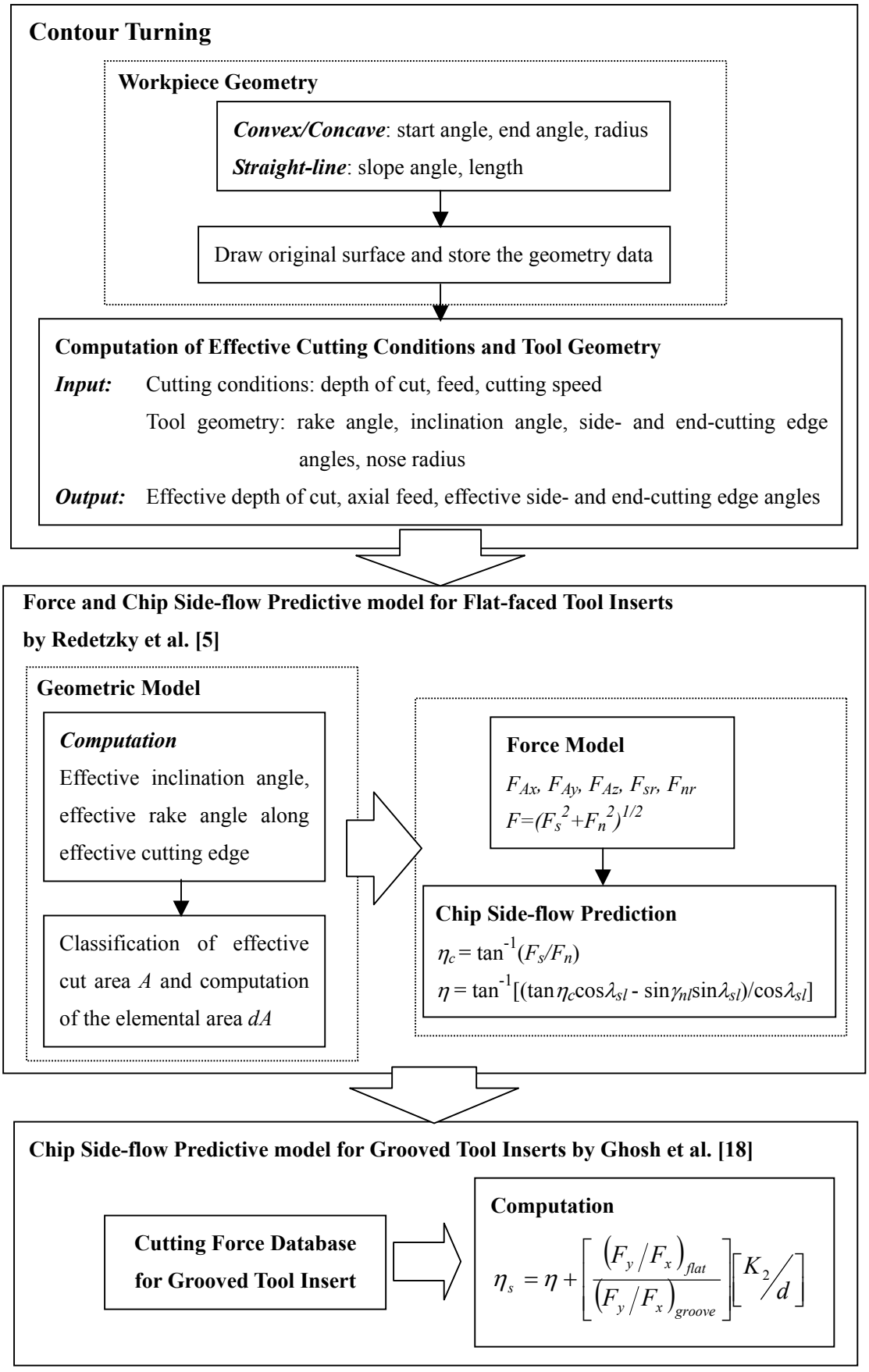

Figure 3.10: Flowchart for predicting chip side-flow in contour turning operations

3.5 Program Results and Validation

Once the databases for the radial and feed forces with grooved tool are created, the predictive program can be applied to contour turning operations. The details of the experimental conditions to create the databases and their results are shown in Chapter 4.

Specific cutting tool, VBMT 332-UM, and work material, AISI 1045 steel are used and a sample workpiece with various geometric shapes (Figure 3.11) is selected as the case study. In order to comprehensively study the effects of contour geometry, the sample workpiece includes convex, concave, and the straight line with positive, negative, and zero slope angles and it is divided by 8 segments according to the geometric shapes as shown in Figure 3.11.

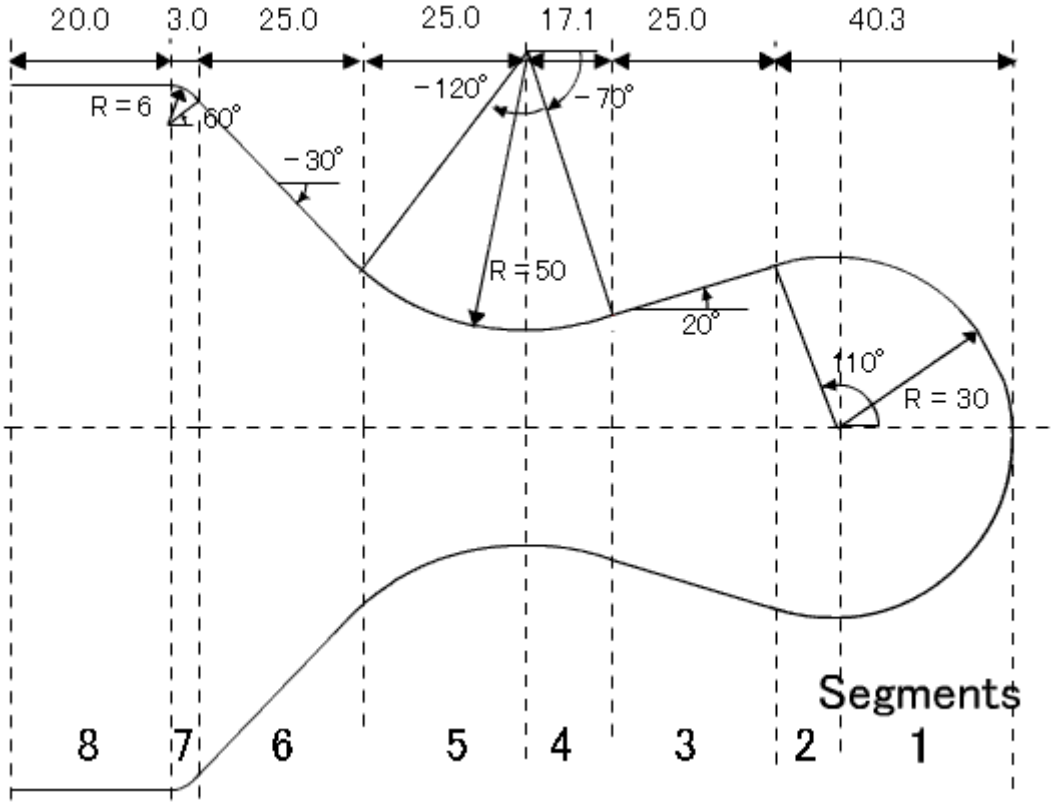

Figure 3.11: The profile of sample workpiece

The program was run under various cutting conditions in finish turning range. Cutting speed was kept constant at 250 m/min. It must be mentioned that the chip side-flow predictions and measurements are referenced with respect to the horizontal X-axis. Figure 3.12 shows the calculated effective cutting conditions and the tool geometry according to the workpiece profile. These parameters were then used as input for a hybrid predictive model to calculate the chip side-flow angles. Figure 3.13 and 3.14 shows the program results for chip side-flow angle prediction for various depths of cut and feeds, respectively. Since this research focuses on the finish turning operations, small depths of cut and feeds, less than nose radius and less than 0.16 mm/rev, were selected.

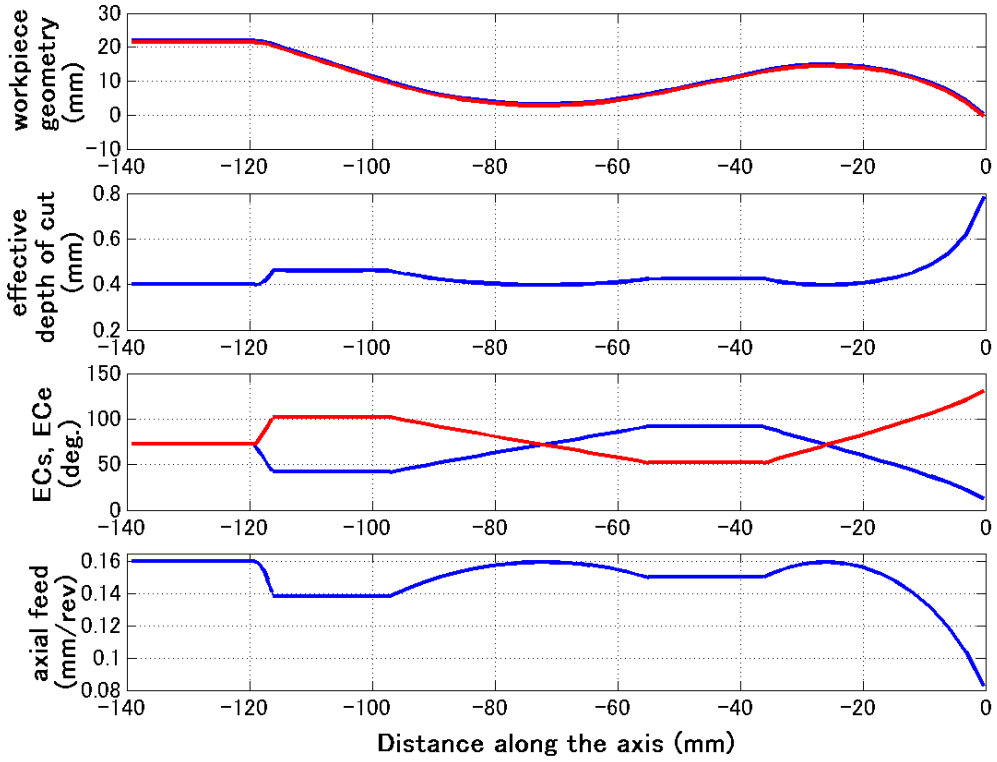

Figure 3.12: Effective parameters according to the workpiece geometry (nominal depth of cut: 0.4 mm, feed: 0.16 mm/rev)

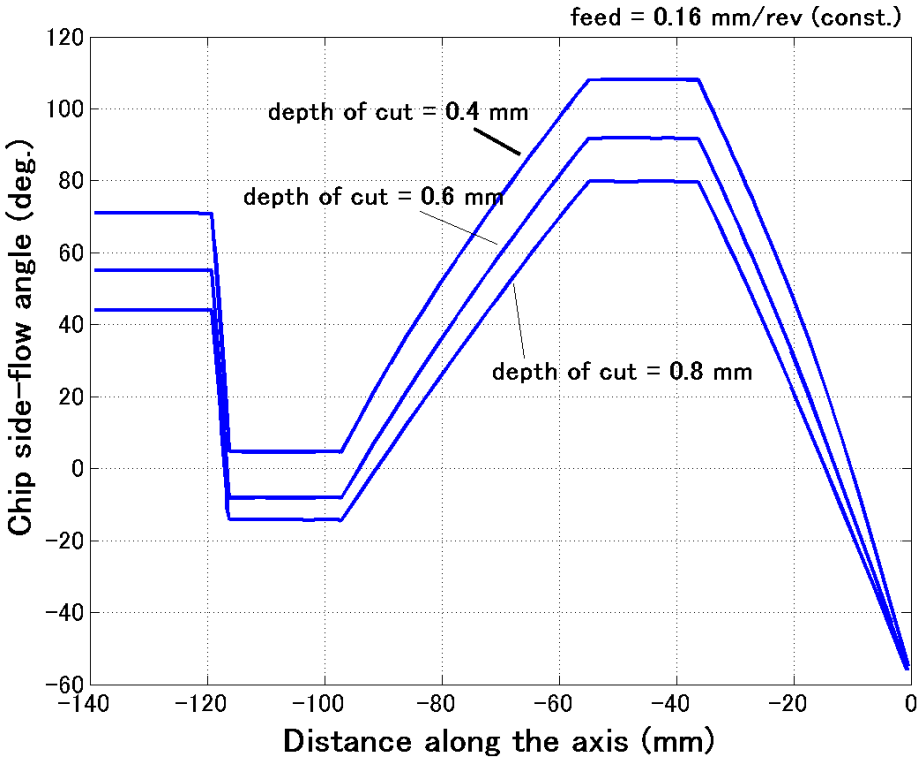

Figure 3.13: Variation of predicted chip side-flow angle for different depths of cut (constant feed: 0.16 mm/rev)

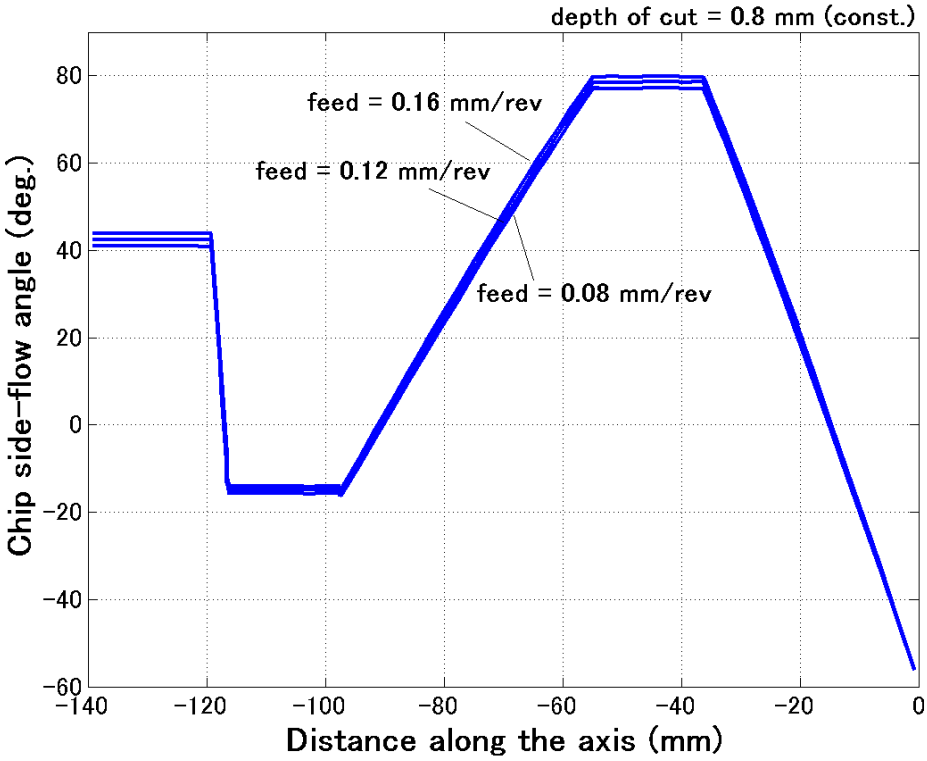

Figure. 3.14: Variation of predicted chip side-flow angle for different feeds (constant depth of cut: 0.8 mm)

As shown in Figure 3.13, and 3.14, chip flow direction is changing rapidly in convex and concave parts, but not in straight parts. This is because the effective cutting conditions and tool geometry are changing rapidly in curved region. The effective depths of cut are larger than nominal depth of cut in all segments, and the maximum effective depth of cut is twice as much as the nominal depth of cut (Figure 3.12). On the contrary, the axial feeds are smaller than tangential feed, and minimum axial feed is half of tangential feed. Also, the range of feeds in finish turning operations is quite small. Thus, the effects of depth of cut play more roll on the chip side-flow changes than the effects of feed in finish turning operations (Figure 3.13 and 3.14).

In Segments 1 and 6, the chip flow angle is negative. This is due to the high gradient of the workpiece profile with negative slope, and thus the axial feed becomes very small while effective depth of cut becomes very large in these regions. Also, the small side-cutting edge angle contributes to negative chip flow angles. On the other hand, the values for the chip side-flow angle in Segment 3 are very high. This is due to the workpiece profile with positive slope and thus the side-cutting edge angle becomes very large.

Experimental validation was carried out with nominal depth of cut 0.4 mm, tangential feed 0.l6 mm/rev to compare with the program result. The chip side-flow angles were measured from snap shots taken from the filming by high speed filming (KODAK motion analyzer). Figure 3.15 shows the method to measure the chip side-flow angle from the reference plane. Figure 3.16 shows the comparison between the predicted and experimentally measured chip side-flow angle. The trend of the chip side-flow is quite similar and the maximum variation between the predicted values and experimental values is less than 15 %.

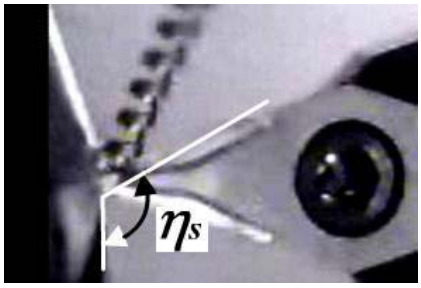

Figure 3.15: Measurement of chip side-flow angle

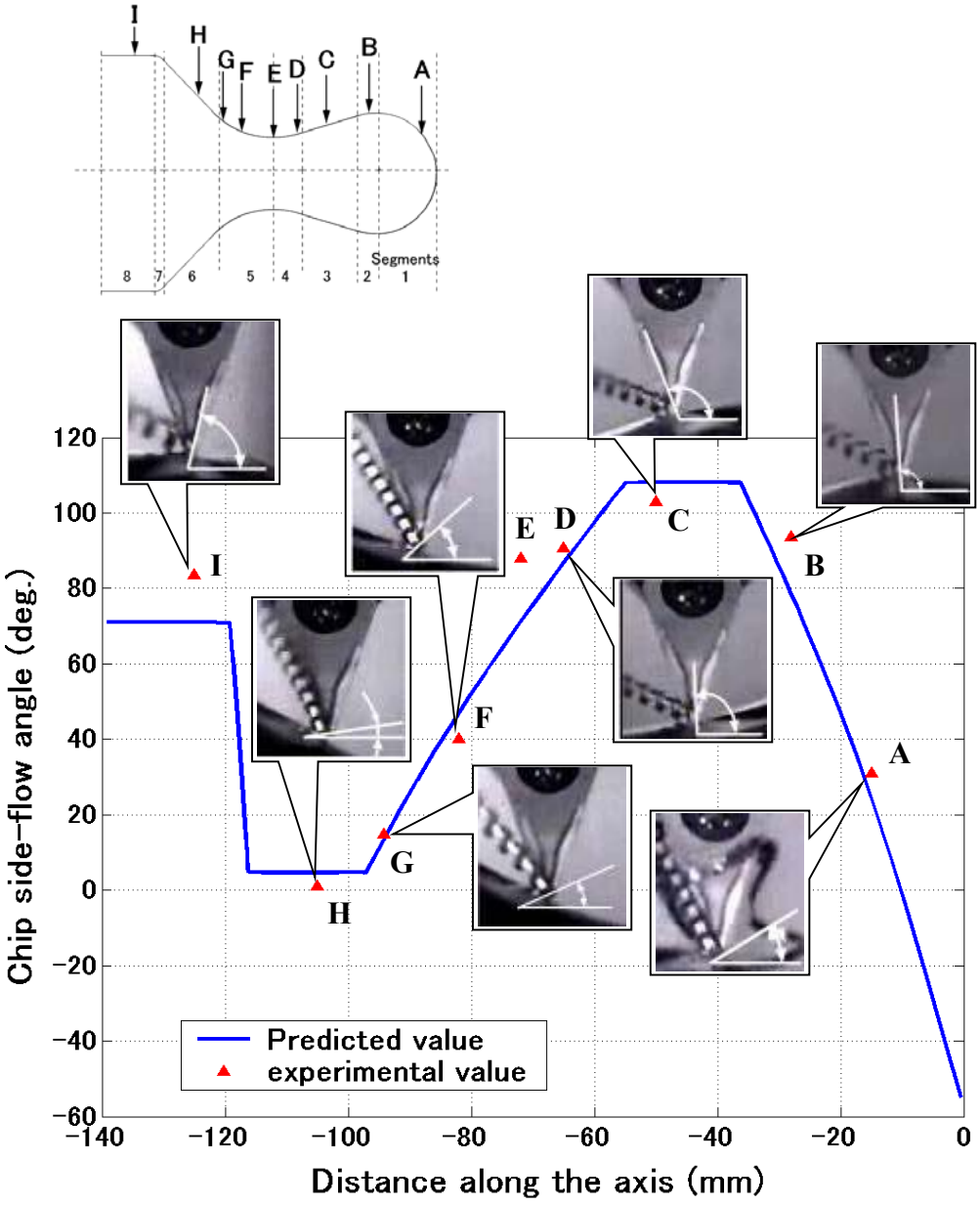

Figure 3.16: Variation of predicted and experimentally measured chip side-flow angle along the contour profile (nominal depth of cut = 0.4 mm, tangential feed = 0.16 mm/rev)

CHAPTER 4

MODELING AND OPTIMIZATION OF CONTOUR FINISH TURNING OPERATIONS

4.1 Introduction: Influencing Factors in Contour Finish Turning Operations

Since its performance immediately reflects the quality of the products, finish turning operations are performed at small depths of cut and feeds, typically less than 1.5 mm, and are less than 0.15 mm/rev, respectively. To obtain high machining performance, it is very important to understand the work and tool material properties and their interactions with the tool and chip-groove geometries used, the cutting conditions selected and the inherent static and dynamic characteristics of the machine tool system before the production process begins. The key factors which affect the cutting process and performance measures of any machining operation including machine tool, cutting tool and work material are shown in Figure 4.1 [38].

To evaluate the machining performance, a number of machinability assessment criteria have to be considered which are not independent, but interrelated with each other. For example, poor chip breakability scratches the machined surface and tool-wear deteriorates the machining accuracy. Jawahir et al. [39] emphasized the importance of the interrelationships among the chip breakability, surface roughness, and specific cutting pressure for finish turning operations.

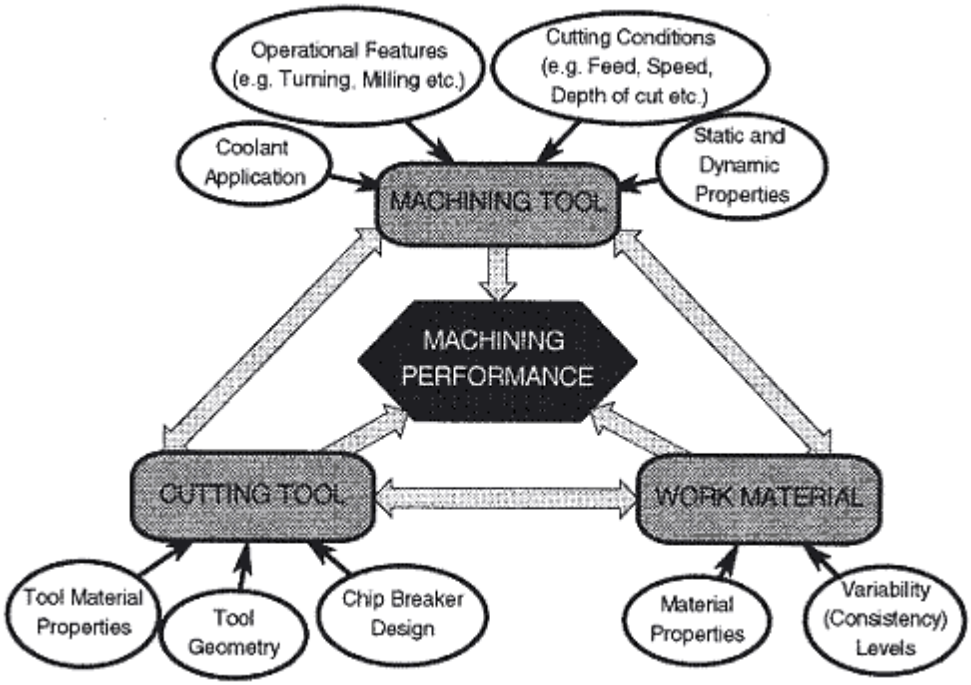

Figure 4.1: Major factors influencing machining performance [38]

Chip breakability consists of four major factors, which are shape and size, side-flow, side-curl, and up-curl. Needless to say that the chip shape and size, side-flow are important factors, especially in contour turning operations because of the wide variation of chip flow angle along the workpiece axis. Since contour workpiece has difference of elevation and hollow, the resultant long snarled chip can scratch the machined surface or intermingle with the workpiece and tool.

4.2 Technological Machining Performance Measures and Experimental Database

Two major technological machining performance measures, chip breakability, and surface roughness, are considered in the optimization criteria. The chip breakability takes into account the chip shape and size, and chip side-flow in this research work.

Since currently available metal cutting theories are unable to predict chip shape and size, cutting forces in complex grooved tools, and surface roughness under the condition of finishing operation range, experimental databases have been created and cubic spline data interpolation method is used to obtain the functions of these measurements. By using as input the effective depth of cut and axial feed into these functions, predictions of chip shape and size, cutting forces, and surface roughness can be made.

4.2.1 Chip Breakability

Chip breakability has to be considered as one of the basic requirements in automated machining systems. Long and snarled chips lead to loss of productive time, out of specification sizes and finishes, rapid tool-wear, and catastrophic tool failures. In finish turning operations, the importance of chip breaking is even greater since the unbroken chip can entangle with the workpiece and easily damage the machined surface. However, the term 'chip breakability' is not uniquely definable owing to the inherent 'fuzziness' in the understanding of the 'acceptability' levels of chip-forms. Hence, in order to quantify the chip breakability, it is considered necessary to develop a subfunction of chip shape and size, and chip side-flow.

- ***Chip shape and size***

Chip shape and size are a major factor in chip breakability, but no standard exists to quantify this factor. Fang and Jawahir [40] presented a new method to quantify chip-forms through a membership value ranging from 0 to 1 by using a fuzzy set-based knowledge-based system. Table 4.1 shows the range of membership values according to the chip shape and size for most common types of chips produced in turning operations.

Table 4.1: The definition of chip shape and size [40]

Membership Value	Fuzzy Definition of Chip Breakability	The Most Likely Chip-forms/Shapes Produced in Machining
0.0-2.0	Absolutely unbroken	Long and snarled Continuous and long coil with large diameter
0.2-0.3	Very difficult to break	Continuous and long Snarled often with few turns or small size
0.3-0.45	Usually difficult to break	Long (continuous and/or broken) Snarled often with few turns or small size
0.45-0.5	Less likely break	Medium size Spiral with few turns
0.5-0.6	More likely break	Short to medium size Flat spiral with medium size Conical spiral with medium size
0.6-0.7	Usually easy to break	Short size and full turn Flat and/or conical spirals with short size
0.7-0.9	Very easy to break	Side-curl arcs and/or up-curl arcs
0.9-1.0	Always broken	Up-curl arcs and connected side-curl arcs

- ***Chip side-flow***

The actual chip flow is a 3-D formation process, and it consists of four major factors: chip side-flow angle, back-flow angle, side-curl radius, and up-curl radius. Although chip back-flow, side- and up-curl contribute to the chip breaking process, the chip flow direction is dominated by chip side-flow. The chip heading for machined surface can easily deteriorate the surface, even though the chip is very small. Therefore, keeping the chip flow in a favorable direction is a very important aspect to control the chip in machining processes.

The hybrid model of Redetzky et al. [5] and Ghosh et al. [18], which are shown in Chapter 3, can be used to predict the chip side-flow angle for complex grooved tool inserts in contour turning operations. The model by Ghosh et al. [18] requires cutting forces with a grooved tool. However, it is very difficult to analytically predict the cutting forces in a grooved tool accurately since the shapes of chip breaker in commercial tool inserts are widely spread and quite complex. Therefore, experimental databases of radial and feed forces are created and then cubic spline interpolation is applied to predict the chip side-flow angle for complex grooved tool inserts.

4.2.2 Surface Roughness

Surface roughness is an important machining performance measure, especially, in finish turning operations. The well known ideal surface roughness equation, which represents the best possible finish that may be obtained for a given tool shape and feed, is given by the following geometric expression [41]:

$$Ra = \frac{0.0321 f^2}{r_e} \tag{4.1}$$

where f represents feed and r_e represents tool nose radius.

This equation works quite well for moderate machining involving medium cutting conditions, but finish turning operations always seem to give much higher measured R_a values than the predicted theoretical values by the equation [39]. This is because the real surface roughness can be attributed to the influence of physical and dynamic phenomena such as friction of the cut surface against tool point and vibrations [42]. Hence, the surface roughness is experimentally measured and cubic spline interpolation is applied to obtain the surface roughness function.

4.2.3 Experimental Database

Full factorial experiments were conducted for a range of feeds: 0.04,0.07,0.10,0.13, and 0.16 mm/rev, and a range of depths of cut: 0.2, 0.6, 1.2, and 2.0 mm on HAAS CNC Turning Center in order to create databases to predict the cutting force, chip shape and size, and surface roughness. The cutting forces were measured by using a tool dynamometer (Kistler 9121) through the amplifier (Kistler 5004 dual mode amplifier) and corrected by data acquisition system (Kistler Dynoware) (Figure 4.2). A particular tool insert (SANDVIK VBMT 332-UM) and work material (AISI 1045 steel) were used under a constant cutting speed of 250 m/min. The rake and inclination angles are 0 degree each, the side- and end-cutting edge angle are both 72.5 degrees, and nose radius is 0.8 mm for this cutting tool.

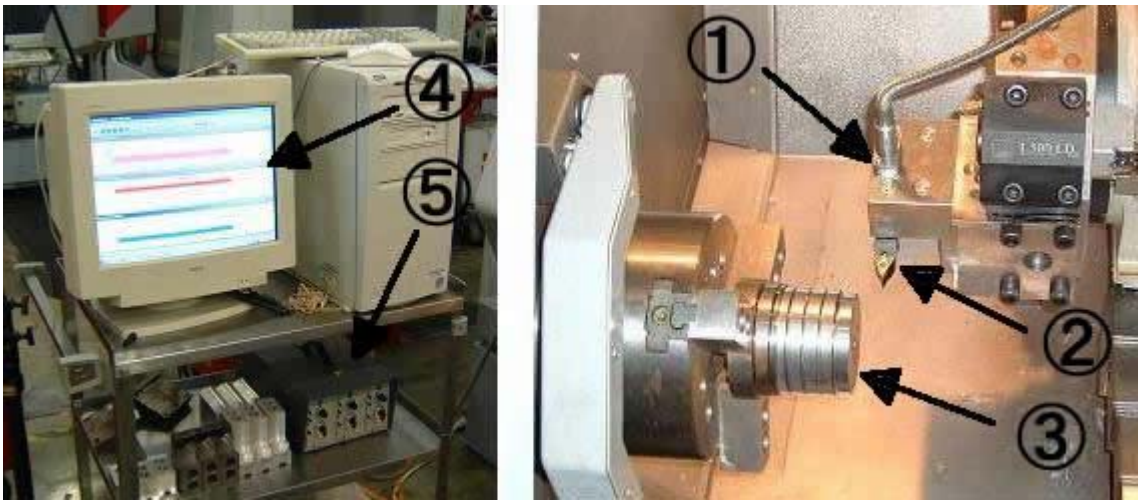

Figure 4.2: Experimental set up

- ***Cutting forces for chip flow prediction***

It has been observed that the effect of cutting speed on cutting forces is much less significant than the feed and depth of cut. Hence, the chip side-flow is least affected by the cutting speed and thus, the effects of cutting speed can be ignored. Tables 4.2 and Table 4.3 show the experimental data for the radial force F_x and the feed force F_y respectively for the given tool insert (VBMT 332-UM) and work material (AISI 1045 steel) where the cutting speed is 250 m/min. Cubic spline interpolation of the test data was then used to obtain the radial and feed force functions. Figures 4.3 to 4.6 show the contours and 3-D surface plots of radial and feed forces respectively.

Table 4.2: Test data for radial force F_x (N) (Cutting speed: 250 m/min, work material: AISI 1045 steel, cutting tool: VBMT 332-UM)

F_x (N)		Feed (mm/rev)				
		0.04	**0.07**	**0.10**	**0.13**	**0.16**
Depth of cut (mm)	**0.2**	26.4	32.3	38.1	42.8	47.5
	0.6	50.9	62.7	79.4	86.1	101.6
	1.2	63.5	83.5	91.8	103.3	119.4
	2.0	86.8	98.1	106.5	126.2	157.7

Table 4.3: Test data for feed force F_y (N) (Cutting speed: 250 m/min, work material: AISI 1045 steel, cutting tool: VBMT 332-UM)

F_y (N)		Feed (mm/rev)				
		0.04	**0.07**	**0.10**	**0.13**	**0.16**
Depth of cut (mm)	**0.2**	9.2	11.4	13.0	13.9	14.9
	0.6	46.6	58.6	73.1	76.2	87.0
	1.2	99.7	132.4	146.1	160.2	186.4
	2.0	172.7	203.0	226.4	266.7	337.6

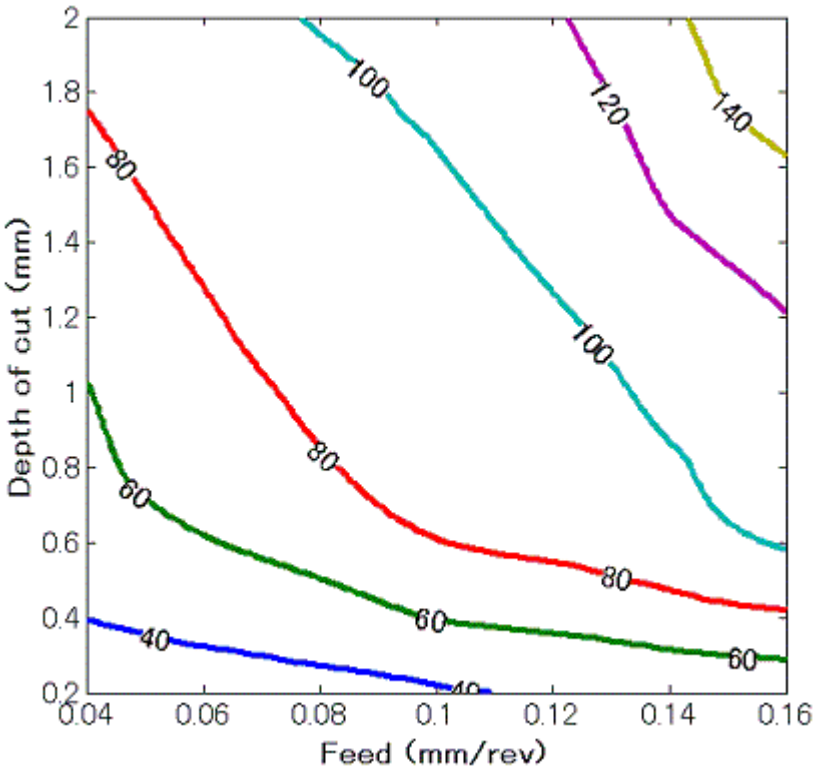

Figure 4.3: The contour of radial force F_x (N)

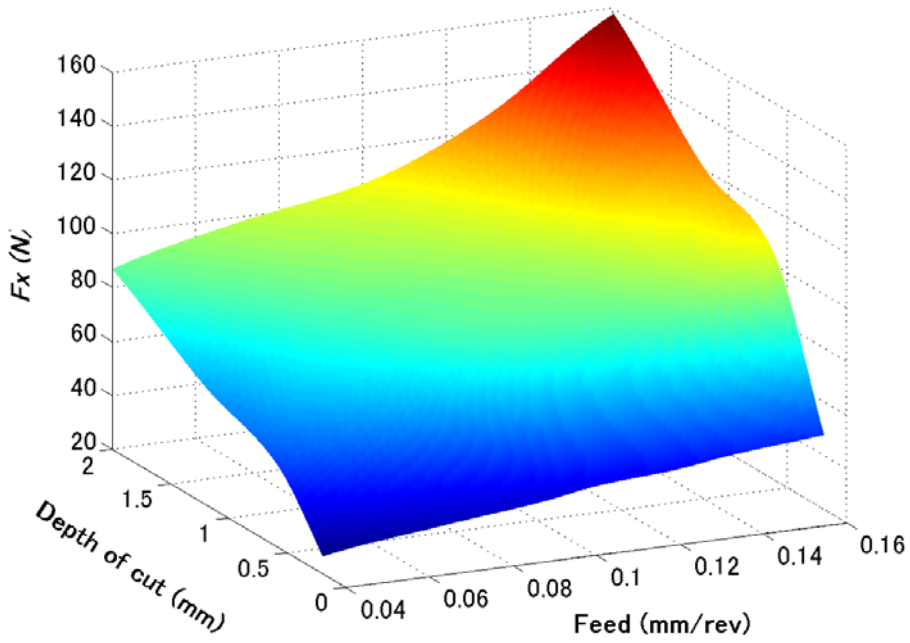

Figure 4.4: The 3-D plot of radial force F_x (N)

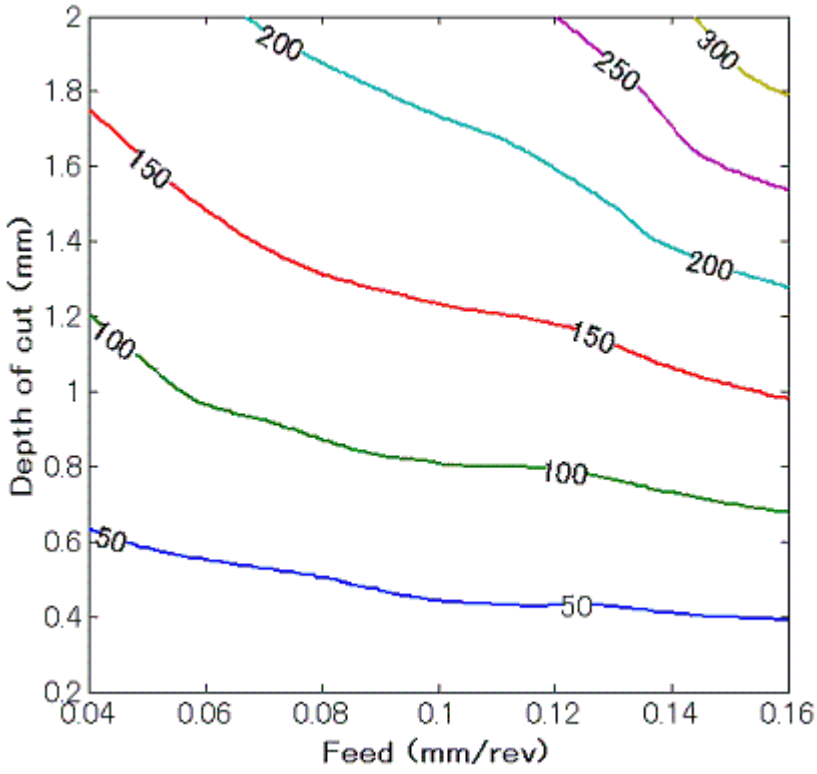

Figure 4.5: The contour of feed force F_y (N)

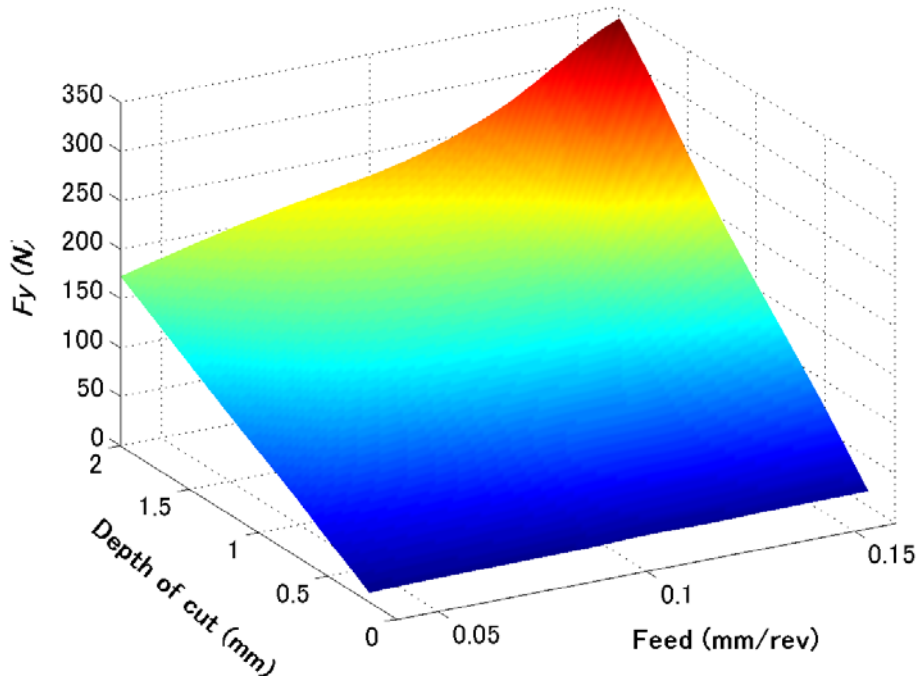

Figure 4.6: The 3-D plot of feed force F_y (N)

- ***Chip shape and size***

The definition of membership values according to the chip-form given by Fang and Jawahir [40], as shown in Table 4.1, was used to estimate the chip shape and size. Generally speaking, smaller cutting speeds tend to produce slightly better chip breakability. However, the effect of cutting speed on chip breakability is not as significant as the effects of feed and depth of cut. Therefore, the cutting speed was kept constant as 250 m/min. Figure 4.7 shows the chip chart of the experimental results using the given tool insert (VBMT 332-UM) and work material (AISI 1045 steel) and Table 4.4 shows the membership values of the chip shape and size.

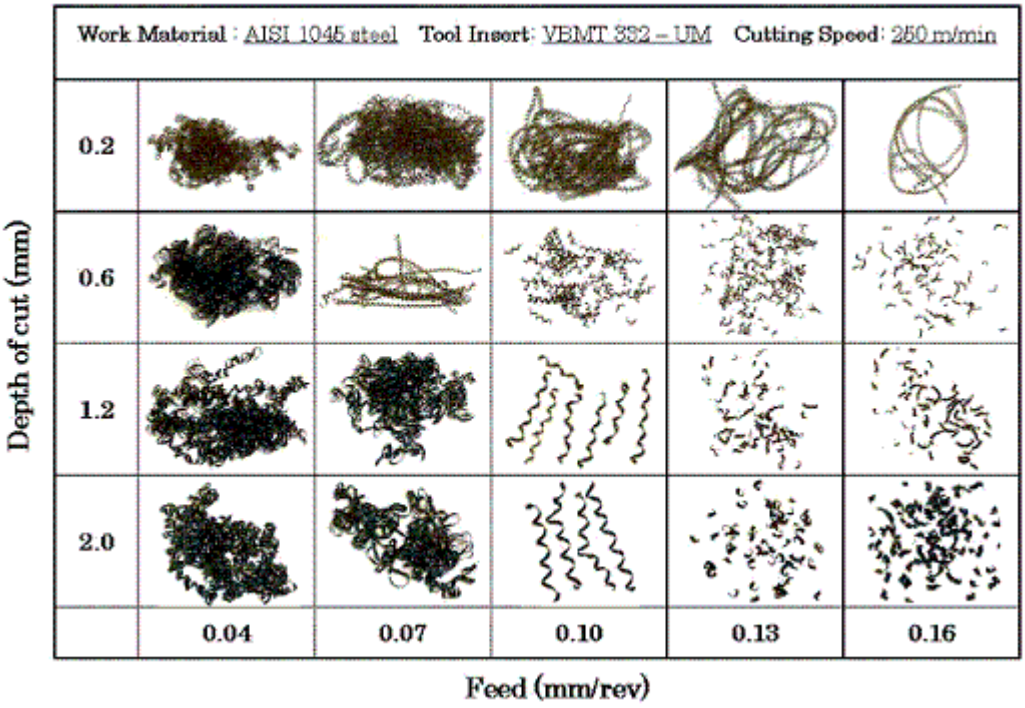

Figure 4.7: Chip chart in terms of feed and depth of cut

Table 4.4: Test data for chip shape and size *CSS* (Cutting speed: 250 m/min, work material: AISI 1045 steel, cutting tool: VBMT 332-UM)

CSS		**Feed (mm/rev)**				
		0.04	**0.07**	**0.1.0**	**0.13**	**0.16**
Depth of cut (mm)	**0.2**	0.2	0.2	0.2	0.3	0.4
	0.6	0.2	0.3	0.6	0.9	0.9
	1.2	0.1	0.1	0.5	0.9	0.9
	2.0	0.1	0.1	0.5	0.8	0.85

A cubic spline interpolation technique was used after creating the database to obtain chip shape and size function. Figures 4.8 and 4.9 show the contour and 3-D surface plots of the experimental results for chip shape and size.

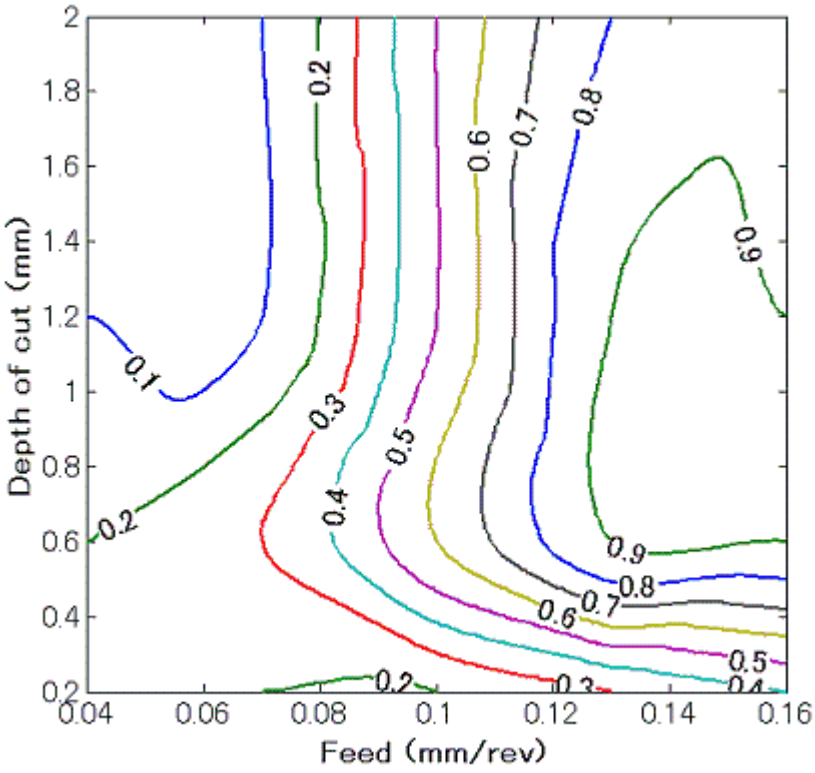

Figure 4.8: The contour of chip shape and size

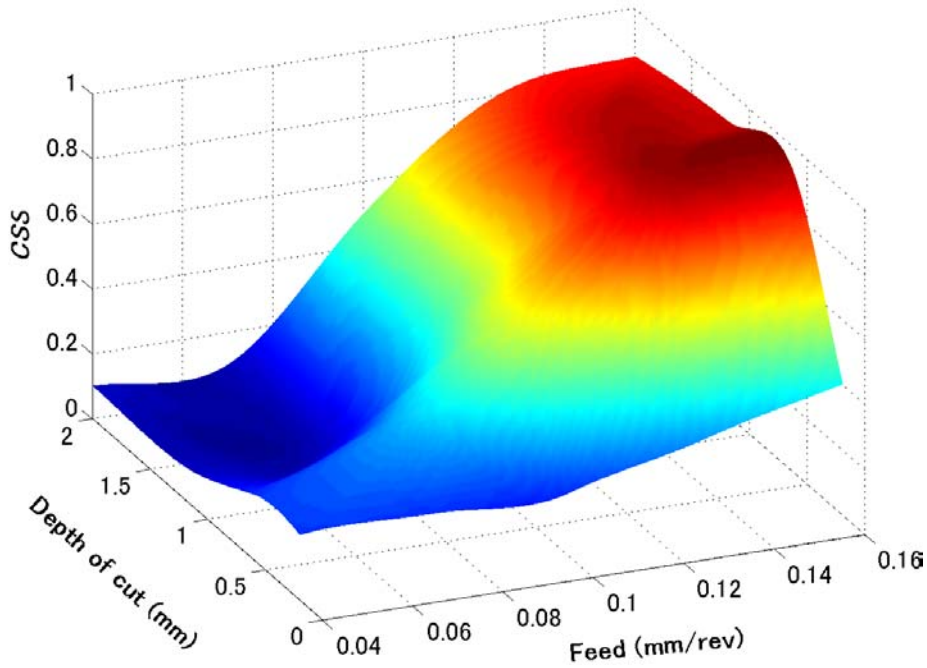

Figure 4.9: The 3-D plot of chip shape and size

• ***Surface roughness***

Since it is very difficult to analytically predict the surface roughness values under the cutting conditions in the finish turning range, an experimental database of surface roughness for varying feeds and depth, where the cutting speed was kept constant as 250 m/min, was created. The equipment used to measure the surface roughness was Taylor-Hobson Form Talysurf Surface Measuring System, and the results are shown in Table 4.5. Cubic spline interpolation technique was applied again and the contour and 3-D surface plots of the experimental results for the surface roughness are shown in Figure 4.10 and Figure 4.11.

Table 4.5: Test data for surface roughness R_a (μm) (Cutting speed: 250 m/min, work material: AISI 1045 steel, cutting tool: VBMT 332-UM)

R_a (μm)		Feed (mm/rev)				
		0.04	**0.07**	**0.10**	**0.13**	**0.16**
Depth of cut (mm)	**0.2**	0.495	0.782	0.896	0.982	1.152
	0.6	0.333	0.541	0.755	0.861	1.111
	1.2	0.369	0.422	0.706	0.892	1.207
	2.0	0.296	0.405	0.683	0.877	1.078

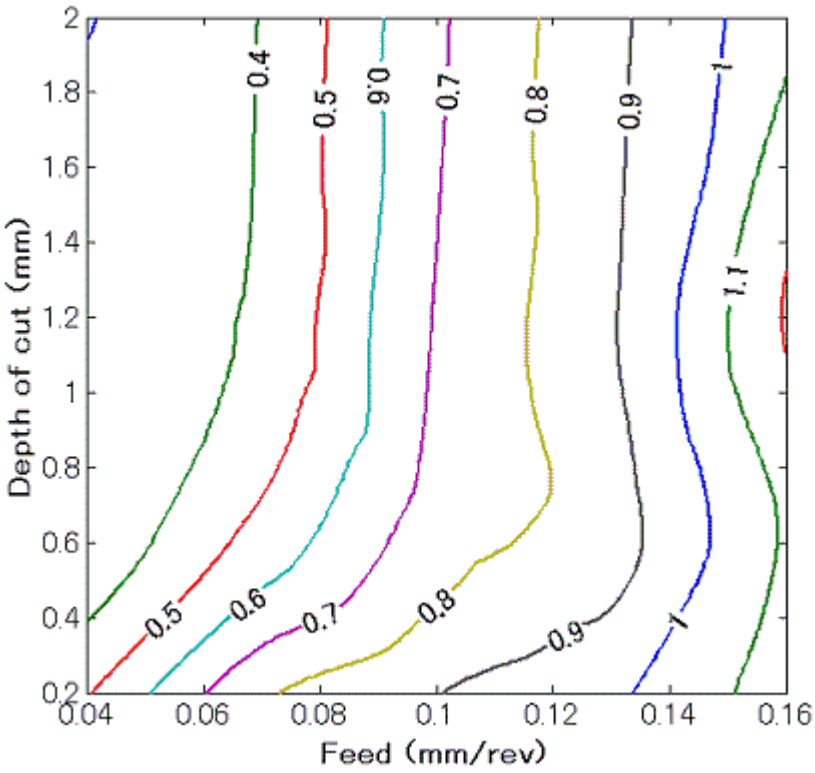

Figure 4.10: The contour of surface roughness R_a (μm)

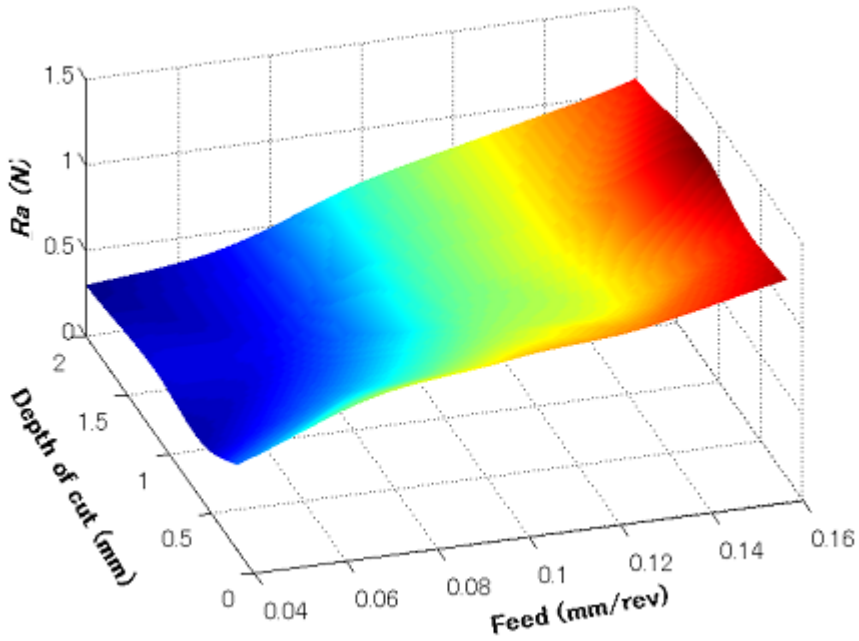

Figure 4.11: The 3-D plot of surface roughness R_a (μm)

4.3 Optimization Criterion

Unlike straight turning, the cutting conditions in contour turning change along the workpiece profile. In some segments of the workpiece, axial feed is very small and the effective depth of cut is very large because of the steep slope, while it is not in other segments. Therefore, optimal cutting conditions are different for each segment. The nominal depth of cut cannot be changed along the workpiece, but feed can be altered easily in the prevailing CNC machine. To obtain the best performance in contour finish turning operations, various feeds according to the segments and a nominal depth of cut along the workpiece are considered to be the design variables.

Da et al. [32] developed a hybrid model for a single-pass straight turning operations based on the multiple machining performance measures, which are surface roughness (R_a), cutting force (F_c), tool-life (T), material removal rate (M_R) and chip breakability (CB). The objective function is constructed as:

$$U(V,f,d) = C_R\left(\frac{R_a^{'} - R_a}{R_a^{'}}\right) + C_F\left(\frac{F_C^{'} - F_C}{F_C^{'}}\right) + C_T\left(\frac{T - T^{'}}{T^{'}}\right) + C_M\left(\frac{M_R - M_R^{'}}{M_R^{'}}\right) + C_{CB}\left(\frac{CB - CB^{'}}{CB^{'}}\right) \tag{4.2}$$

where each term is normalized by using the user-provided information concerning machining performance requirements. C_i (i = R, F, T, M, and CB) are weighting factors considered as the contribution coefficient of i-th machining performance variable to the value of the operation. These weighting factors satisfy two conditions:

$$\text{(1) } C_R + C_F + C_R + C_M + C_{CB} = 1;$$

$$\text{(2) } 0 \le C_i \le 1 \quad (i = \text{R,F,T,M,CB}) \tag{4.3}$$

Corresponding constraints on these machining performance measures are assumed as

Ra' $F_C^{'}$, *T'*, M_R' and *CB'*.

In a similar manner, the optimization objective for contour finish turning problems is the sum of the objectives of all segments along the workpiece. In each segment, equally spaced 5 data points are evaluated represented by $U_{i,j}$, where *i* is segment number and *j* is number of the data point in that segment (Figure 4.12). Chip breakability is a sub-function of chip shape and size and chip side-flow angle.

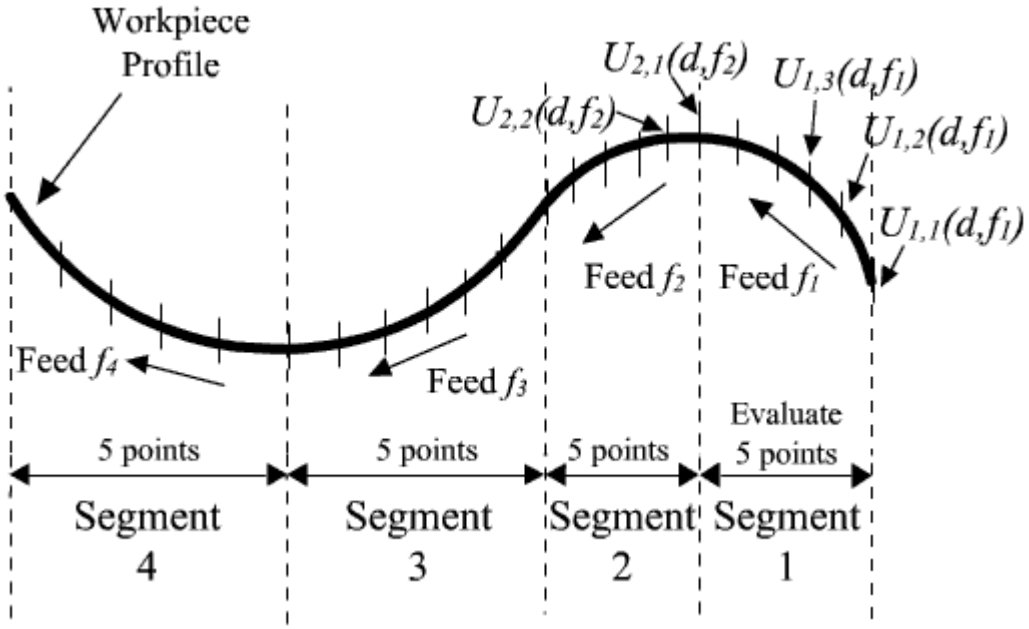

Figure 4.12: Evaluation data points

The overall objective function is:

$$
\begin{aligned}
U(d, f_i, (i = 1,2,...N)) &= \sum_{i=1}^{N}\sum_{j=1}^{5} U_{i,j}(d, f_i) \\
&= \sum_{i=1}^{N}\sum_{j=1}^{5}\left\{ C_R \cdot (\frac{R_a^{'} - R_{a\,i,j}}{R_a^{'}}) + C_{CB} \cdot CB_{i,j}(CSS, \eta) \right\}
\end{aligned}
\qquad (4.4)
$$

$$
\text{where} \quad CB_{i,j}(CSS, \eta) = CSS_{i,j} \times (\frac{\eta_{i,j} - \eta_{\min}}{\eta_{\max} - \eta_{\min}})
$$

N is the total number of segments, *d* is the nominal depth of cut, f_i is the feed for *i*-th

segment. The index i and j denote j-th data point in the i-th segment. The parameters, $R_{ai,j}$, and $CB_{i,j}$, represent the surface roughness, and chip breakability, at the j-th data point in the i-th segment respectively and chip breakability is the function of chip shape and size ($CSS_{i,j}$) and chip side-flow angle ($\eta_{i,j}$). η_{max}, and η_{min} represent the possible maximum and minimum chip side-flow angle respectively under the cutting conditions range for finish turning. C_R, and C_{CB} are weighting factors considered as the contributing coefficients for the machining performance measures.

Hence, the optimization problem becomes

Maximize: $U(d,f_i)$, $(i = 1,2,....,N)$

With respect to: $d, f_i, (i = 1,2,....,N)$

Subject to:

$$d_{\min} \le d \le d_{\max}$$

$$f_{\min} \le f_i \le f_{\max}$$

$$R_{ai} \le R_a^{'}, \quad CSS_i \ge CSS' \qquad (i = 1,2,.....,N)$$

$$C_R + C_{CB} = 1$$

$$0 \le C_j \le 1 \qquad (j = R, CB)$$

The parameters R_{ai} and CSS_i denote the average surface roughness and chip shape and size in a segment respectively. The overall optimization algorithm flow-chart is shown in Figure 4.13. This optimization method is based on the determination of a combination of optimal depth of cut and feed for each segment in order to maximize the utility function. The optimization algorithm determines a common, optimal depth of cut for all segments, because of the need to keep the nominal value constant throughout the profile. The optimal depth of cut and feeds would maximize the total utility function U for the whole profile, which is a summation of all local utility functions $U_{i,j}$, throughout the profile, and it satisfies all constraints.

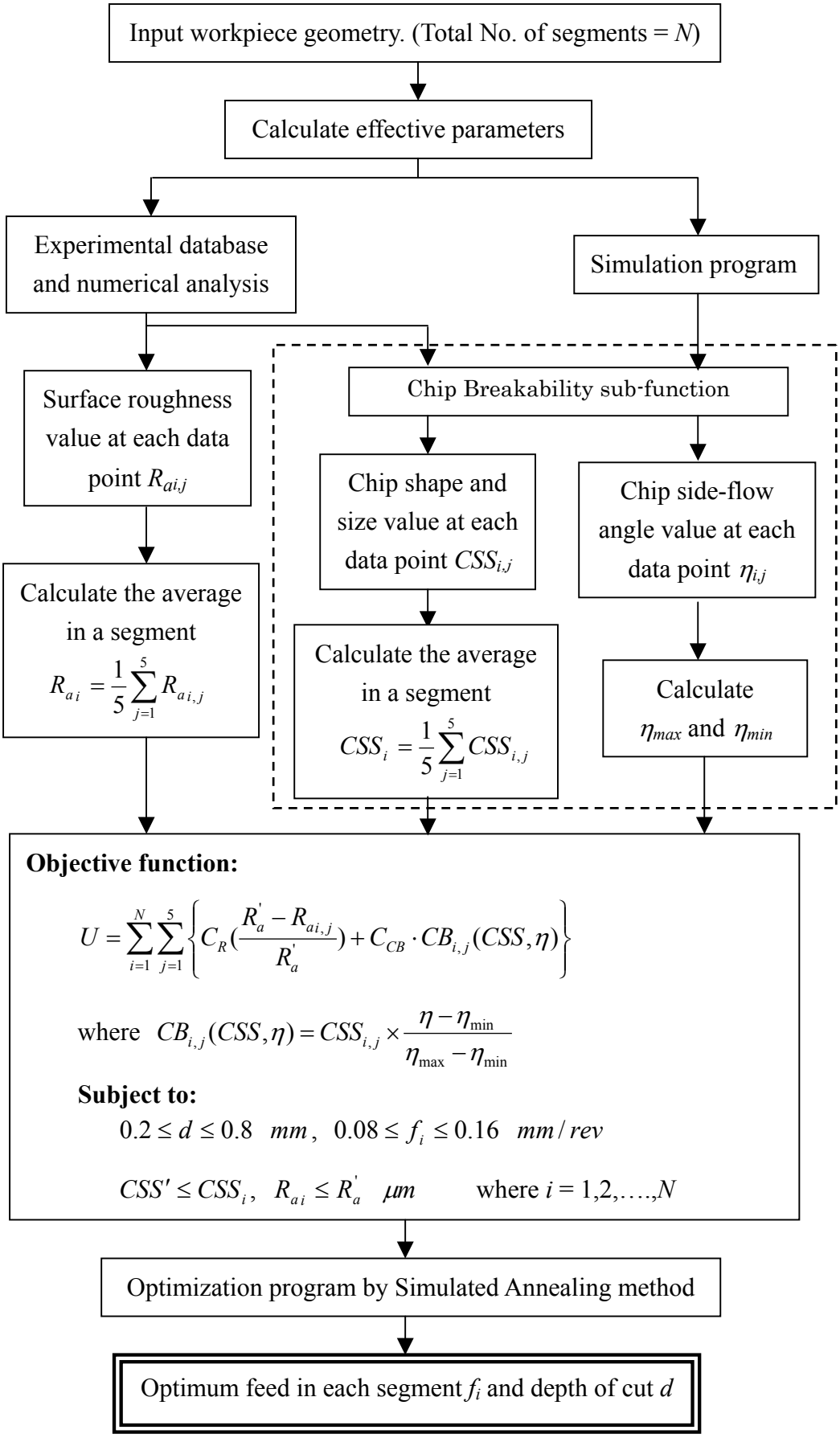

Figure 4.13: Overall optimization algorithm flowchart

4.4 Introduction to Nonlinear Optimization Problem

If the objective function and constraints can be expressed as a linear equation, the optimization problem is called a Linear Programming Problem (LP). For these problems, the optimization can be achieved easily by conducting well-established searching methods, such as simplex method, steepest descent method and Newton method. On the other hand, if any of the functions in the objective and constraint functions is nonlinear, then the problem is called a Nonlinear Programming Problem (NLP). NLP problem is much more complex than LP problem and quite often cannot be solved by the searching method mentioned above because of the difficulty of calculating the derivative of the objective function or existence of local optimal points. For these problems, it may be necessary to use meta-heuristic methods which may not give an exact global optimum, but would provide satisfactory optimum within the practical searching time. Unfortunately, most of optimization problems in machining are NLP problems. There are many meta-heuristic methods developed and some of the popular methods are listed below with their advantages and disadvantages. Table 4.6 shows the characteristics of the commonly used optimization methods in NLP problems. In this thesis research, Simulated Annealing method is used as the optimization method.

Table 4.6: Characteristics of commonly used optimization methods

	Basic concept	Advantage	Disadvantage
Random search	Randomly search the optimal points in all feasible region	• Algorithm is very easy • Applicable any kind of problem	• It takes much time to obtain global optimal points • It often doesn't converge in the practical time
Multi-start local optimization	Start from randomly chosen various initial points. Each point proceeds to the direction with better solution.	• Algorithm is very easy • Applicable any kind of problem • Accuracy is good	• It takes time to converge • The point of convergence highly depends on initial points.
Taboo search	Search to the better solution and mark that region. Then searching is prohibited inside the marked region for a while	• Faster than normal searching method.	• Design of parameter is difficult task • Program code is not easy
Genetic Algorithms	This method models human gene. Provide better gene to children from lots of parents	• It is able to obtain "relative minimum or maximum" (not global optimal) solution in practical time even in very complex problem • It has wide range of applicable problem • There are lots of method is investigated not to converge to local optimal points.	• Program code is very complex • There is no general way for determining parameter, cording • Convergence to global optimal is slow
Simulated Annealing	This method models the material annealing process. Searching direction goes to worse region with specific probability not to converge to local optimal points	• It does not converge to local optimal easily • It has a wide range of applicable problem • Convergence to global optimal is faster than others • Algorithm is relatively easy	• Setting parameter is not easy • The accuracy and speed of convergence depend on initial set up • The calculation is large in amount

4.5 Simulated Annealing Method

In an annealing process, the metal, initially at high temperature and disordered, is slowly cooled down so that the material grain structure can be stable. This process is time consuming, but if the cooling is conducted in a very fast rate, the material will be fragile. The system at any time needs to be approximately in thermodynamic equilibrium. As cooling proceeds, the system becomes more ordered and approaches a "frozen" ground state at $T = 0$. Hence the process can be thought of as an adiabatic approach to the lowest energy state. The Simulated Annealing Method for optimization imitates this process in the computer program.

Most of NLP problems do not involve single-peaked patterns, but multi-peaked patterns with some local minimum or maximum. However, traditional optimization methods tend to search only in a better direction from the current position. This make the results fall into a local optimal easily. On the other hand, in simulated annealing method, the optimization process is not required to proceed uniformly downhill, but is allowed to make occasional uphill moves. The acceptable probability of an uphill move is determined by the parameter T called “temperature”. The value is expressed as $exp(-\Delta E/\kappa T)$, where κ is a constant. At the start of the annealing process, T has a relatively large value and it can be move in all feasible regions. As the random walk progresses, the value of T gradually decreases and the acceptable uphill moves will be smaller. This causes that the random walk is to be effectively constrained. By reducing temperature T sufficiently slowly, the random walk can escape the higher valleys during its earlier stages, and can be expected to terminate at the global minimum. However, if temperature T reduces at a very fast rate, it cannot go over some uphills and tends to fall into a local optimal.

Figure 4.14 shows the model of Simulated Annealing and Figure 4.15 shows the program algorithm flowchart.

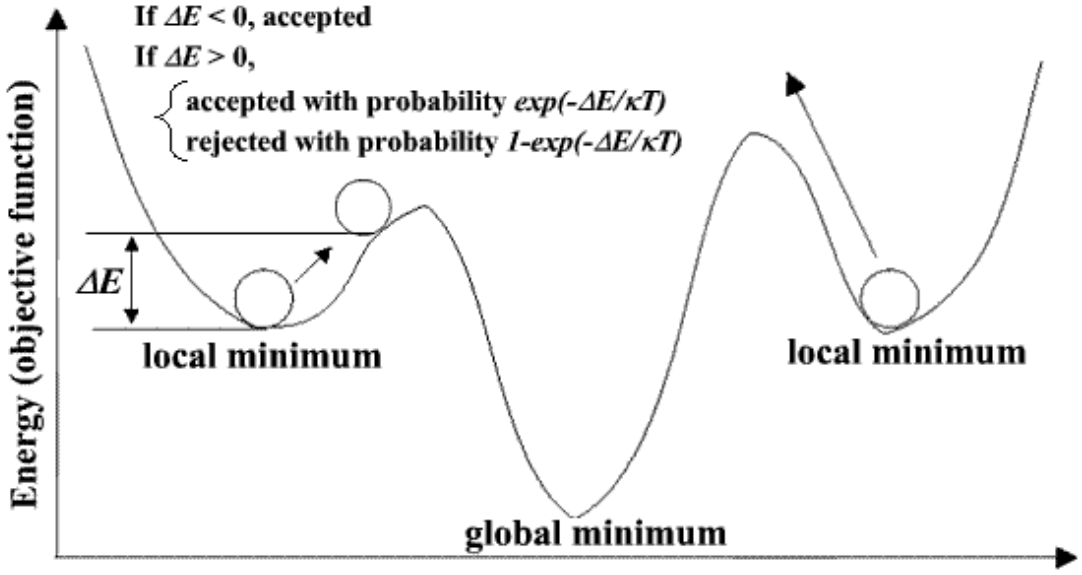

Figure 4.14: Model for Simulated Annealing (SA) method

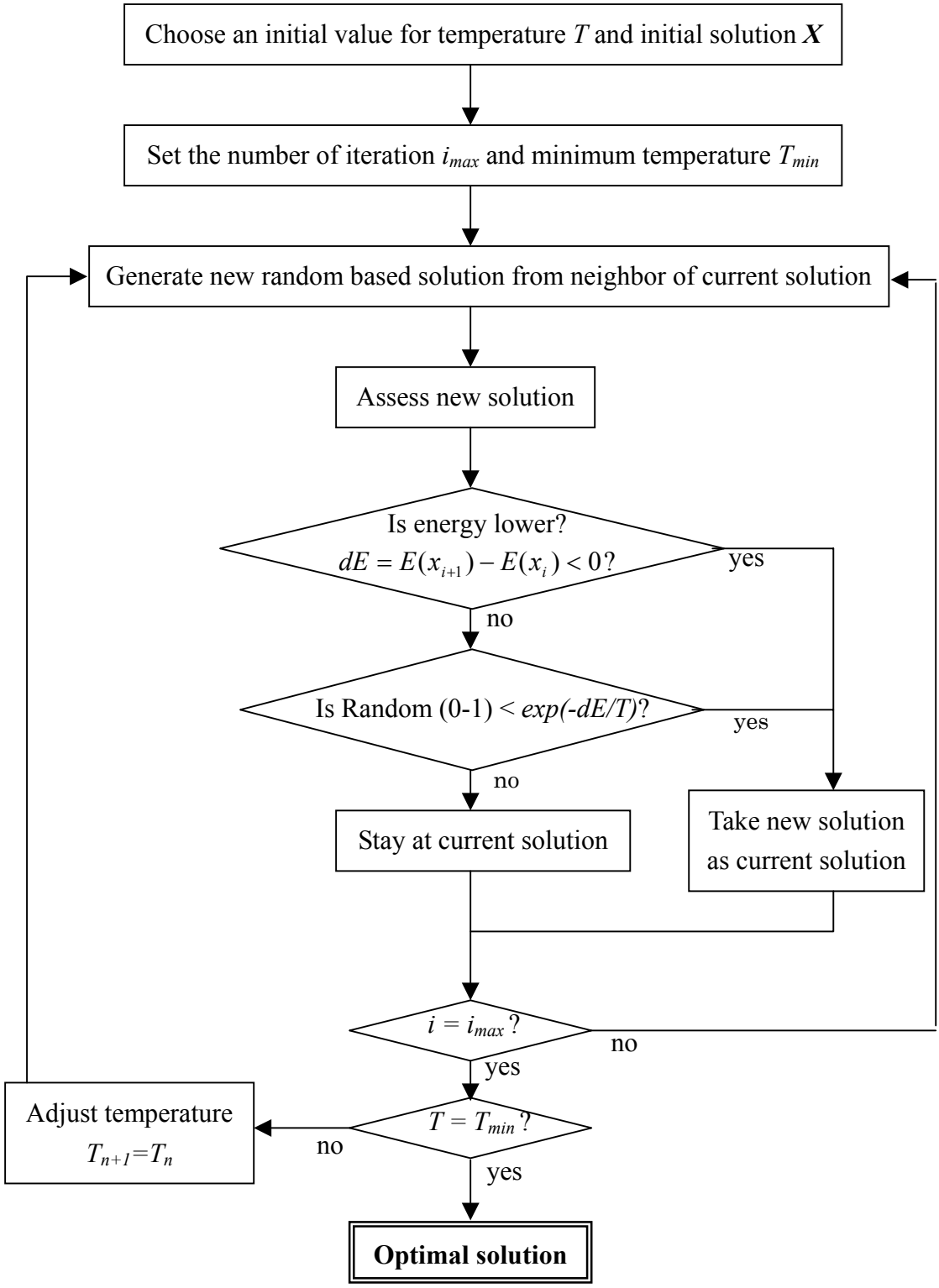

Figure 4.15: Flowchart of general Simulated Annealing method

CHAPTER 5

OPTIMIZATION RESULTS AND ANALYSIS

5.1 Conditions for Case Study and Program Results

Several representative cases are analyzed and presented in this chapter to demonstrate the application of the methodology mentioned in the previous two chapters. The optimal feed for each workpiece segment and the optimal depth of cut will be determined to maximize the machining performance in terms of chip breakability and surface roughness with the required limitation in finish contour turning operations. A specific cutting tool, VBMT 332-UM, and work material, AISI 1045 steel are used and a sample workpiece with various geometric shapes (Figure 5.1) is again selected for the case study. This sample workpiece has convex, concave, and the straight line contours with positive, negative, and zero slope angles and it is divided by 8 segments according to the geometric shapes as shown in Figure 5.1.

The parameters required for the Simulated Annealing (SA) optimization program are shown in Table 5.1. In order to reduce the calculation time, a high cooling rate is selected. After every 40 iterations, the temperature is reduced by 75% and the total number of iterations is 400 times.

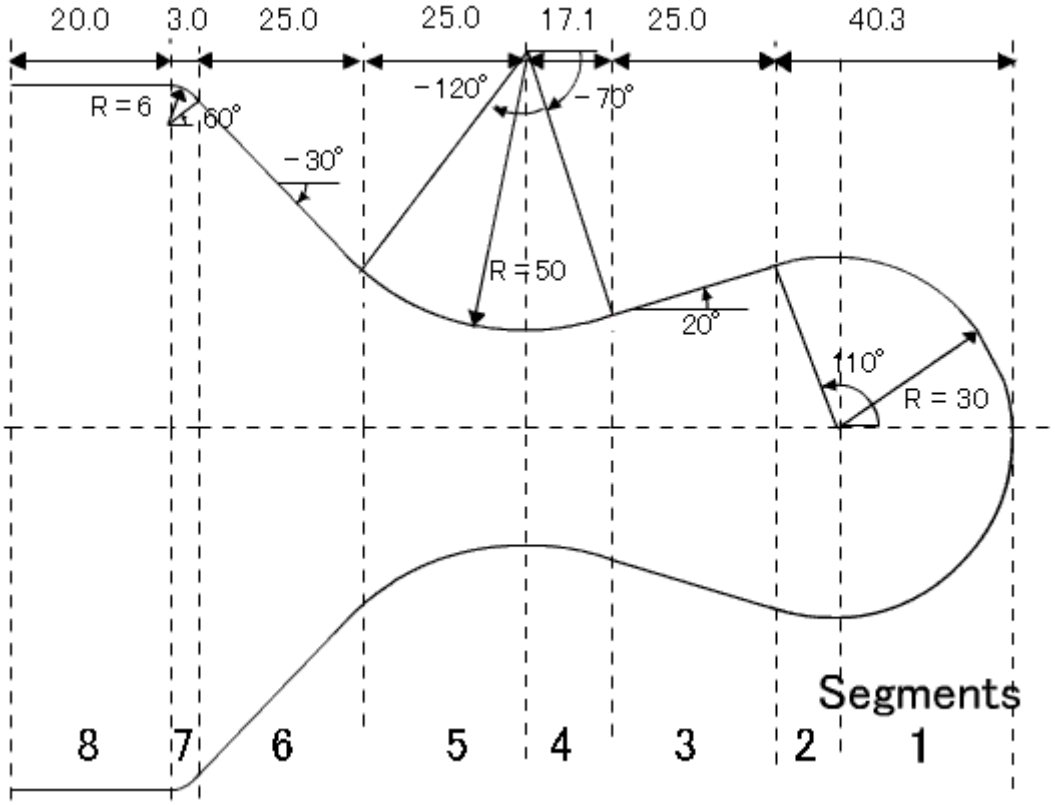

Figure 5.1: The profile of sample workpiece

Table 5.1: Parameters of SA optimization program

Maximum temperature	3
Minimum temperature	$9.51*10^{-3}$
Cooling rate	0.75
Neighborhood range's adjustment interval	20
Total number of iteration	400

Table 5.2 shows the weighing factors and constraints for three cases. The optimization results and the predicted machining performance for each case are shown in Table 5.3, 5.4, 5.5 respectively. Figure 5.2 shows the optimal depth of cut and feeds along the workpiece profile and Figure 5.3 shows the predicted machining performance under the optimal cutting conditions for Case 1. Figures 5.4 to 5.11, shows the contour plots of the objective function as well as the constraints in each segment for Case 1. Similarly, Figure 5.12 and Figure 5.22 show the optimal cutting conditions, Figure 5.13 and Figure 5.23 show the predicted machining performance, and Figures 5.14 to 5.21 and Figure 5.24 to Figure 5.31 show the contour plots for Case 2 and Case 3, respectively.

Table 5.2: Weighting factors and constraints

		Case 1	Case 2	Case 3
Weighting Factors	C_R	0.5	0.2	0.8
	C_{CB}	0.5	0.8	0.2
V (m/min)		250	250	250
f (mm/rev)		0.08 – 0.16	0.08 – 0.16	0.08 – 0.16
d (mm)		0.2 – 0.8	0.2 – 0.8	0.2 – 0.8
R_a' (μm)		1.0	1.0	1.0
CSS'		0.7	0.7	0.7

Table 5.3: Optimization results for Case 1

Weighting Factors			**C_R = 0.5, C_{CB} = 0.5,**							
Segment No.			**1**	**2**	**3**	**4**	**5**	**6**	**7**	**8**
Optimum Cutting Conditions	***d* (mm)**		**0.4731**							
	***f* (mm/rev)**		0.1546	0.1316	0.1383	0.1261	0.1272	0.1381	0.1280	0.1280
Predicted Average Machining Performance	**R_{ai} (μm)**		0.8864	0.8777	0.8746	0.8550	0.88458	0.8258	0.8505	0.8756
	CB(f,d)	**CSS_i**	0.7010	0.7816	0.8177	0.7352	0.7275	0.7804	0.7426	0.7660
		η (deg.)	-4.0863	66.0050	85.3648	66.0325	17.0264	-13.2646	18.4538	47.1625

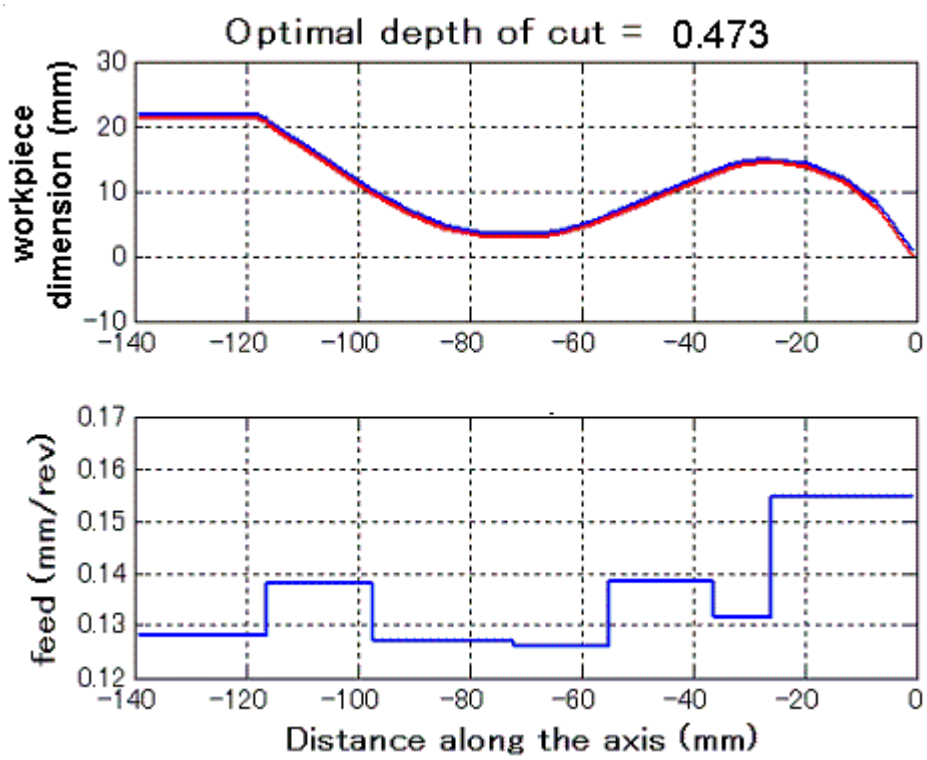

Figure 5.2: Optimized cutting conditions followed by workpiece geometry for Case 1

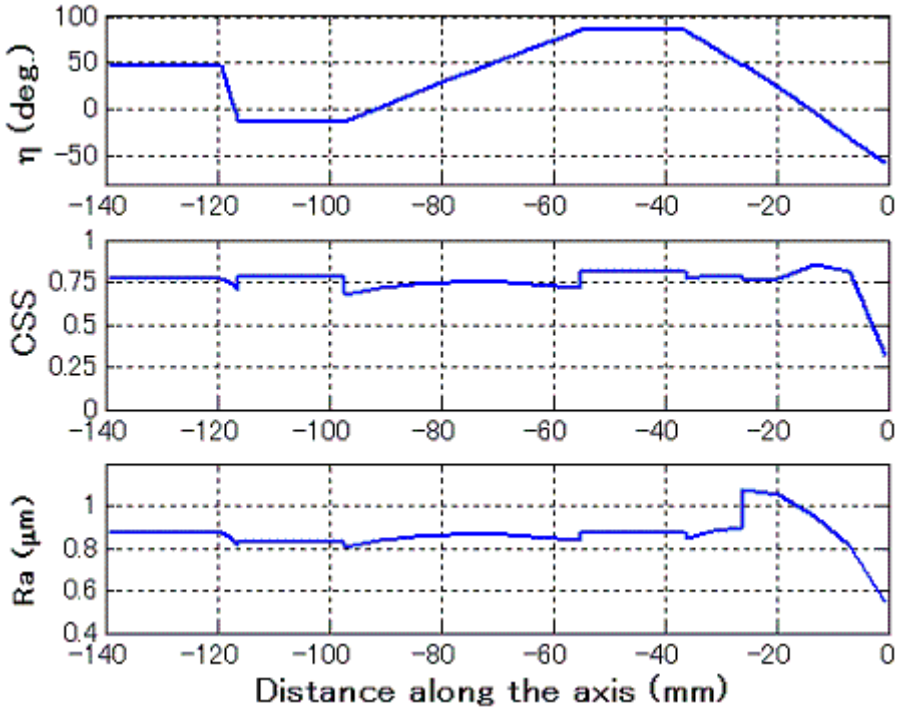

Figure 5.3: Predicted machining performance along the axis for Case 1

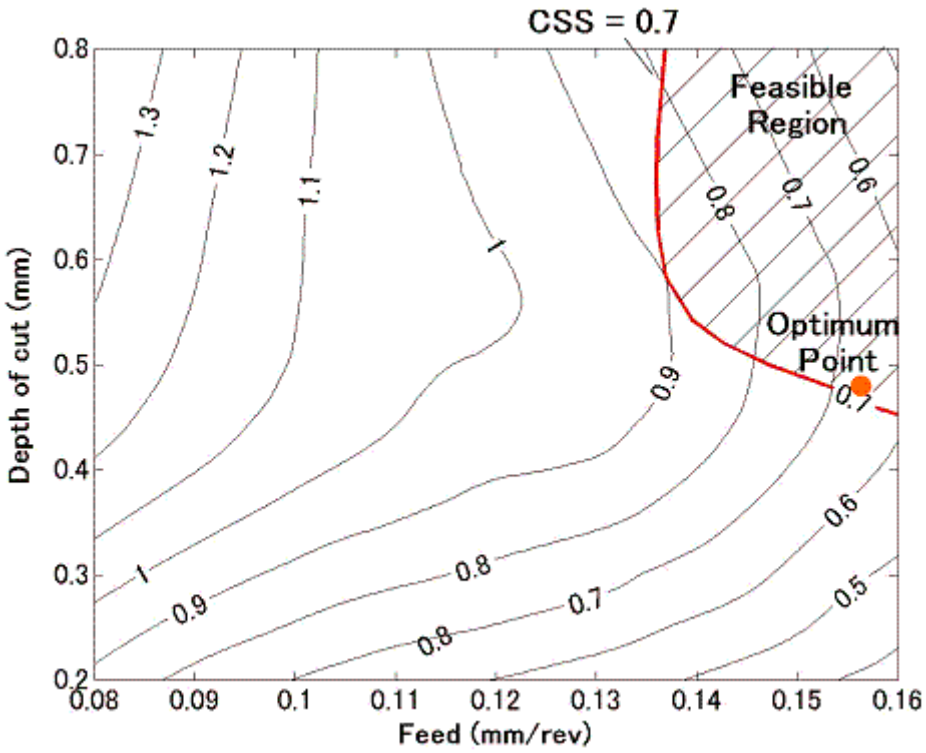

Figure 5.4: Optimization results for contour plot of Segment 1 for Case 1

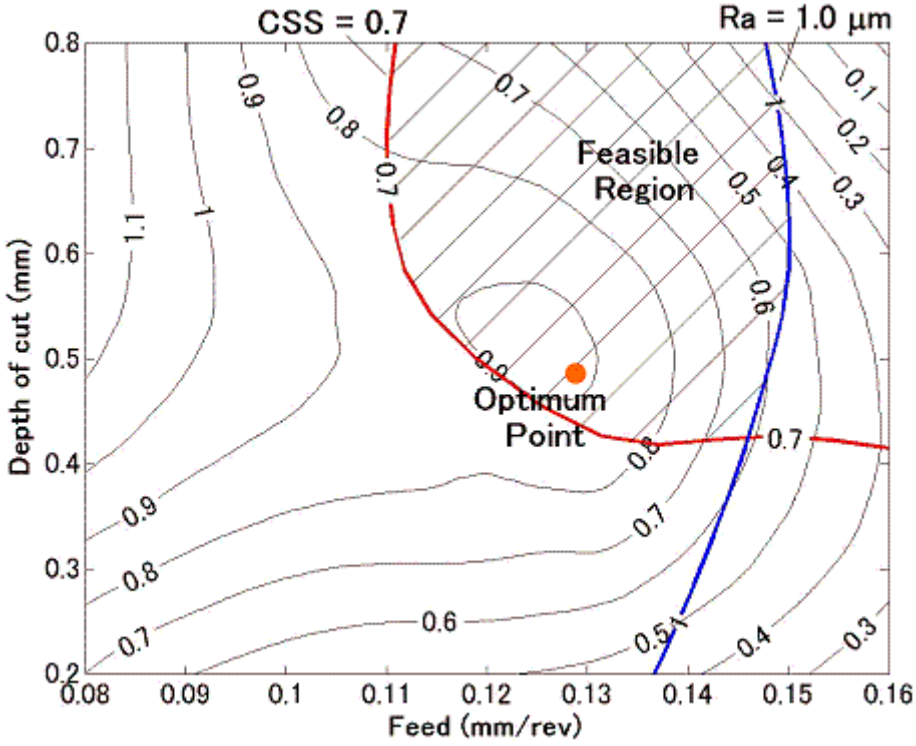

Figure 5.5: Optimization results for contour plot of Segment 2 for Case 1

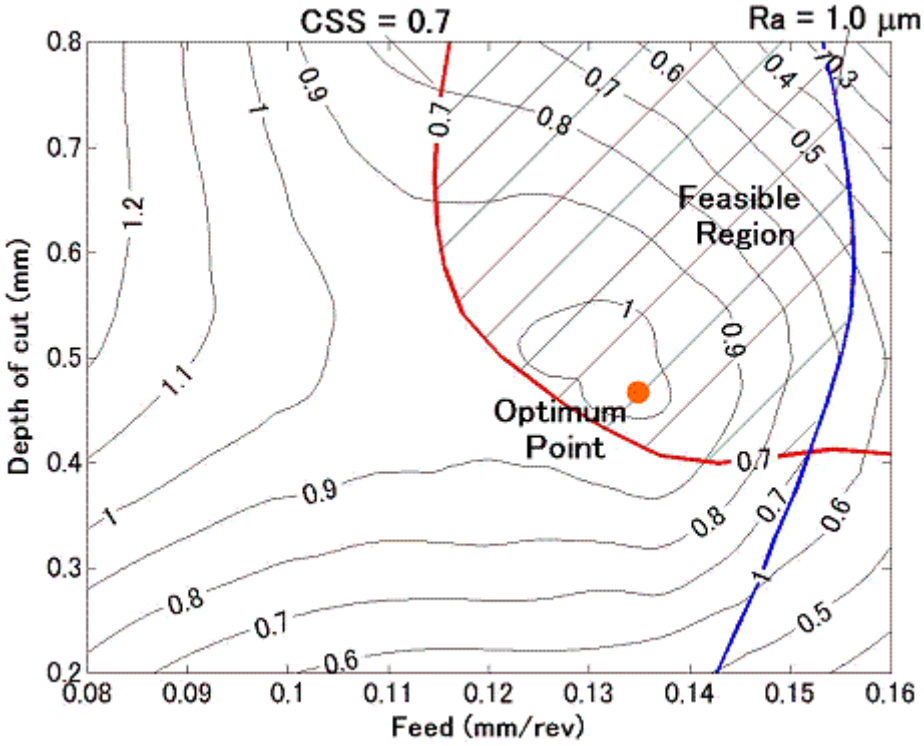

Figure 5.6: Optimization results for contour plot of Segment 3 for Case 1

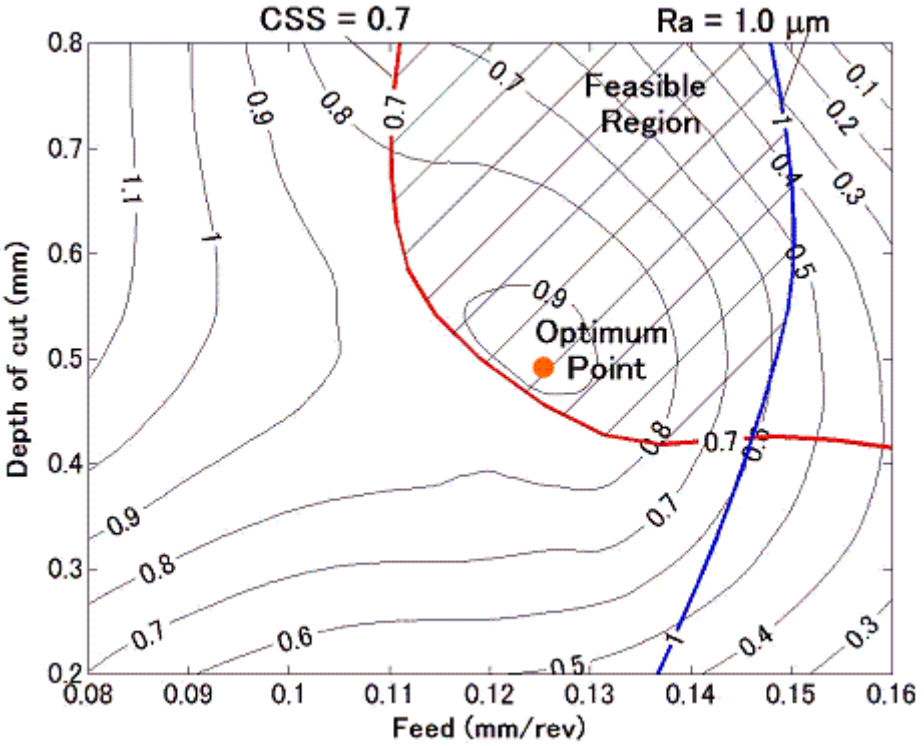

Figure 5.7: Optimization results for contour plot of Segment 4 for Case 1

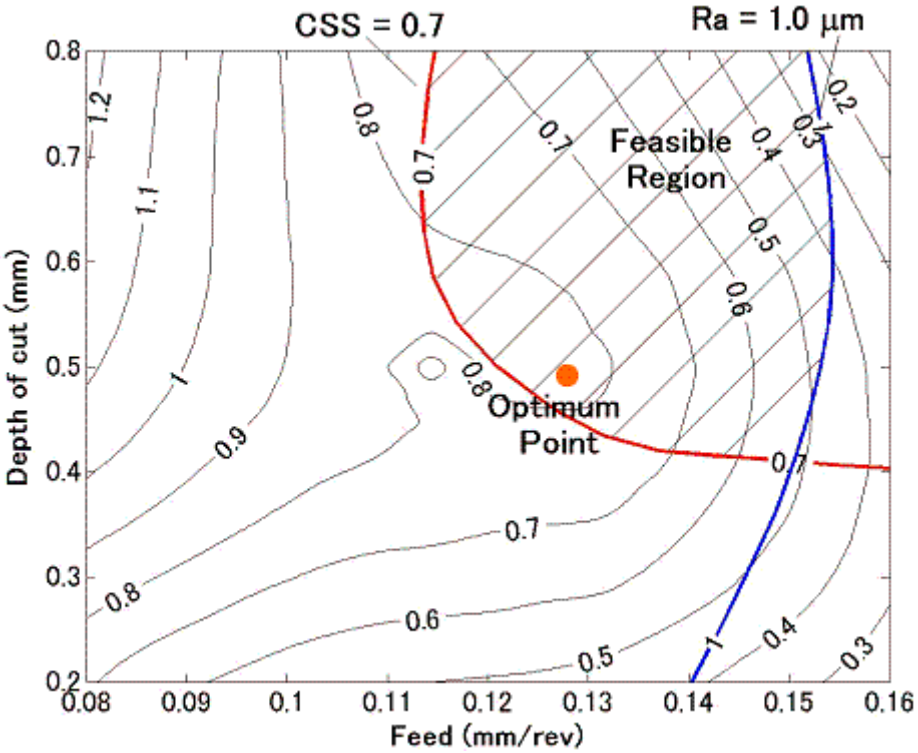

Figure 5.8: Optimization results for contour plot of Segment 5 for Case 1

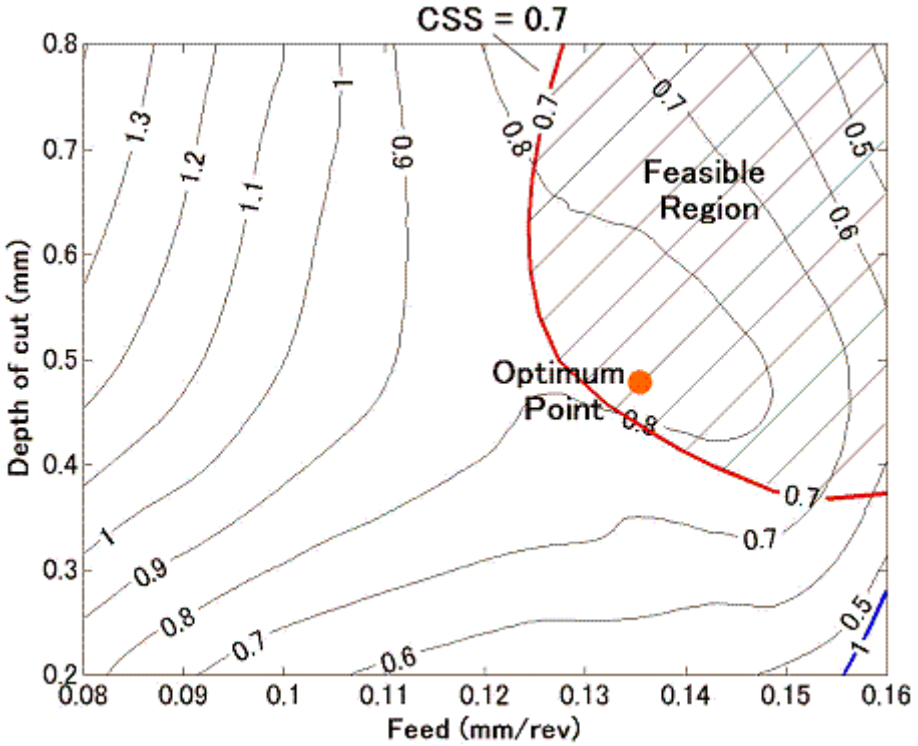

Figure 5.9: Optimization results for contour plot of Segment 6 for Case 1

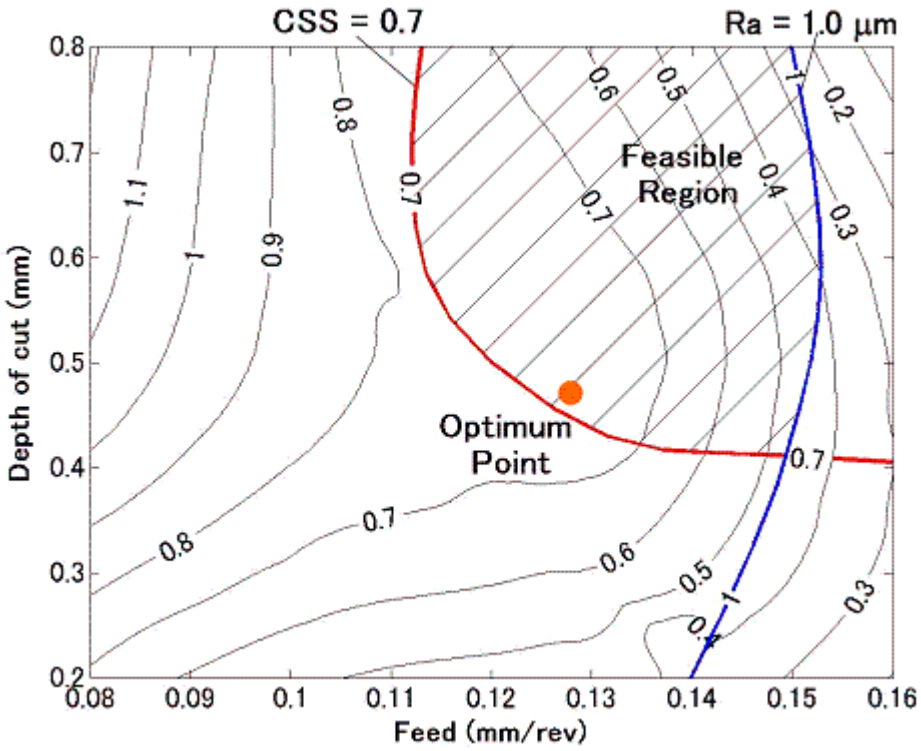

Figure 5.10: Optimization results for contour plot of Segment 7 for Case 1

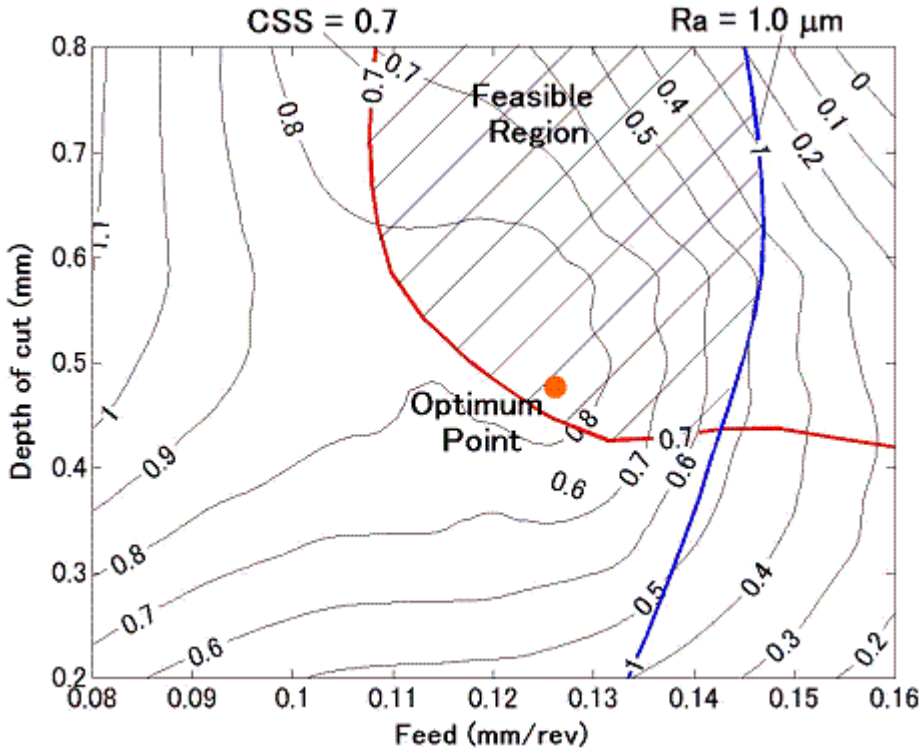

Figure 5.11: Optimization results for contour plot of Segment 8 for Case 1

Table 5.4: Optimization results for Case 2

Weighting Factors			C_R = 0.2, C_{CB} = 0.8							
Segment No.			**1**	**2**	**3**	**4**	**5**	**6**	**7**	**8**
Optimum Cutting Conditions	***d* (mm)**		**0.4518**							
	***f* (mm/rev)**		0.1600	0.1331	0.1349	0.1380	0.1338	0.1432	0.1311	0.1312
Predicted Average Machining Performance	R_{ai} **(μm)**		0.9232	0.8921	0.8664	0.9267	0.8795	0.8448	0.8699	0.8989
	CB(f,d)	CSS_i	0.7002	0.7510	0.7617	0.7587	0.7427	0.7935	0.7336	0.7436
		η_i **(deg.)**	-3.1963	67.2630	86.6702	67.6887	18.3129	-12.2858	20.4542	48.3100

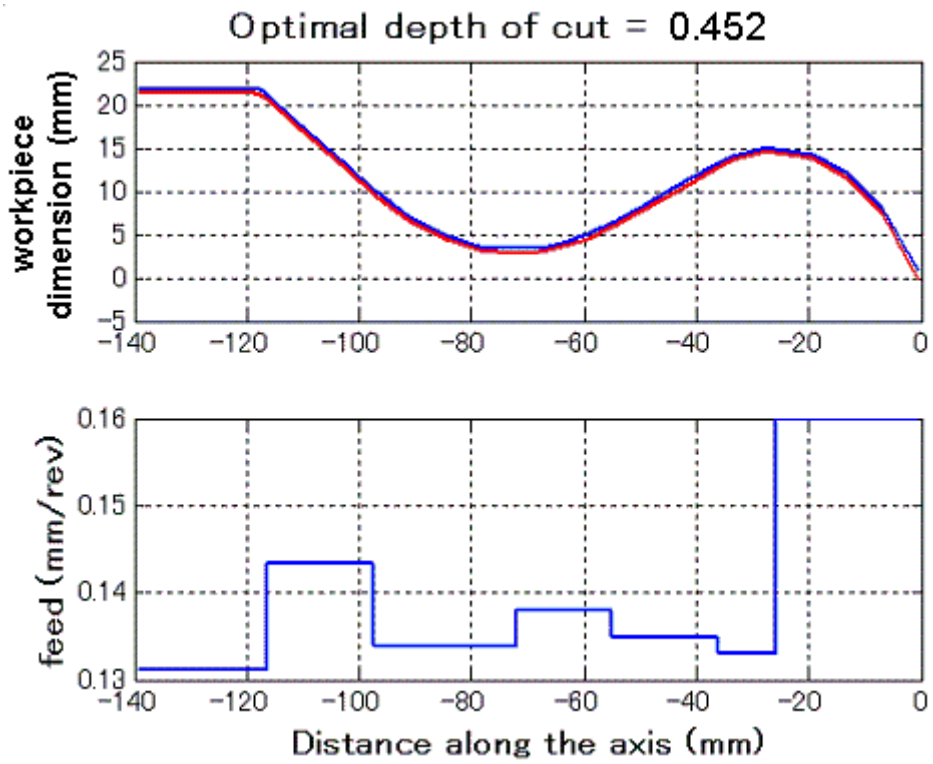

Figure 5.12: Optimized cutting conditions followed by workpiece geometry for Case 2

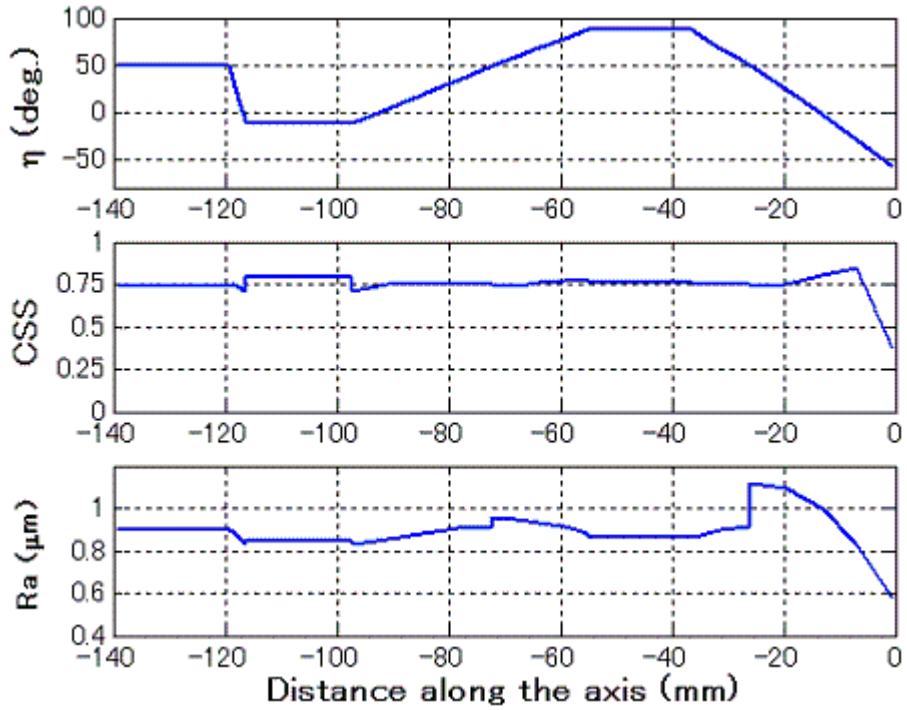

Figure 5.13: Predicted machining performance along the axis for Case 2

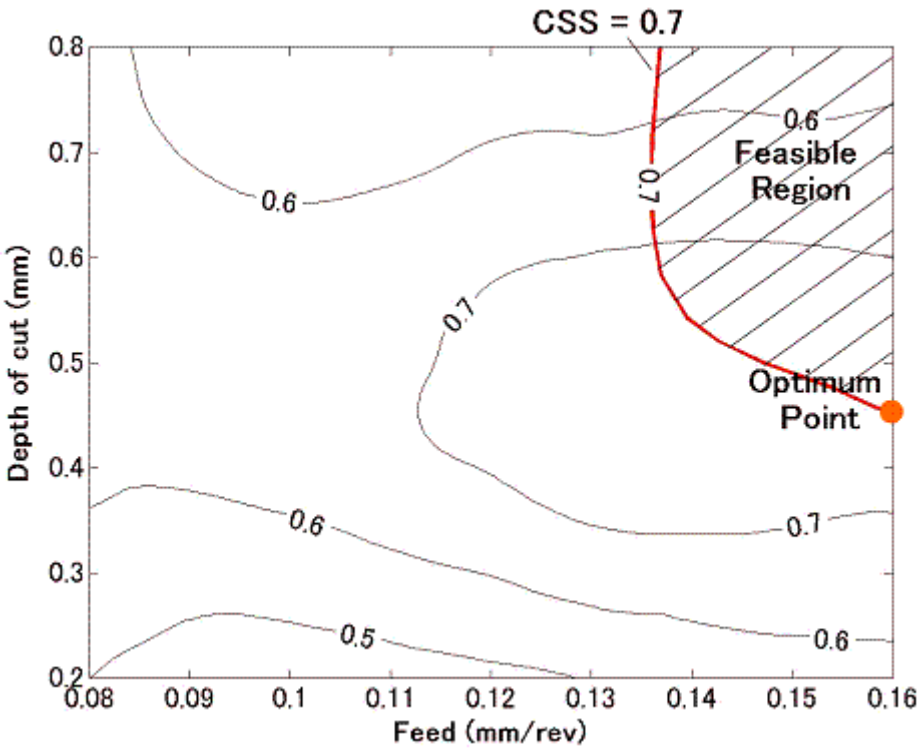

Figure 5.14: Optimization results for contour plot of Segment 1 for Case 2

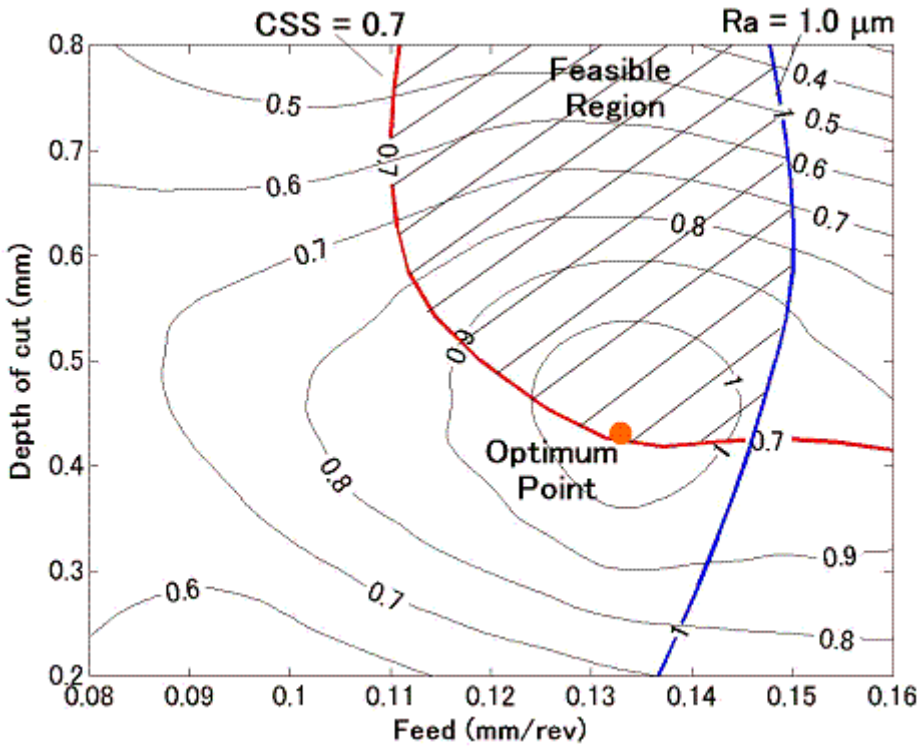

Figure 5.15: Optimization results for contour plot of Segment 2 for Case 2

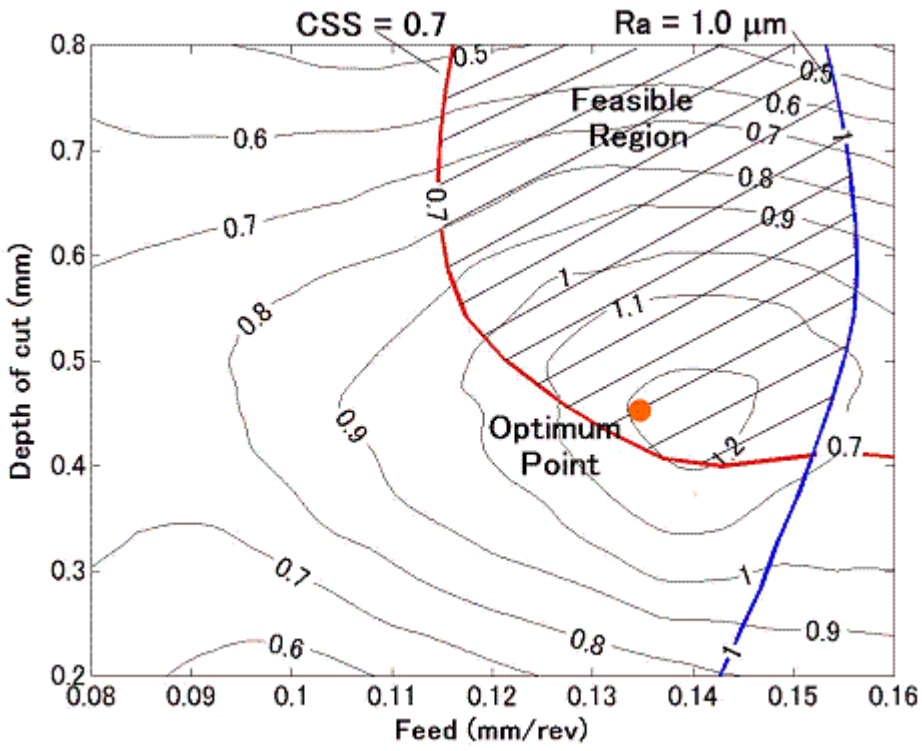

Figure 5.16: Optimization results for contour plot of Segment 3 for Case 2

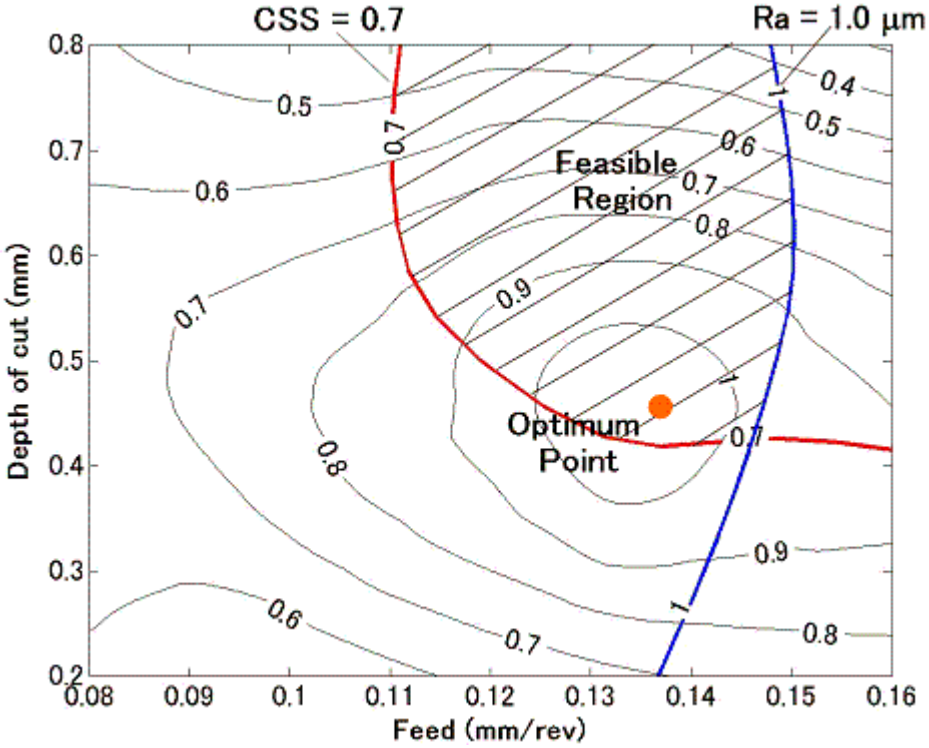

Figure 5.17: Optimization results for contour plot of Segment 4 for Case 2

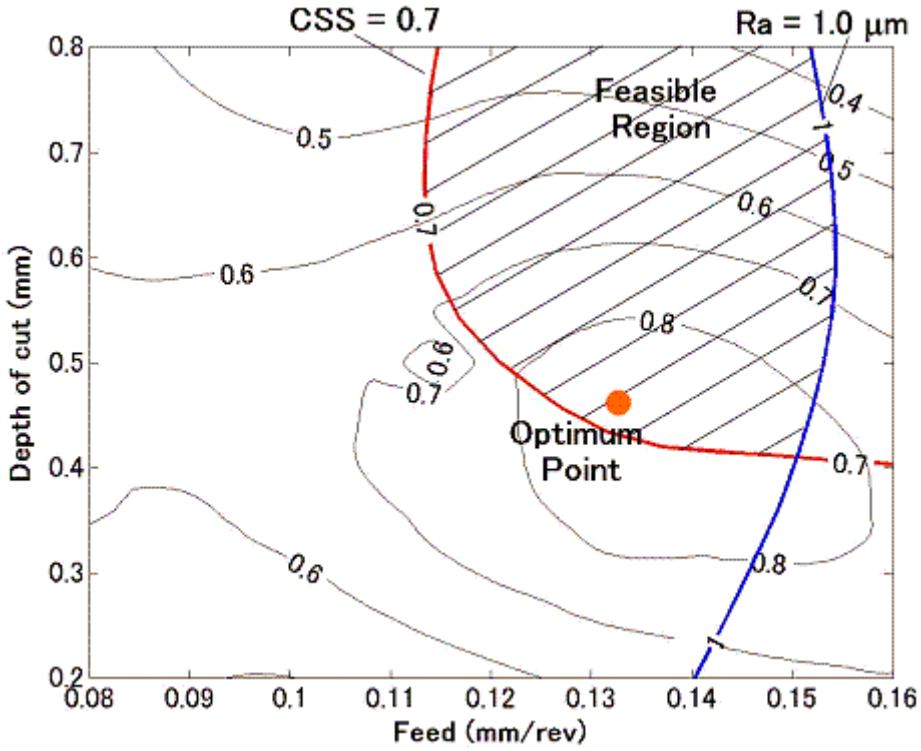

Figure 5.18: Optimization results for contour plot of Segment 5 for Case 2

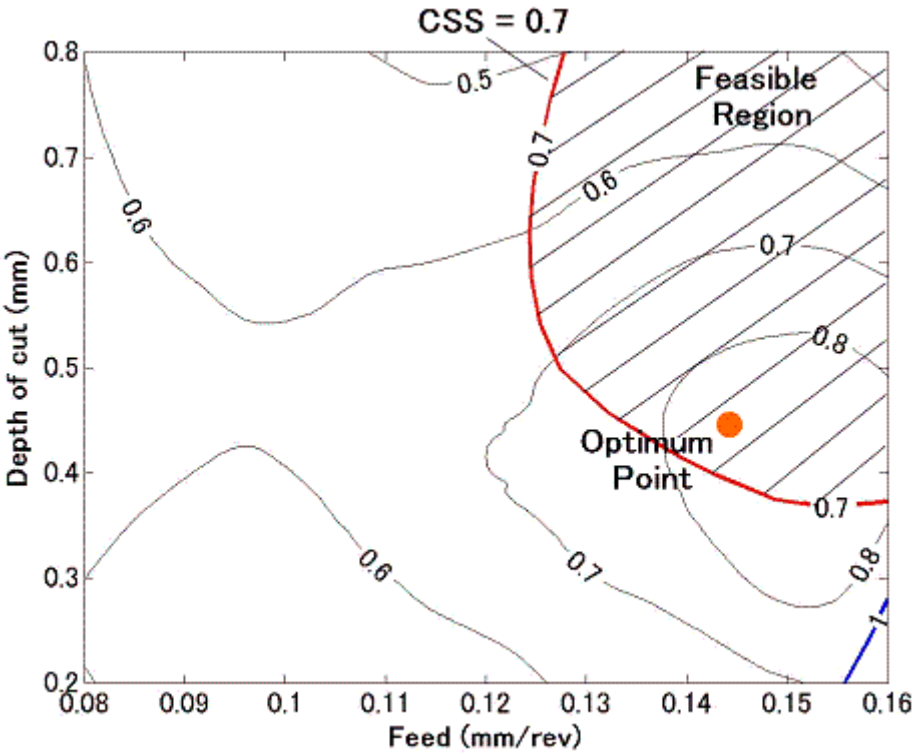

Figure 5.19: Optimization results for contour plot of Segment 6 for Case 2

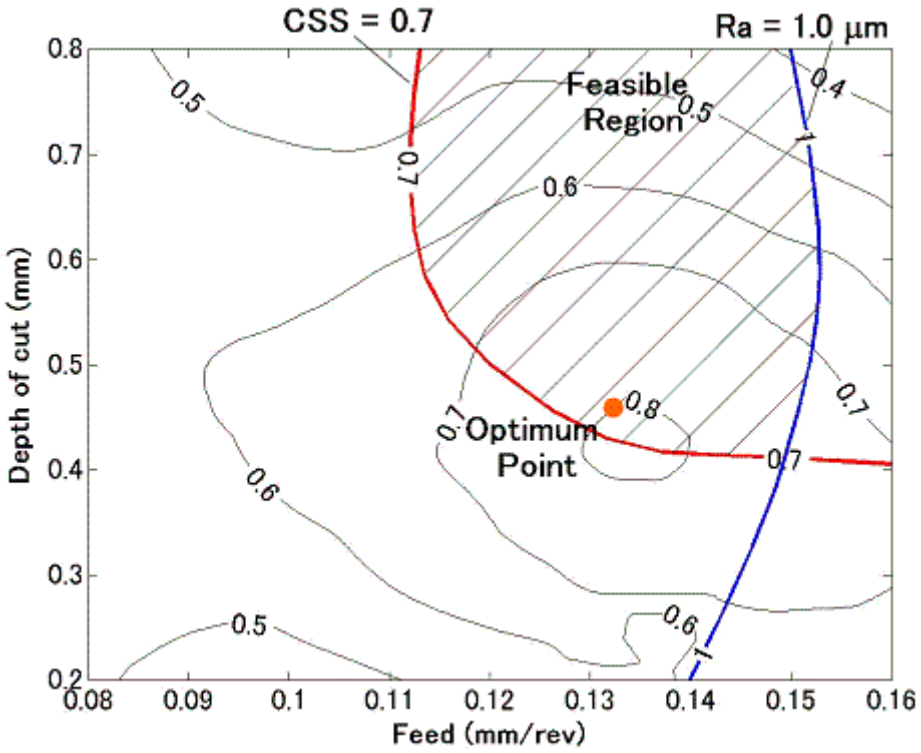

Figure 5.20: Optimization results for contour plot of Segment 7 for Case 2

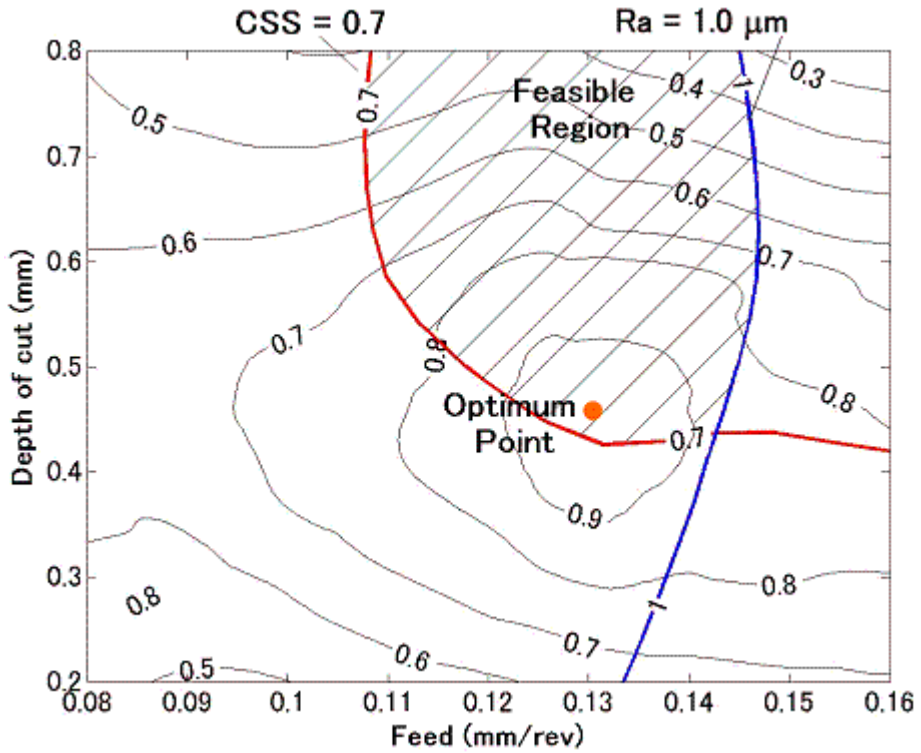

Figure 5.21: Optimization results for contour plot of Segment 8 for Case 2

Table 5.5: Optimization results for Case 3

Weighting Factors			C_R = 0.8, C_{CB} = 0.2							
Segment No.			**1**	**2**	**3**	**4**	**5**	**6**	**7**	**8**
Optimum Cutting Conditions	d (mm)		0.5760							
	f (mm/rev)		0.1375	0.1133	0.1274	0.1186	0.1293	0.1308	0.1143	0.1184
Predicted Average Machining Performance	R_{ai} (μm)		0.7694	0.7968	0.8140	0.8079	0.8288	0.7909	0.7901	0.8151
	$CB(f,d)$	CSS_i	0.7020	0.7138	0.8209	0.7705	0.8398	0.7609	0.7075	0.7889
		η_i(deg.)	-7.3506	59.7237	79.3048	60.4350	12.9240	-16.2843	15.0500	41.9064

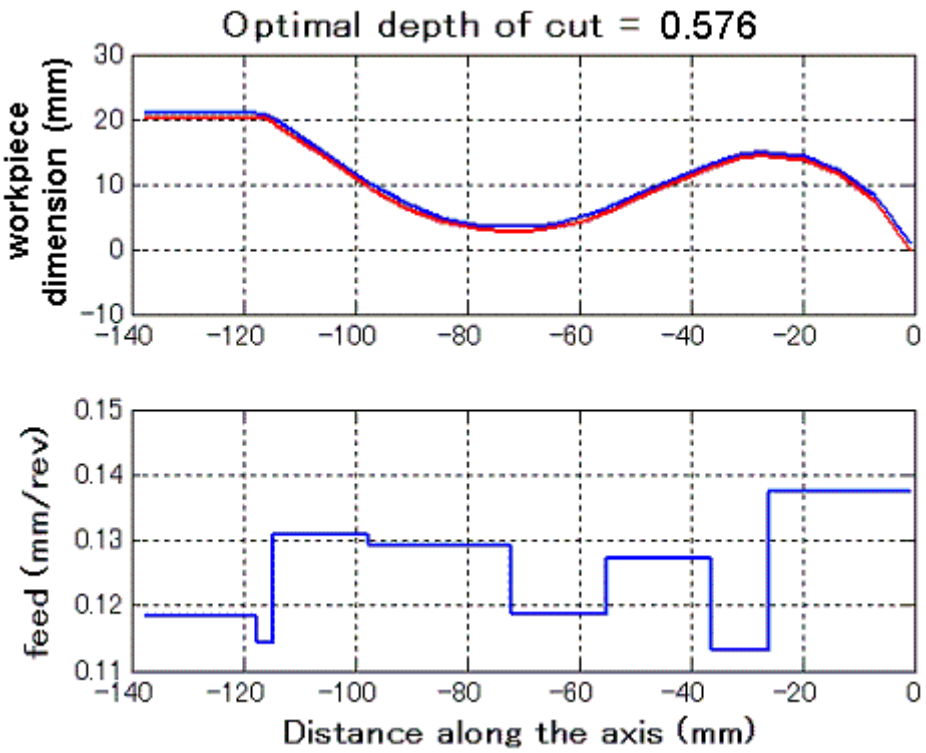

Figure 5.22: Optimized cutting conditions followed by workpiece geometry for Case 3

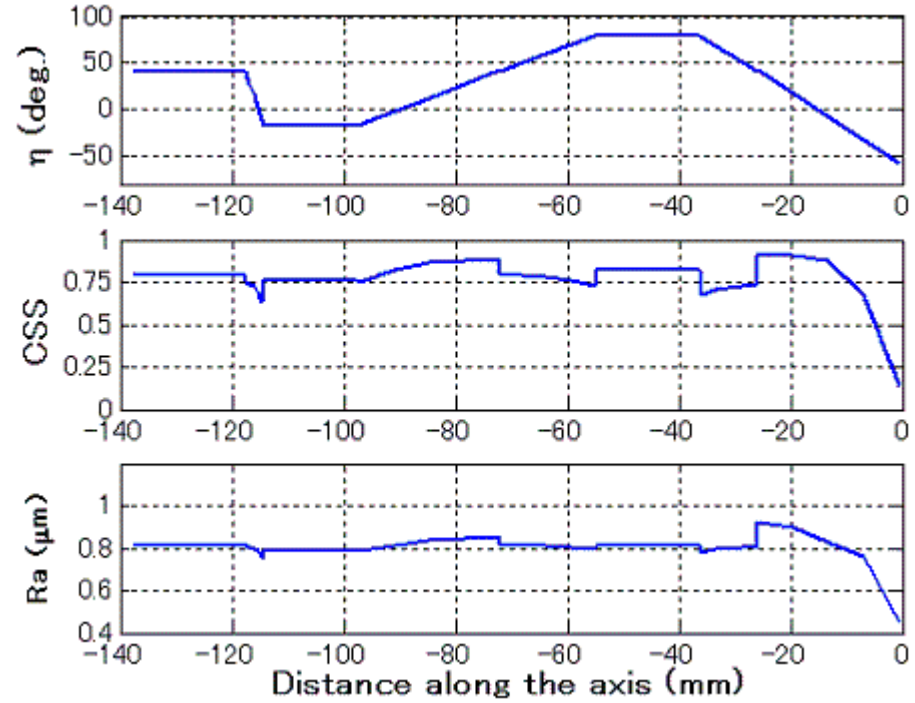

Figure 5.23: Predicted machining performance along the axis for Case 3

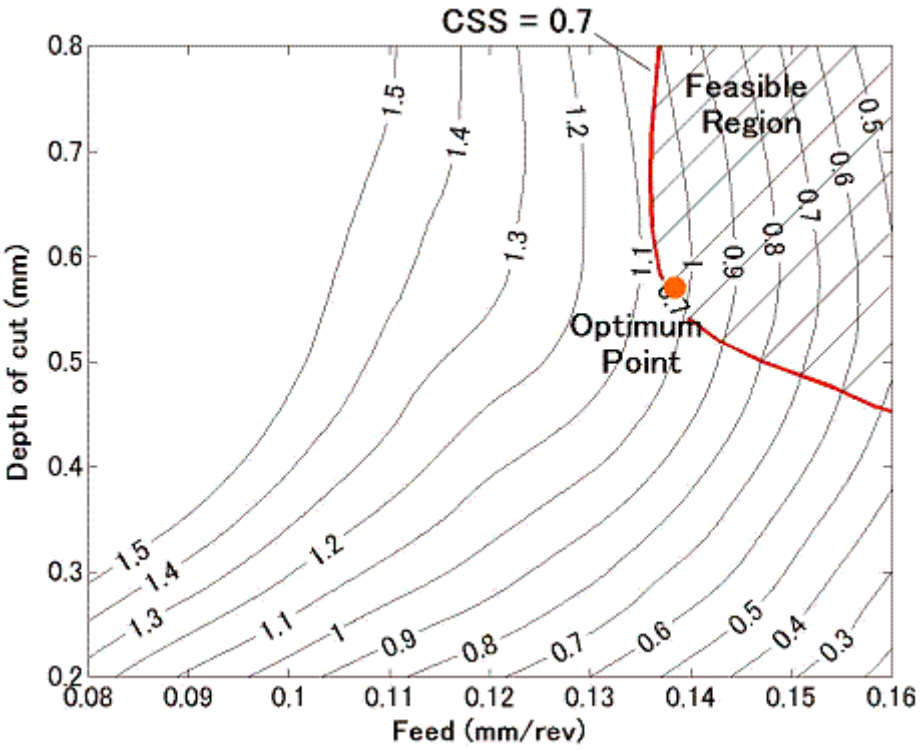

Figure 5.24: Optimization results for contour plot of Segment 1 for Case 3

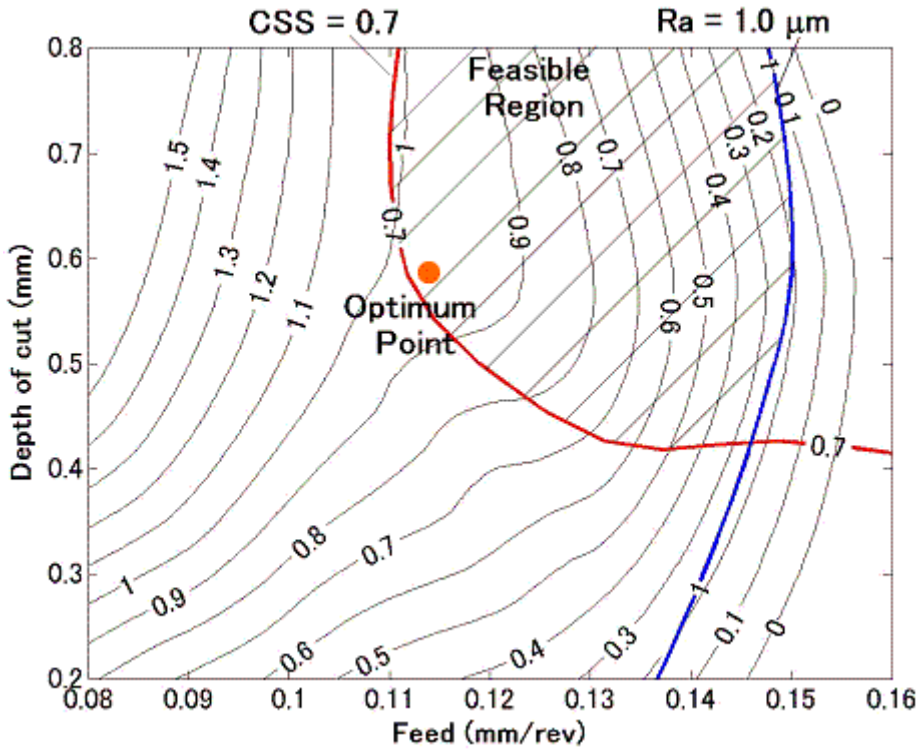

Figure 5.25: Optimization results for contour plot of Segment 2 for Case 3

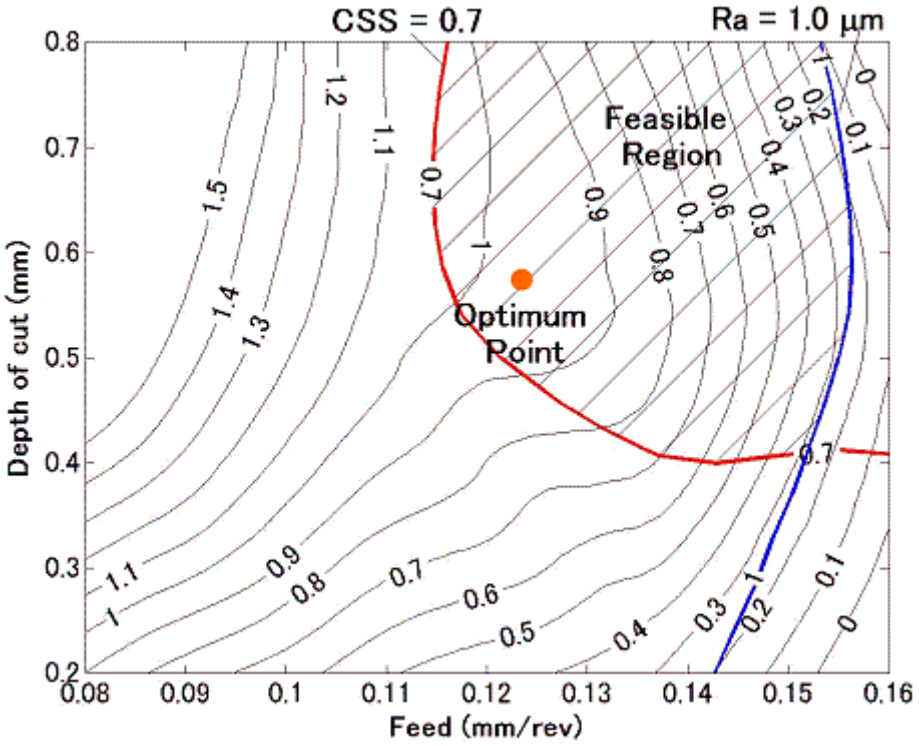

Figure 5.26: Optimization results for contour plot of Segment 3 for Case 3

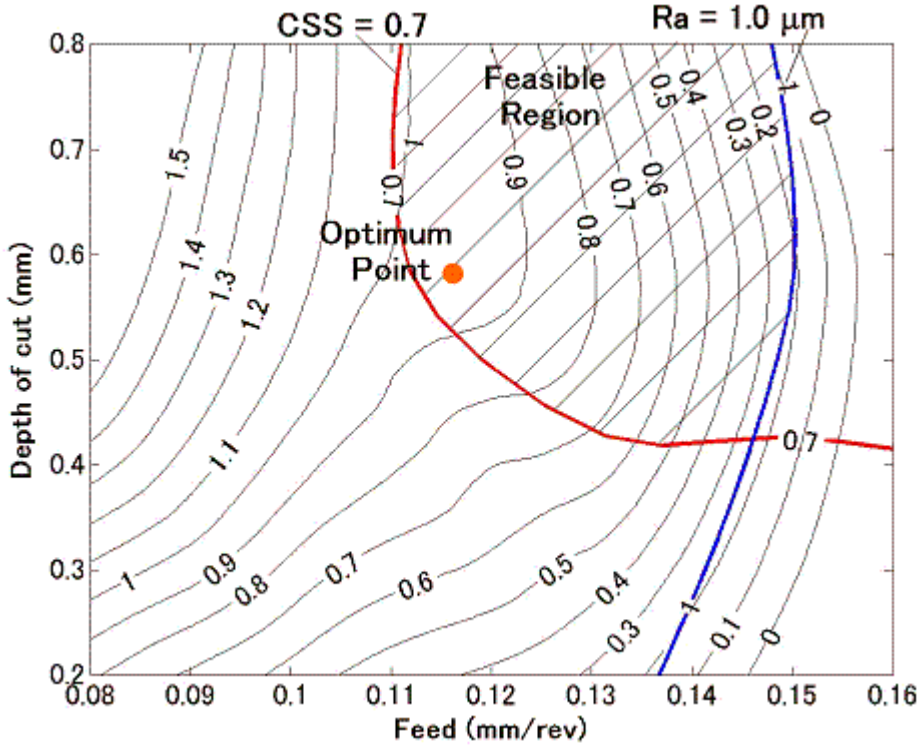

Figure 5.27: Optimization results for contour plot of Segment 4 for Case 3

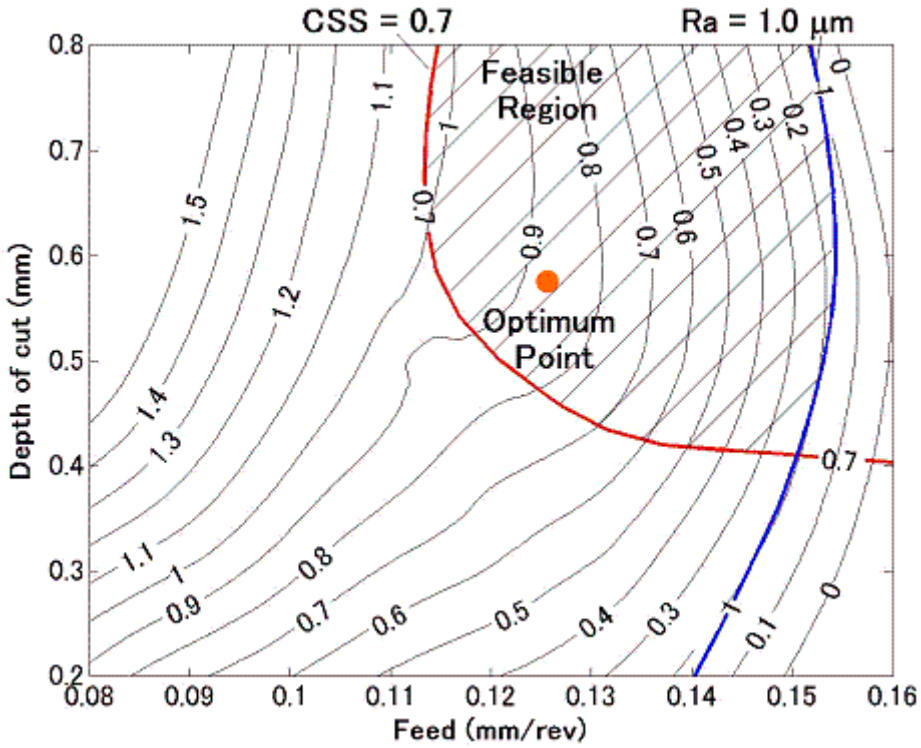

Figure 5.28: Optimization results for contour plot of Segment 5 for Case 3

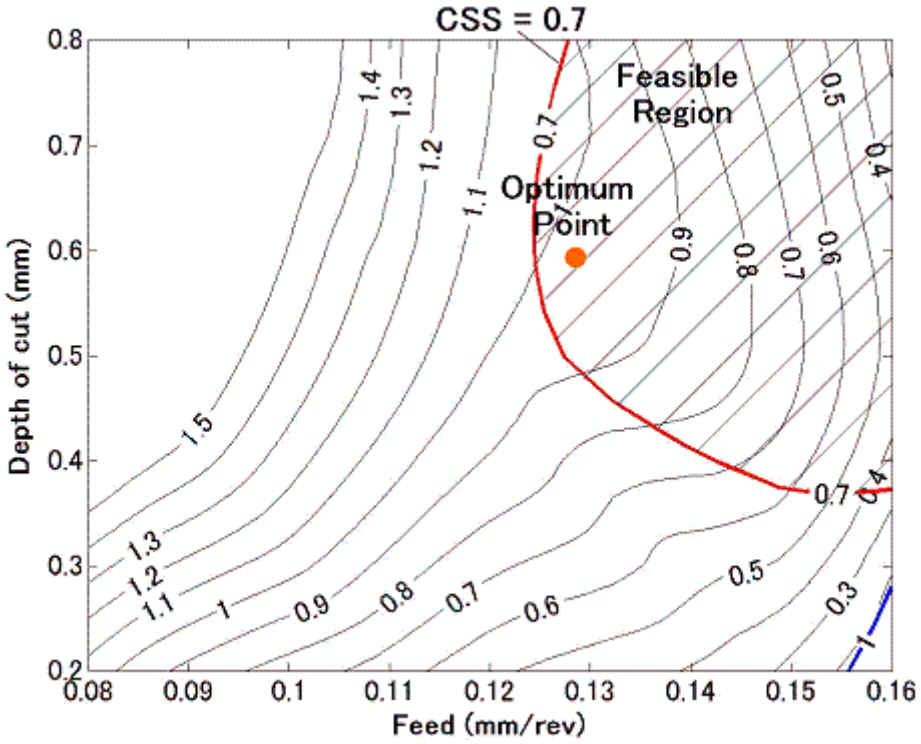

Figure 5.29: Optimization results for contour plot of Segment 6 for Case 3

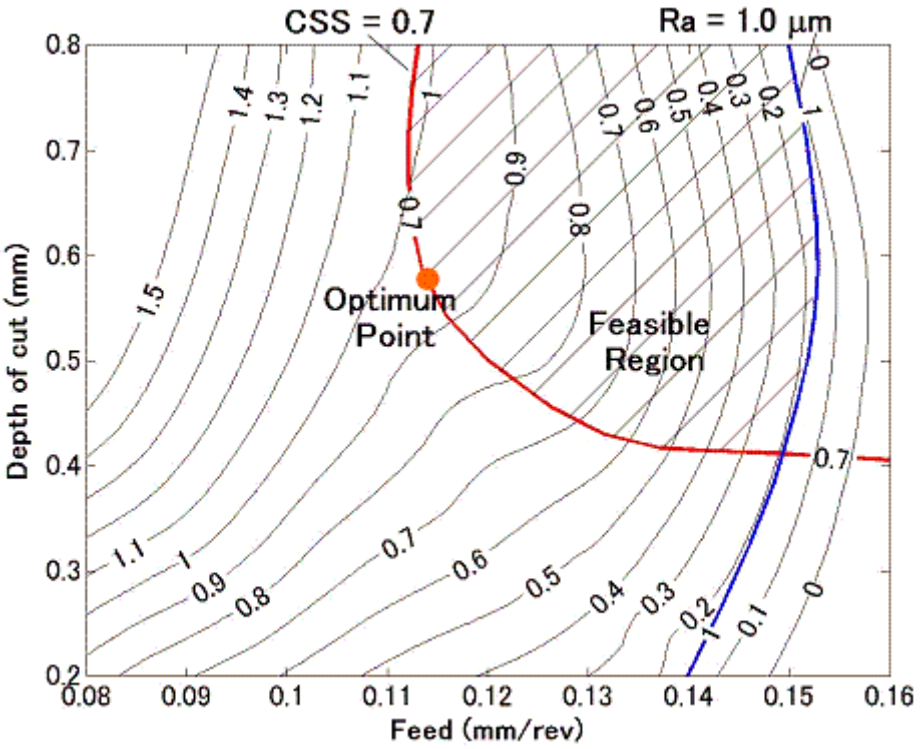

Figure 5.30: Optimization results for contour plot of Segment 7 for Case 3

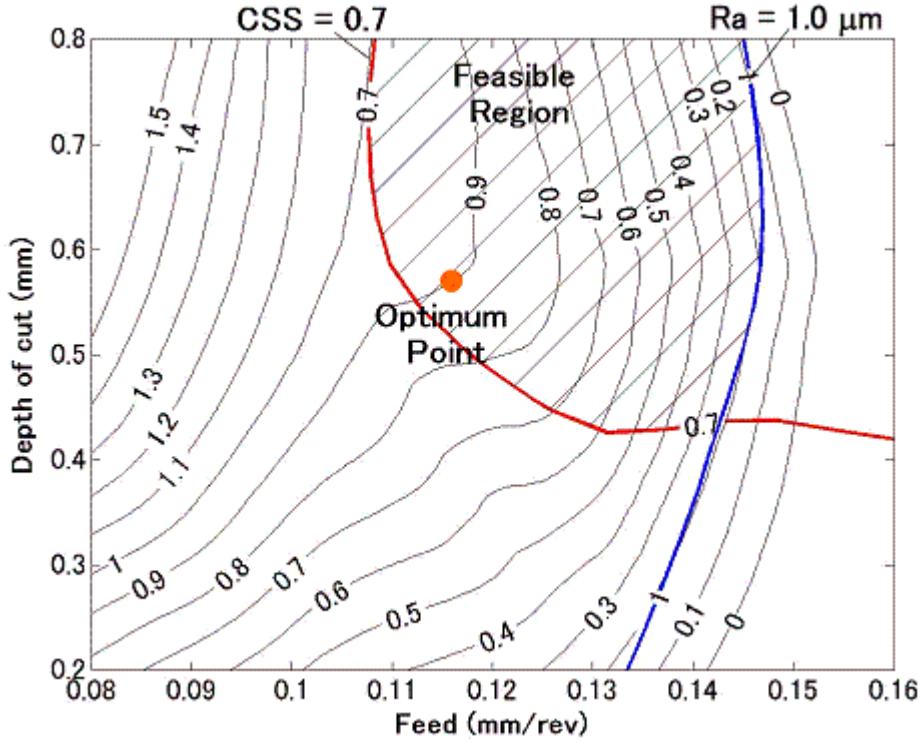

Figure 5.31: Optimization results for contour plot of Segment 8 for Case 3

5.2 Analysis of the Program Results

As shown in Section 5.1, the optimum feeds are changing thoroughly between the segments. This is because some regions have sharp curves and the effective cutting conditions in these regions change rapidly, while they do not change much in other regions. The optimal depth of cut and feeds are satisfied the all constraints and maximize the total utility function.

Figures 5.32, 5.33, and 5.34 show the comparison between the results for Cases 1, Case 2, and Case 3 according to the surface roughness, chip shape and size, and chip side-flow angle. When the weighting factor for chip breakability is larger than the weighting factor for surface roughness, the chip side-flow angle increases by 10-30% and the average chip shape and size, and surface roughness in the segments are satisfying the constraints where the membership value of chip shape and size is 0.7, and surface roughness is 1.0 μm. Thus, this optimum cutting conditions can provide a more favorable chip flow direction with required chip shape and surface roughness. On the other hand, when the weighting factor for surface roughness is larger, the optimum feeds are relatively smaller than other two cases. The average value of surface roughness in the whole workpiece profile is around 0.8 μm, and all chip shapes and sizes are satisfying the constraints. When the weighting factors are given equally, the results give well-balanced machining performance between chip breakability and surface roughness.

The reason for the negative chip side-flow angle at Segment 1 and 6 is due to the high gradients of the workpiece profile. In these regions, the axial feed becomes very small while effective depth of cut becomes very large. Chip side-flow angle decreases with

decreasing feed and increasing depth of cut. Also, the effective side-cutting edge angle is very small in these regions allowing for chip to flow negative directions.

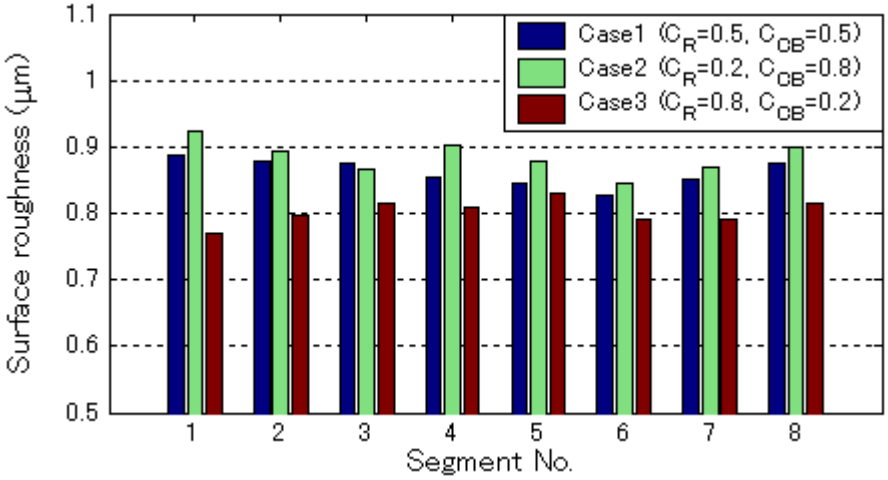

Figure 5.32: Predicted average surface roughness values for Cases 1, 2 and 3

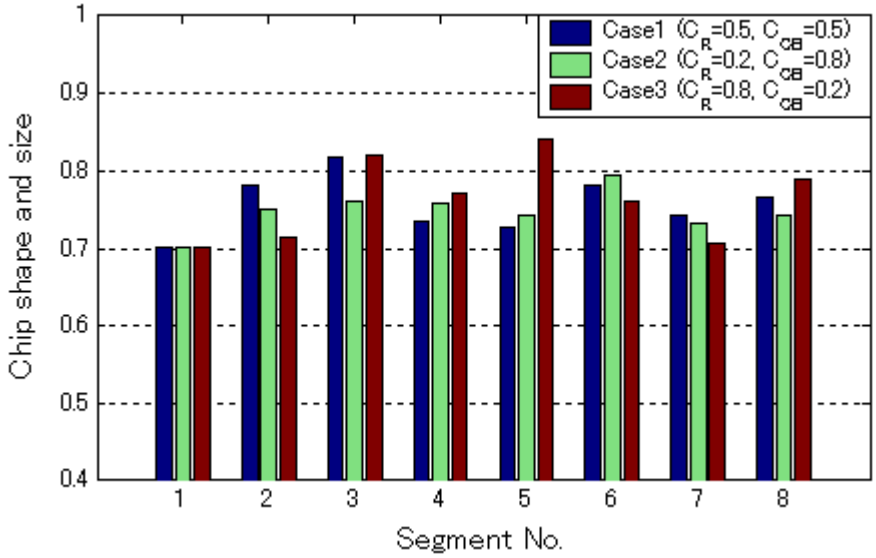

Figure 5.33: Predicted average chip shape and size for Cases 1, 2 and 3

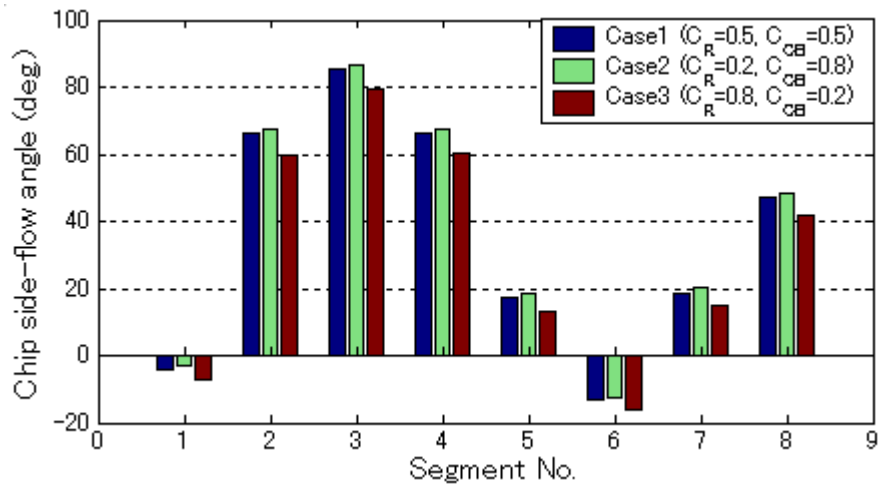

Figure 5.34: Predicted average chip side-flow angle for Cases 1, 2 and 3

5.3 Program Results Validation

Three additional experiments were conducted to validate the optimization results using the workpiece with the profile shown in Figure 5.1. The work material is AISI 1045 steel and VBMT 332-UM is used as the cutting tool. As a comparison, one of the experiments was carried out under the optimum cutting conditions for Case 2, which was 0.4518 mm depth of cut, and various feeds shown in Table 5.4, and other two experiments were carried out under the depth of cut close to the optimum, which was 0.4 mm, and small and large feeds, which were 0.10 mm/rev and 0.16 mm/rev respectively. The cutting speed was kept constant at 250 m/min in all of three experiments. In order to compare the machining performance between optimum cutting conditions and randomly selected cutting conditions, a high speed filming camera (KODAK motion analyzer) was used to record the chip breakability. Surface roughness was also measured.

Figure 5.35 shows the snap shots from the high speed filming at four selected positions, which are Segment 1, 3, 5, and 8. Since the gradient of the initial position (Segment 1) is very steep, the axial feed becomes much smaller than tangential feed. In these conditions, it is difficult for the chip to break and hence the chip tends to be long. In the case of the constant feed at 0.10 mm/rev, long and snarling chips totally adhered to the toolface and did not fall off till the end of the machining. These adhered chips were also affecting the chip flow of subsequently formed chips. This can deteriorate the machined surface as well as the adhered chip itself.

Segment 1	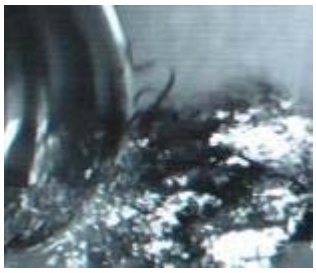		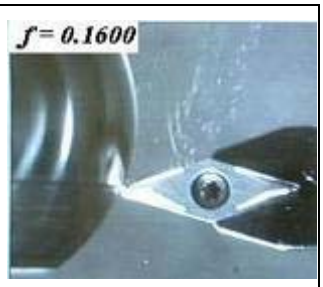
Segment 3			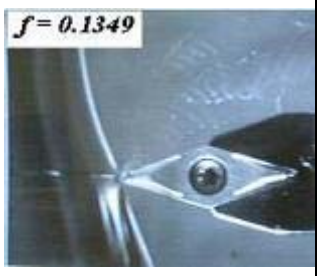
Segment 5			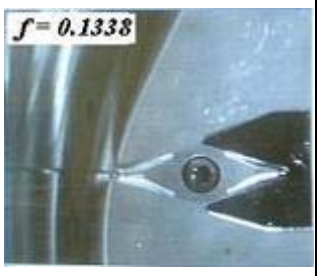
Segment 8		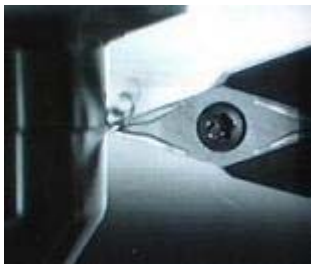	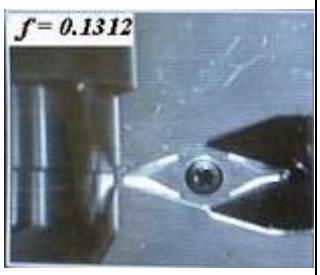
	f = 0.10 mm/rev (constant) d = 0.4 mm (constant)	f = 0.16 mm/rev (constant) d = 0.4 mm (constant)	Optimization results (C_R = 0.2, C_{CB} = 0.8) d = 0.4518 (constant)

Figure 5.35: Comparison of the chip breakability between randomly selected cutting conditions and optimization program results for Case 2 at the Segments 1, 3, 5, and 8 from above.

Comparing with the 0.16 mm/rev constant feed and optimum feeds, the chip shape is notably different even with the same feed in Segment 1. This is because of the difference in the depth of cut. The difference in the nominal depth of cut is only 0.05 mm. However, when it comes to the effective depth of cut, the difference between the constant conditions and optimum conditions becomes large at the initial point due to the high gradient of the workpiece profile. According to Figure 4.8, chip shape and size are very sensitive in the region of small depth of cut and hence, the chip shape is completely different. Also, in other segments, all of the optimum feeds are less than 0.16 mm/rev, but the chip breakability is still almost same or even better than the constant feed of 0.16 mm/rev.

Figure 5.36 shows the measured surface roughness after conducting these three experiments. In accordance with the theory, a smaller feed gives the smaller surface roughness value and larger feed gives the larger surface roughness. However, the surface roughness value of the 0.01 mm/rev constant feed at the Segment 8 is extremely high. A major reason for this can be that the snarling chip on the tool face prevents the chip from flowing properly and the chip bounces back onto the machined surface, thereby, damages it. For the feed of 0.16 mm/rev, the surface roughness value is about 0.2 μm higher than the optimum cutting conditions in the Segment 1 in spite of the same feed values. This can be a result of the snarling chip deteriorating the machined surface. On the other hand, the results for the optimum cutting conditions are well balanced and under control.

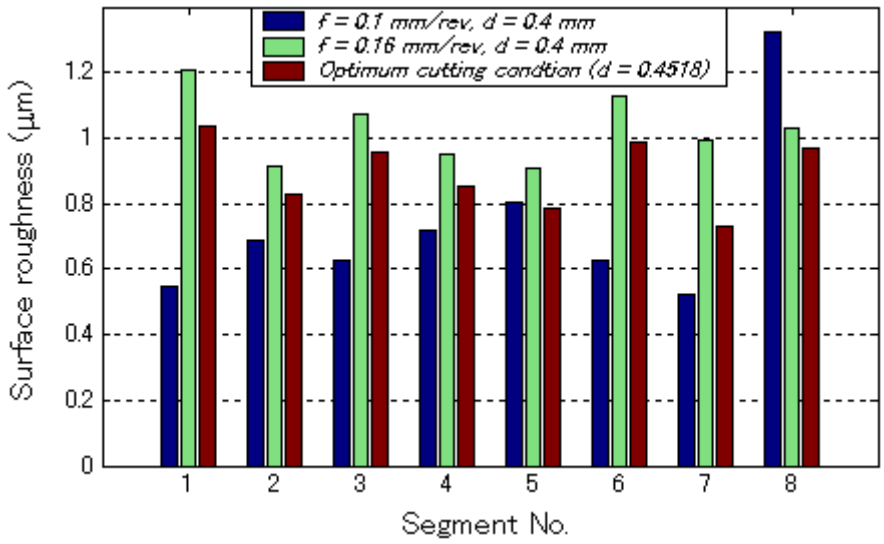

Figure 5.36: Comparison of the surface roughness between constant conditions and optimum cutting conditions

In summary, the experimental results show that the optimum cutting conditions give better chip breakability in any regions of the workpiece profile. When it comes to the surface roughness, the constant feed of 0.10 mm/rev gives better surface roughness in most of the segments, but it also has irregular and high surface roughness, presumably, because of the poor chip breakability. On the contrary, the surface roughness is quite controllable under the optimum cutting conditions. Since these optimum cutting conditions are the results from the Case 2 in Section 5.1, which is weighting on chip breakability much more than surface roughness, this optimization results are quite successful.

CHAPTER 6

CONCLUSIONS AND FUTURE WORK

6.1 Summary of Present Research Work

Contour turning operations are more practical comparing to straight turning. Almost all industrial products have some curvatures to be machined and the cutting conditions are continuously changing along the workpiece profile. In this research work, two major accomplishments are made:

1, Chip side-flow prediction with complex grooved tool inserts in contour turning operations

2, Optimization of machining performance in contour finish turning operations

The hybrid models of Redetzky et al. [5] and Ghosh et al. [18] are applied, with calculated effective cutting parameters and tool geometries, to simulate the chip side-flow angles along the workpiece profile. Since this simulation model does not depend on the workpiece geometry, it can be applied to any workpiece geometry by changing the input parameters of the workpiece profile as long as the work material and cutting tool remain the same. Hence, it is also possible to modify or optimize the original product design features using this simulation program to make the chip flow in the most favorable direction.

Once the simulation model is established, then the next step was to optimize the cutting conditions to improve the machining performance. Two major machining performance measures, chip breakability, and surface roughness are selected in this thesis work because of their relative importance to finishing operations. The goal of this optimization is determine the optimum cutting conditions according to the workpiece segments in order to improve the machining performance. By configuring weighting factors and constraints for chip breakability and surface roughness, the best cutting conditions, fulfilling the required machining performance, can be obtained.

The results of the validation experiments show that small constant feeds tend to give good surface roughness, but the chip breakability is so poor that surface is deteriorated. On the other hand, a larger constant feed tends to give good chip breakability but surface roughness is poor as expected. Moreover, even a small difference in the depth of cut gives a larger difference in the chip breakability because of the effective depth of cut making the effect of the depth of cut larger in contour turning operations. The optimum cutting conditions give better chip breakability and surface roughness with the performance fulfilling requirements. In other word, it is maximizing the machining performance under the user-selected constraints.

6.2 Suggestions for Future Work

This research work focused on optimizing cutting conditions, namely the feeds and depth of cut. Since all simulation and optimization results are stored as data, it is possible to integrate this with other software. For example, by integrating suitable

CAD software with this optimization program, the all required data could be automatically used as input for the optimization program from CAD. Also, the CNC-code to operate the CNC turning machine can be provided as the output of the optimization results since all workpiece configurations and cutting conditions are stored. In effect, this new optimization method can greatly help the machining process planners by providing the most-needed optimization module in the computer-aided process planning systems (CAPP).

It is also possible to determine the optimum cutting tool configurations and chip breaker from tool selections. By creating a database for each tool insert, an evaluation of which tool gives a larger utility function can be made, but this requires much more experimental work.

Another possibility is to optimize a product design in order to make chip flow in a favorable direction. In most cases, the design of a product has some flexibility to change unless the change affects the product's function and concepts. By giving constraints for workpiece geometry, optimum product design can be determined.

APPENDIX

GRAPHICAL USER INTERFACE

In most computer programming, the usability is one of the main factors to determine the quality of the work as well as the capacity of the program itself. Even high capability computer programming work will be wasted, if it is too difficult to handle it, or the usage is limited. Programming code is not easy to understand with no knowledge of the programming language. Thus, it is very important to develop the program with more user-friendly for easy use.

In this thesis work, an optimization program for contour finish turning operations has been developed. The optimization program can determine the optimal cutting conditions, namely, feeds and depths of cut, in contour turning operations based on the chip breakability and surface roughness criteria. The user can apply this program for any workpiece profile by changing input data such as the workpiece geometry and the tool inserts. However, it is quite difficult to input the data to the program code since the program code is very complicated. Therefore, Matlab-based Graphical User Interface (GUI) has been developed in this research so that it can be easy to have access by industries or researchers as shown in Figure A.1.

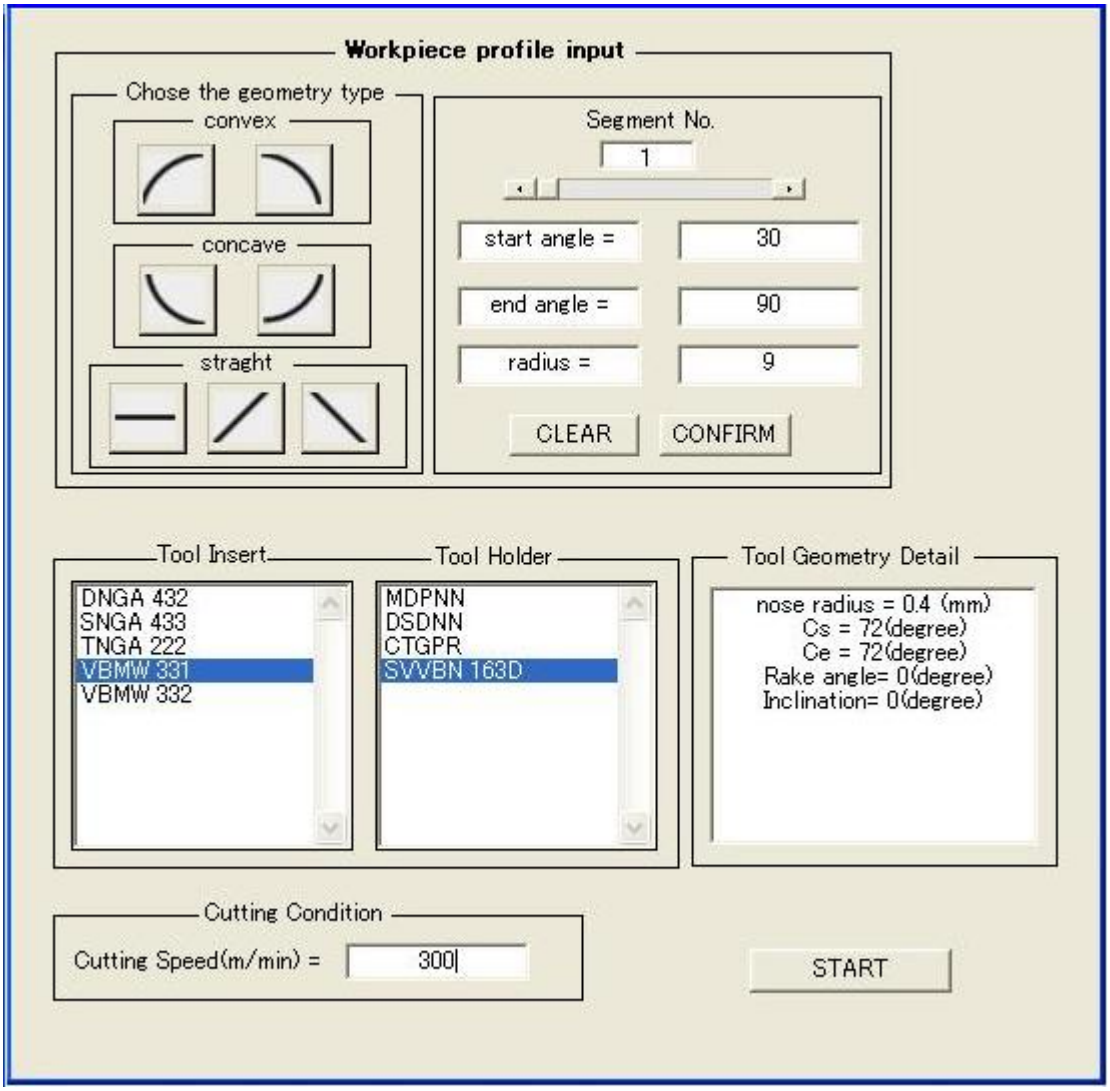

Figure A.1: Matlab-based graphical user interface

In order to use this optimization program, the only thing needed is to follow the graphics and input the workpiece geometry data, choose tool insert and holder, and input the cutting speed at the proper box. The description of this GUI is as follows:

1. Choose the geometry type from the left upper figure for the segment.
2. If convex or concave shape was chosen, the dialog box at the right upper shows start angle, end angle and radius. Then, enter the data on the right side box according to your workpiece geometry. If a straight line was chosen, the dialog box shows the slope and length. Then enter the data.

3. Click the “CONFIRM” button if the input data is correct. Then the figure that you input will show up on the different window (Figure A.2). If not click the “CLEAR” button and go back to 1 again.
4. Choose the workpiece geometry type of the next segment, and repeat 2-3 until the figure creates the whole workpiece profile that you want.
5. Choose the tool insert and holder which you need to use from the left lower dialog box. Then, details of the tool inserts and the tool holder such as nose radius, side-cutting edge angle, end-cutting edge angle, rake angle and inclination angle will show up on the right side dialog box.
6. Enter the cutting speed on the lower right dialog box. Then, click “START” to run the optimization program.
7. Results of the optimal cutting conditions will show up on a different window after finishing the program (Figure A.3).

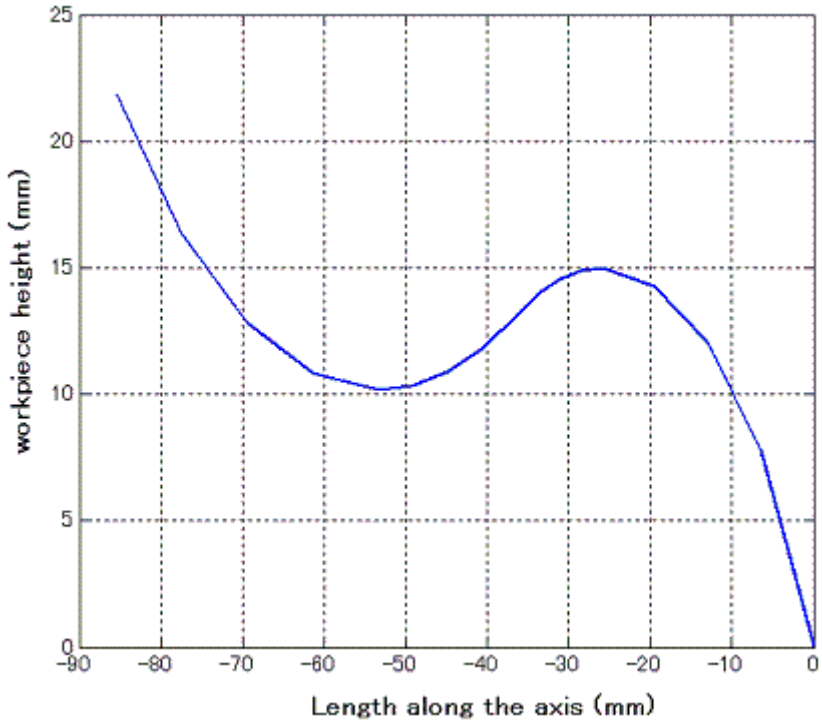

Figure A.2: Constructed geometry figure
(After "CONFIRM" button is clicked, the figure will show up)

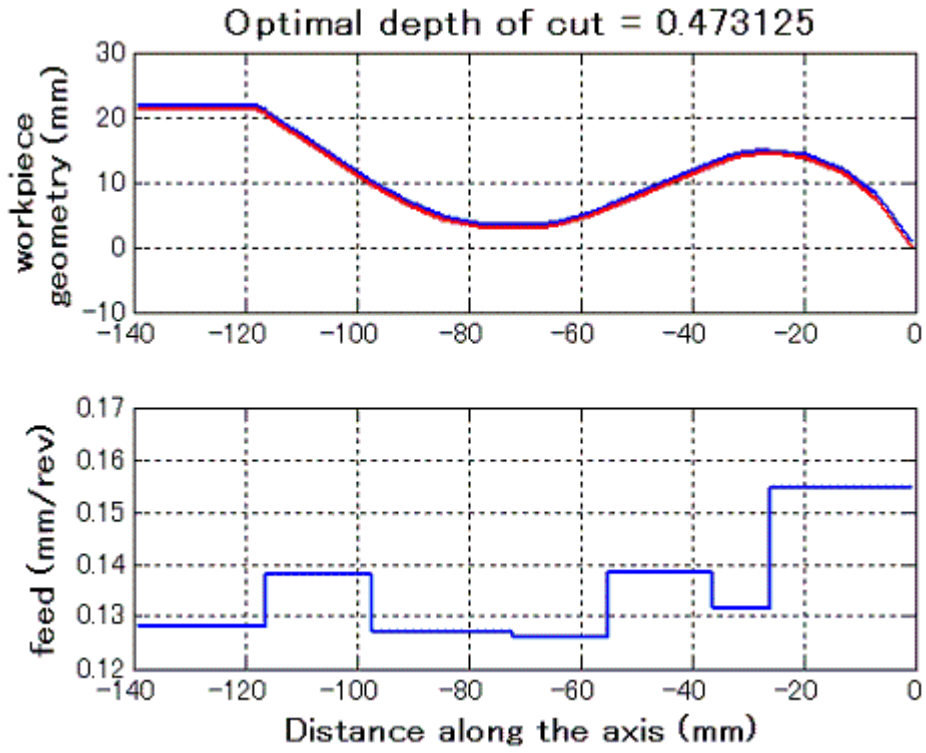

Figure A.3: The program output figure

REFERENCES

[1] I.S. Jawahir and C.A. van Luttervelt, "Recent Developments in Chip Control Research and Application", *Annals of the CIRP*, Vol 42 (2), 1993, p. 659.

[2] I.S. Jawahir, "The Chip Control Factor in Machinability Assessments: Recent Trends", *Journal of Mechanical Working Technology*, Vol. 17, 1988, p. 213.

[3] X. Wang, Z.J. Da, A.K. Balaji, and I.S. Jawahir, "Performance-based Optimal Selection of Cutting Conditions and Cutting Tools in Multi-pass Turning Operations using Genetic Algorithms", *Int. J. Production Research,* Vol. 40 (9), 2002, p. 2053.

[4] L.V. Colwell, "Predicting the Angle of Chip Flow for Single-Point Cutting Tools", *Trans. ASME*, 76, 1954, p. 199.

[5] M. Redetzky, A.K. Balaji, and I.S. Jawahir, "Predictive Modeling of Cutting Forces and Chip Flow in Machining with Nose Radius Tools", *Proc. 2nd CIRP Int. Workshop on Modeling of Machining Operations*, Nantes, France, January 1999, p. 160.

[6] R. Ghosh, "An Investigation of 3-D Chip Flow, Curl and Breaking in Machining with Grooved Tools", *PhD Thesis*, University of Kentucky, 1996.

[7] K. Okushima and K. Minato, “On the Behavior of Chip in Steel Cutting”, *Bull. Jap. Soc. Mech. Eng*. Vol. 2(5), 1959, p. 58.

[8] G.V. Stabler, “The Fundamental Geometry of Cutting Tools”, *Proc. Inst. Mech. Eng.*, Vol. 165, 1951, p. 14.

[9] G.V. Stabler, “The Chip Flow Law and Its Consequences”*, Proc. 5th Intl. J. Mach. Tool Des. Res. Conf*., Pergamon, Oxford, 1964, p. 243.

[10] K. Nakayama, “Chip Form Geometry – Study on the Form of Chip in Metal Cutting (Part 1)”, *J of JSPE*, Vol. 38, 7, 1972, p. 34.

[11] K. Nakayama, M. Ogawa and H. Takeyama, “Basic Rules on the Form of Chip in Metal Cutting”, *Annals of the CIRP*, Vol. 27, 1978, p. 17.

[12] H.T. Young, P. Mathew and P.L.B. Oxley, “Allowing for Nose Radius Effects in Predicting the Chip Flow Direction and Cutting Forces in Bar Turning”, *Proc. Inst. Mech. Eng*., C201 (C3), 1987, p. 213.

[13] J. Wang and P. Mathew, “Development of a General Tool Model for Turning Operations Based on a Variable Flow Stress Theory”, *Int. J. Mach. Tools Manufact*., Vol. 35(1), 1995, p. 71.

[14] J. Wang, “Development of a chip flow model for turning operation”, *International*

Journal of Machine Tools & Manufacture, Vol. 41, 2001, p. 1265.

[15] J.A. Arsecularatne, P. Mathew, and P.L.B Oxley, "Prediction of Chip Flow Direction, Cutting Forces in Oblique Machining with Nose Radius", *Proc. Inst. Mech. Eng*., 209, 1995, p. 305.

[16] J.A. Arsecularatne, R.F. Fowle, and P. Mathew, "Prediction of Chip Flow Direction, Cutting Forces and Surface Roughness in Finish Turning", *Journal of Manufacturing Science and Engineering*, Vol. 120, Feb 1998, p. 1.

[17] R. Ghosh and I.S. Jawahir, "New Methodology for Estimating the Chip-Flow Direction in Oblique Machining Using Measured Cutting Forces", *CRMS Internal Report*, Manufacturing Process, 1/1993, University of Kentucky, 1993.

[18] R. Ghosh, X.D. Fang, and I.S. Jawahir, "Estimation of Chip Side-flow in Machining with Complex Grooved Tools Using a Force Ratio Method", *Proc. Conf. On The Physics of Machining Processes II*, Chicago, November 1994, p. 233.

[19] M. Redetzky, "Prediction of Feed Force and Passive Force and Their Application in Technical Constraints for Ensuring Precision Manufacturing", Dresden Techn. Univ., Dr.-Ing. Diss, 1979.

[20] M. Redetzky, "A Novel Methodology for An Universal Prediction of All

Components of The Resultant Cutting Force", Wiss. Z. Techn. Hochsch. Karl-Marx-Stadt, 27(6), 1985, p. 951.

[21] M. Redetzky, "Prediction of The Chip-flow Direction in Turning with Carbide Tools", Wiss. Z. Techn. Univ. Magdeburg, 31(7), 1987, p. 40.

[22] M. Redetzky, R. Ghosh and I.S. Jawahir, "A Predictive Model for Cutting Forces and Chip Flow in Finish Turning with Flat-faced Tools", *CRMS Internal Report* MC/1, University of Kentucky, 1995.

[23] F.W. Taylor, "On the Art of Cutting Metals", *Transactions of the ASME*, Vol. 28, 1907, p. 31.

[24] W.W. Gilbert, "Economics of Machining", *Machining – Theory and Practice*, *American Society for Metals*, 1950, p. 465.

[25] W.W. Gilbert, "Machining with Carbides and Oxides", *American Society of Tool and Manufacturing Engineering*, 1962.

[26] K. Okushima, and K. Hitomi, "A Study of Economical Machining; An Analysis of the Maximum Profit Cutting Speed", *International Journal of Production Engineering Research*, Vol. 3(1), 1964, p. 73.

[27] L.H. Tee, S.C. Ho, and M.F. DeVries, "Economic Machining Charts", *ASME*

Paper, 1965, No. MR 69.

[28] G. Boothroyd and P. Rusek, “Maximum Rate of Profit Criteria in Machining”, Journal of Engineering for Industry, *Transactions of the ASME*, Vol. 98, 1976, p. 217.

[29] D.S. Ermer, “Optimization of the Constrained Machining Economics Problem by Geometric Programming”, *Journal of Engineering for Industry*, *Transactions of ASME*, Vol. 93, 1971, p. 1067.

[30] J.S. Agapiou, “The optimization of Machining Operations Based on a Combined Criterion, Part1: The Use of Combined Objectives in Single-pass Operations”, *ASME Journal of Engineering for Industry*, Vol. 114, 1992, p. 500.

[31] Z.J. Da, J.P. Stabler, X.D. Fang, and I.S. Jawahir, “Optimum Machining Performance in Finish Turning with Complex Grooved Tools”, *Manufacturing Science and Engineering*, MED-vol. 2-1/MH-vol. 3-1, ASME, 1995, p. 703.

[32] Z.J. Da, J.P. Stabler, and I.S. Jawahir, “Multiple Criteria Optimization of Finish Turning Operations Based on a Hybrid Model”, *Proceeding of the 1996 ASME Design Engineering Technical Conferences and Computers in Engineering Conference*, Irvine, California, 1996.

[33] M.C. Chen, and C.T. Su, “Optimization of Machining Conditions for Turning

Cylindrical Stocks into Continuous Finished Profiles", *Int. J. Prod. Res*., Vol. 36(8), 1998, p. 2115.

[34] X. Wang, "Optimization of Multi-pass Turning Operations using Genetic Algorithms", *M.S thesis*, University of Kentucky, 2001.

[35] R. Saravanan, P. Asokan, and K. Vijayakumar, "Machining Parameters Optimization for Turning Cylindrical Stock into a Continuous Finished Profile Using Genetic Algorithm (GA) and Simulated Annealing (SA)", *Int. J. Adv. Manuf. Technol*, Vol. 21, 2003, p. 1.

[36] S. Chen, "Chip Flow and Chip Control in Contour Turning of Cast Aluminum Automotive Alloy Wheels", *MS Thesis*, University of Kentucky, 2002.

[37] A.K. Balaji, and I.S. Jawahir, "A Machining Performance Study in Dry Contour Turning of Aluminum Alloys with Flat-faced and Grooved Diamond Tools", *Machining Science and Technology*, Vol. 5(2), 2001, p. 269.

[38] Z. J. Da, "Optimization of Finish Turning Operations Based on a Hybrid Model", *PhD Thesis*, University of Kentucky, 1997.

[39] I.S. Jawahir, N. Qureshi, and J.A. Aresecularatne, "On the Interrelationships of Some Machinability Parameters in Finish Turning with Cermet Chip Forming Tool Inserts", *Int. J. Mach. Tools Manufact*., Vol. 32(5) 1992, p. 709.

[40] X. D. Fang and I.S. Jawahir, “On predicting Chip Breakability in Machining of Steels with Carbide Tool Inserts Having Complex Chip Groove Geometries”, *Journal of Materials Processing Technology*, Vol. 28, 1991, p. 37.

[41] G. Boothroyd, and W.A. Knight, “Fundamentals of Machining and Machine Tools”, 2nd Edition, Marcel Dekker, Inc., 1989.

[42] M. Thomas, Y. Beauchamp, A.Y. Youssef, and J. Masounave, “Effect of Vibrations on Surface Roughness During Lathe Dry Turning Process”, *Computers ind. Engng*, 31(3/4), 1996, p. 637.

VITA

The author was born on 8th of August, 1979 in Hamamatsu, Shizuoka prefecture, Japan. He received his Bachelors in Mechanical Engineering from Nagoya University, Japan in 2003. He continued study to the graduate school in Nagoya University, and he was selected as an exchange student to the University of Kentucky in Fall 2003. In Spring 2004, he transferred to the University of Kentucky to pursue the M.S degree.

Masaya Hagiwara

05 / 03 / 2005